Sinteza i simulacija strategije upravljanja umjereno-hibridiziranim vozilom paralelne arhitekture P2

Miletić, Marin

UNIVERSITY OF ZAGREB

FACULTY OF MECHANICAL ENGINEERING AND NAVAL ARCHITECTURE

MASTER'S THESIS

Marin Miletić

Zagreb, 2018.

UNIVERSITY OF ZAGREB

FACULTY OF MECHANICAL ENGINEERING AND NAVAL ARCHITECTURE

MASTER'S THESIS

Mentor:

Full Prof. Joško Deur, PhD

Student:

Marin Miletić

Zagreb, 2018.

IZJAVA

Pod punom moralnom odgovornošću izjavljujem da sam rad radio samostalno koristeći se znanjem stečenim tijekom studija te navedenom literaturom.

STATEMENT

I declare that I have done this study using knowlegde and skills gained during my university studies and using specified scientific literature.

ZAHVALA

Na početku bih se htio zahvaliti prof. dr. sc. Jošku Deuru na prihvaćanju mentorstva i za korisne sugestije tokom izrade ovog rada. Zatim, zahvaljujem se dr.sc. Branimiru Škugoru na korisnim savjetima. Nadalje zahvaljujem se mr. sc. Nikoli Naranči za pruženu priliku i za omogućivanje izrade diplomskog rada unutar tvrtke AVL - AST d.o.o. Zahvaljujem se kolegama iz ureda, na korisnim savjetima.

Najsrdačnije se zahvaljujem mojoj obitelji, ocu Zoranu, majci Marini i sestri Eni na neizmjernom strpljenju i podršci tokom studija i izrade ovog rada. Zahvalu upućujem i svojim prijateljima koji su bili uz mene tokom studija i pružali mi podršku.

Na koncu, zahvaljujem se svojoj djevojci Lari, na pruženoj potpori tokom izrade ovog rada.

Marin Miletić

ACKNOWLEDGMENT

At the beginning I would like to thank to Full Prof. Joško Deur, PhD for accepting the mentorship for this master's thesis and for useful suggestions during this study. Next, I would like to thank to Branimir Škugor, PhD for useful advises. Further, I would like to thank MPhil Nikola Naranča for giving me the opportunity to make my master's thesis within the AVL - AST d.o.o. I express my gratitude to my colleagues from the office for giving me useful advises during my graduation.

I would like to thank my family, father Zoran, mother Marina and my sister Ena for their tremendous patience and support during the study. I would like to thank my friends who were with me during the study and gave me support.

Finally, I thank my girlfriend Lara for her support during this work.

Marin Miletić

SVEUČILIŠTE U ZAGREBU
FAKULTET STROJARSTVA I BRODOGRADNJE
Središnje povjerenstvo za završne i diplomske ispite
Povjerenstvo za diplomske radove studija strojarstva za smjerove:
proizvodno inženjerstvo, računalno inženjerstvo, industrijsko inženjerstvo i menadžment, inženjerstvo materijala te mehatronika i robotika

Sveučilište u Zagrebu Fakultet strojarstva i brodogradnje	
Datum:	Prilog:
Klasa:	
Ur. broj:	

DIPLOMSKI ZADATAK

Student: **MARIN MILETIĆ** Mat. br.: 0035194500

Naslov rada na hrvatskom jeziku: **Sinteza i simulacija strategije upravljanja umjereno-hibridiziranim vozilom paralelne arhitekture P2**

Naslov rada na engleskom jeziku: **Design and simulation of control strategy for a mild hybrid electric vehicle given in parallel architecture P2**

Opis zadatka:

Powertrain of a Mild Hybrid Electric Vehicle (MHEV) is usually designed in a parallel configuration. Among different parallel HEV architectures, P2 architecture in which the electric machine is integrated between the internal combustion engine (ICE) and an automatic transmission is widely used in applications. Design of an effective MHEV control strategy is a key step towards minimising fuel consumption for a given vehicle hardware architecture and various driving cycles. The overall control strategy is based on integration of individual control functionalities such as e-creep, e-sailing, regenerative braking, e-boost and similar. The focus of the thesis is on development of the following MHEV control functionalities: torque assist, e-boost, load point moving and load point shifting, their integration with other, previously developed functionalities, and verification of the overall control strategy within the AVL CRUISE simulation environment.

To this end, the main tasks of the thesis are as follows:

1. Develop the aforementioned individual MHEV control functionalities and implement them within the AVL CRUISE environment by using the built-in C compiler;
2. integrate these individual control functionalities together with the previously developed ones and verify the overall control strategy by means of AVL CRUISE simulations for different certification driving cycles;
3. implement more detailed simulation model through adopting more detailed ICE model from AVL CRUISE M environment and setting up co-simulation model within the AVL Model.CONNECT environment;
4. analyse the main features of MHEV powertrain response when using the final control strategy, with the emphasis on fuel efficiency gains in comparison with the conventional vehicle and the MHEV without newly developed control functionalities.

All references should be included in a reference list and an acknowledgement of all received help should be provided.

Zadatak zadan: 27. rujna 2018.

Rok predaje rada: 29. studenog 2018.

Predviđeni datum obrane: 05. prosinca 2018. 06. prosinca 2018. 07. prosinca 2018.

Zadatak zadao: prof. dr. sc. Joško Deur

Predsjednica Povjerenstva: prof. dr. sc. Biserka Runje

Contents

List of Figures

List of Tables

List of Symbols and Units

Symbol	Description	Unit
A_{ek}	Brake specific fuel consumption,	g/kWh
b_w	Smoothing function bandwidth,	-
C	Load Point Shifting scaling factor	-
Cl_{ice}	Internal combustion engine clutch state,	-
e_{SoC}	State of charge control error,	%
G_{curr}	Current gear,	-
G_{new}	New LPS functionality desired gear,	-
i	Battery current,	A
$i_{DCT,curr,gear}$	DCT current transmission ratio,	-
$i_{DCT,new,gear}$	DCT new transmission ratio,	-
i_{tisg}	TISG transmission ratio,	-
k	Fuel consumption correction factor,	-
K_P	State of charge controller proportional gain,	W/%
m_{eq}	Equivalent mass fuel consumption,	g
$\dot{m}_{eq}$	Equivalent mass flow fuel consumption,	g/s
$m_{eq,downshift}$	Equivalent mass fuel consumption - downshift,	g
$m_{eq,upshift}$	Equivalent mass fuel consumption - upshift,	g
P_{alt}	Alternator power,	kW
P_{batt}	Battery power,	W
$P_{batt,c}$	Battery charging power,	W
$P_{batt,dc}$	Battery discharging power,	W
$P_{batt,max}$	Maximal battery power,	W
P_{eCreep}	eCreep power limit,	kW
P_{em}	Electric drive power,	W
$P_{em,eBoost}$	E-Boost available power,	W
$P_{em,max}$	Electric drive maximal power,	W

$P_{em,TA}$	TA available power,	W
$P_{el,cons}$	Electrical consumer power losses,	W
P_{des}	Desired power,	W
P_{ice}	Internal combustion engine power,	W
P_{max}	Start-stop switch on power,	W
$P_{max,regen}$	Maximal regeneration power limit,	kW
P_{min}	Start-stop switch off power,	W
$P_{eSailing}$	eSailing/TA/E-Boost power limit,	kW
R_0	Rolling resistance factor	-
R	Battery resistance	Ω
R_c	Battery charging resistance,	Ω
R_{dc}	Battery discharging resistance,	Ω
SoC	State of charge,	%
$SoC_{initial}$	Initial state of charge,	%
SoC_{final}	Final state of charge,	%
SoC_m	Current state of charge,	%
SoC_{ref}	Desired state of charge,	%
t	Time,	s
$t_{coupling}$	Coupling time step	ms
$t_{last-stop}$	Time from last ICE stop,	s
$t_{last-start}$	Time from last ICE start,	s
t_{sim}	Simulation time,	s
t_{start}	ICE start time,	s
t_{TA}	TA time delay,	s
U_{oc}	Battery open circuit voltage,	V
V_f	Fuel consumption,	l/100 km
$V_{f,corr}$	Corrected fuel consumption,	l/100 km
v_{veh}	Vehicle velocity,	m/s
W	Weighting factor,	-
Q_{max}	Maximum battery charge,	Ah
$\eta_{batt,c}$	Battery charging efficiency,	-
$\eta_{batt,dc}$	Battery discharging efficiency,	-

$\eta_{em,c}$	Battery charging efficiency,	-
τ_{em}	Electrical drive torque,	Nm
$\tau_{em,avaliable}$	Electrical drive available torque,	Nm
$\tau_{em,c}$	Electrical drive torque - state of charge controller,	Nm
$\tau_{em,max}$	Electrical drive maximal torque,	Nm
$\tau_{DCT,in}$	DCT transmission input shaft torque,	Nm
$\tau_{DCT,out}$	DCT transmission output shaft torque,	Nm
τ_{ice}	Internal combustion engine torque,	Nm
$\tau_{ice,c}$	Internal combustion engine torque - state of charge controller,	Nm
$\tau_{ice,ECMS}$	Internal combustion engine torque - ECMS maps,	Nm
$\tau_{ice,opt}$	Internal combustion engine optimal torque,	Nm
ω_{em}	Electrical drive angular velocity,	min^{-1}, rpm, rad/s
ω_{ice}	Internal combustion engine angular velocity,	min^{-1}, rpm, rad/s
$\omega_{in,DCT}$	DCT transmission input shaft angular velocity,	min^{-1}, rpm, rad/s
$\omega_{in,DCT,new}$	New calculated DCT transmission input shaft angular velocity,	min^{-1}, rpm, rad/s
$\omega_{out,DCT}$	DCT transmission output shaft angular velocity.	min^{-1}, rpm, rad/s

List of Abbreviations

Abbreviation	Description
BEV	Battery Electric vehicle
BSFC	Brake Specific Fuel Consumption
CD	Charge Depleting
CS	Charge Sustaining
DCT	Dual Clutch Transmission
EM	Electric Motor
ERHEV	Extended Range Hybrid Electric Vehicle
FHEV	Full Hybrid Electric Vehicle
FMI	Functional Mock-up Interface
FMU	Functional Mock-up Unit
FWD	Front Wheel Drive
HEV	Hybrid Electric Vehicle
HHV	Hybrid Hydraulic Vehicle
HMV	Hybrid Mechanical Vehicle
ICE	Internal Combustion Engine
LPM	Load Point Moving
LPS	Load Point Shifting
M/G	Motor/Generator
MHEV	Mild Hybrid Electric Vehicle
MHV	Micro Hybrid Vehicle
NEDC	New European Driving Cycle
PHEV	Plug-in Hybrid Electric Vehicle
TA	Torque Assist
WLTP	Worldwide Harmonised Light Vehicle Test Procedure
US06	Supplemental Federal Test Procedure

Sažetak

Zagađenje okoliša, efekti staklenika i potencijalna nestašica fosilnih goriva predstavljaju trenutne globalne probleme u svijetu. Direktna posljedica tih problema jest moderni tijek razvoja automobilske industrije, koja se smatra odgovornom za navedene probleme. Nadalje, u svijetu postoji ideja elektrifikacije te stapanja elektro-energetskog sustava s transportnim sustavom. Kao rješenje trenutno se nude hibridna električna vozila. Jedna od ključnih izazova kod razvoja hibridnih električnih vozila jest optimalna raspodjela energije na pogonskim sustavima, koja će minimizirati potrošnju goriva i emisiju štetnih plinova. Za danu arhitekturu pogona hibridnog električnog vozila, potrebno je razviti nadređenu strategiju upravljanja koja će raditi navedenu raspodjelu energije. Tema ovog rada upravo jest sinteza i simulacija strategije upravljanja umjereno-hibridiziranim električnim vozilom paralelne arhitekture P2. Umjereno-hibridizirano električno vozilo nudi razne mogućnosti razvoja hibridnih funkcionalnosti, koje će na temelju nadređenog sustava upravljanja smanjiti potrošnju goriva i emisiju štetnih plinova. Kroz ovaj rad prestavljen je unazadni i dan unaprijedni matematički model umjereno-hibridizanog električnog vozila unutar AVL CRUISE ™-a. Zatim je provedena sinteza i implementacija hibridnih funkcionalosti kao što su asistiranje momentom (eng. Torque Assist), pojačavanje momentom (eng. E-Boost), pomicanje radne točke u vertikalnom smjeru (eng. Load Point Moving) i pomicanje radne točke u horizontalnom smjeru (eng. Load Point Shifting). Razvijene funkcionalnosti su integrirane u jedan zajednički model te je proveden odziv na nekoliko certifikacijskih voznih ciklusa u svrhu analize smanjenja potrošnje goriva. Kasnije je razvijen ko-simulacijski model unutar AVL Model.CONNECT ™-a sa složenijim modelom motora s unutarnjim izgaranjem unutar AVL CRUISE ™ M-a. Odziv ko-simulacijskog modela proveden je na istim certifikacijskim voznim ciklusima, kao što je bio slučaj i s osnovnim modelom.

Ključne riječi: *hibridno električno vozilo, umjereno-hibridizirano električno vozilo, P2 arhitektura, hibridne funkcionalnosti, optimalno upravljanje, ko-simulacija, AVL, CRUISE ™, Model.CONNECT ™*

Summary

Environment pollution, greenhouse effect, and the potential fossil fuel scarceness represent the current global problems worldwide. The direct consequence of those problems is the modern course of development of automotive industry, which is considered responsible for those problem. Also, the idea of electrification and electrical energy system amalgamation with the transport system is present nowadays. Hybrid electric vehicles are currently being offered as a solution to these problems. One of the key aspects of hybrid electric vehicles development is the optimal energy management of the power sources, which is aimed to minimize the fuel consumption and harmful gas emissions. For a given powertrain architecture, it is necessary to develop a supervisory control strategy which will carry out the energy management within the system. The topic of this thesis is the design and simulation of a control strategy for a mild hybrid electric vehicle given in parallel architecture P2. Mild hybrid electric vehicle offers a fair amount of hybrid functionalities development, which will ensure fuel economy gains and harmful gas emissions reduction. Through this thesis, a backward powertrain model was developed, and the forward powertrain model was given within the AVL CRUISE ™ environment. Then the design and implementation of hybrid functionalities such as Torque Assist, E-Boost, Load Point Moving and Load Point Shifting were carried out. The developed functionalities were integrated into one model. Model's response was tested on several certification driving cycles for the fuel consumption analysis purposes. Later on a Co-Simulation model within the AVL Model.CONNECT ™ was developed, with a more complex internal combustion engine model taken from the AVL CRUISE ™ M. The Co-Simulation response was carried out on the certification driving cycles as it was the case with the basic CRUISE ™ model.

Keywords: *hybrid electric vehicle, mild hybrid electric vehicle, P2 architecture, hybrid functionalities, optimal control, Co-Simulation, AVL, CRUISE ™, Model.CONNECT ™*

Prošireni sažetak

Cilj ovog diplomskog rada jest sinteza i simulacija hibridnih funkcionalnosti upravljanja umjereno-hibridiziranim električnim vozilom u svrhu smanjenje potrošnje goriva i emisije štetnih plinova unutar AVL programskih paketa CRUISE ™, CRUISE ™ M i Model.CONNECT ™-a.

Spoznaje o zagađenju okoliša, efektima staklenika i nestašici fosilnih goriva postaju jedan od najvećih globalnih problema današnjice. Sve te spoznaje čine veliki izazov za moderni razvoj autoindustrije koja bi trebala ponuditi rješenje za navedene teze. Kao jedno od rješenja trenutno se nude hibridna električna vozila. Jedna od ključnih stvari kod razvoja hibridnih električnih vozila jest optimalna raspodjela energije na pogonskim sustavima koja će minimizirati potrošnju goriva i emisiju štetnih plinova. S obzirom na arhitekturu pogona hibridnog električnog vozila, potrebno je razviti nadređenu strategiju upravljanja koja će raditi navedenu raspodjelu energije. Kao što je navedeno na početku, tema ovog rada jest sinteza i simulacija strategije upravljanja umjereno-hibridiziranim električnim vozilom paralelne arhitekture P2. Umjereno-hibridizirano električno vozilo nudi razne mogućnosti razvoja hibridnih funkcionalnosti, koje će na temelju nadređenog sustava upravljanja smanjiti potrošnju goriva i emisiju štetnih plinova.

Ovaj rad je organiziran u sedam poglavlja s zaključkom, čiji sadržaj je sažet kako slijedi.

Poglavlje 1 - 'Uvod' - U uvodu je dana motivacija te osnovni pregled svojstava umjereno-hibridiziranih električnih vozila. Također dan je kratak opis paralelne arhitekture hibridnih vozila u općem smislu te detaljniji opis glavnih karakteristika i mogućih funkcionalnosti podskupa paralelne arhitekture P2.

Poglavlje 2 - 'MHEV matematički model' - Na početku ovog poglavlja dan je unazadni model pogona umjereno-hibridiziranog električnog vozila. Kao glavni dio unazadnog modela pogona dan je dinamički model baterije, za koji je stanje napunjenosti

baterije (SoC) jedina varijabla stanja. Zatim dane su karakteristike korištenog pogonskog sustava odnosno karakteristika motora s unutarnjim izgaranjem i električnog motora. Nadalje je opisana temeljna ideja strategije minimizacije ekvivalentne potrošnje goriva (ECMS). Zatim je dan kratak opis implementacije unazadnog modela u MATLAB Simulink okruženju. Nakon toga slijedi opis unaprijednog modela pogona koji uključuje i dinamiku prijenosa momenta. Dan je opis najvažnijih komponenti unaprijednog modela unutar AVL CRUISE ™ simulacijskog okruženja.

Poglavlje 3 - 'Razvoj MHEV funkcionalnosti' - Unutar ovog poglavlja dan je detaljan opis, implementacija i simulacijsko ispitivanje razvijenih hibridnih funkcionalnosti. Prvo je dan opis i odziv funkcionalnosti asistiranje momentom (eng. Torque Assist). Zatim pokazan je razvoj funkcionalnosti pojačavanja momentom (eng. E-Boost), za koji je dan opis i odziv na CRUISE ™ i ko-simulacijskom modelu. Nakon toga je dan opis i implementacija Load Point Moving funkcionalnosti. Unutar tog dijela, nalazi se opis optimizacijskog problema kojeg rješava funkcionalnost pomicanja radne točke u vertikalnom smjeru(eng. Load Point Moving) i njegova implementacija. Također tu se nalazi još i opis razvijenog eksplicitnog regulatora stanja napunjenosti baterije (SoC-a) kao dodatak samoj funkcionalnosti. Dana je i usporedba između modela s i bez eksplicitnog regulatora SoC-a. Na koncu je dan opis i implementacija funkcionalnosti pomicanja radne točke u horizontalnom smjeru (eng. Load Point Shifting). Za svaku funkcionalnost, definiran je i dijagram toka, koji objašnjava logiku uključivanja pojedine funkcionalnosti.

Poglavlje 4 - 'Integracija i simulacijska provjera upravljačke strategije' - U ovom poglavlju dan je opis integracije pojedinih funkcionalnosti u jedan zajednički model, te implementacije 'cjelovite' strategije upravljanja kao alternativa za model s odvojenim funkcionalnostima. Nakon toga, dan je odziv različitih upravljačkih strategija na certifikacijskim voznim ciklusima s fokusom na analizu potrošnje goriva.

Poglavlje 5 - 'Razvoj ko-simulacijskog modela MHEV-a' - Ovo poglavlje prikazuje kratki opis dinamičkog modela motora s unutarnjim izgaranjem unutar AVL CRUISE ™ M-a i razvoj ko-simulacijskog modela unutar AVL Model.CONNECT ™-a. Razvijeni co-simulacijski model iskorišten je za usporedbu odziva upravljačke strategije s i bez detaljno-modeliranog motora s unutarnjim izgaranjem.

Poglavlje 6 - 'Simulacijska provjera upravljačke strategije na MHEV co-simulacijskom modelu' - Slično kao i u poglavlju 4, dan je odziv co-simulacijskog modela na certifikacijskim voznim ciklusima s fokusom na analizu potrošnje goriva.

Poglavlje 7 - 'Zaključak' - Unutar zaključka dan je opis trenutnog stanja rada, zatim najvažniji rezultati analize potrošnje goriva za CRUISE ™ i co-simulacijski model te predložene točke nastavka i poboljšanja samog rada.

Chapter 1

Introduction

1.1 Basic terms

Hybrid (lat. *hybrida*) is a word which originally means an offspring of two animals or plants of different breeds, varieties, species or genera [1]. Hybrid, in a technical sense of the word, means a machine which in principle has at least two power sources in their powertrain structure. Most common hybrid powertrains include an internal combustion engine, ICE (Gasoline, Diesel), in a combination with an electrical motor, EM. These vehicles comprising ICE and EM drive, are called Hybrid Electric Vehicles or HEVs [2]. Similar to HEVs, there are Hybrid Hydraulic Vehicles or HHVs, which contain hydraulic accumulators as an energy storage and a hydraulic pump as an actuator instead of an electrical motor and a battery [3]. In addition, there are also Hybrid Mechanical Vehicles or HMVs, which use flywheel as an energy storage [3]. In this thesis, the focus will be on HEVs, especially on their subgroup Mild Hybrid Electric Vehicles or MHEVs.

1.2 Motivation

In the last two decades, strengthens the trend of introducing HEVs due to fosill fuel consuption and emission reductions [4]. Global carbon - dioxide (CO_2) emissions from fossil fuel use were 35.9 Gt (gigatonnes) in 2014 [5]. Fossil fuel emissions were 0.6% above emissions in 2013 and 60% above emissions in 1990 [5]. Due to these facts, new approaches to vehicle development needed to be introduced. For instance the automotive industry has had a big challenge in developing and implementing hybrid systems in their powertrain structure. HEVs are a good example of emission reductions and are becoming more popular. Some of

the advantages of HEV powertrains are [2] :

- Energy recuperation via regenerative braking,
- Pure electrical driving at low velocities,
- ICE downsizing and optimal loading for better efficiency,
- Power boost.

Due to these facts, there is a need for optimal HEV powertrain control development to achieve the best possible performance in terms of reducing fuel consumption and gas emissions. To this end, the topic of this thesis is to implement several hybrid functionalities (drive control) on an MHEV model given in P2 architecture.

1.3 Mild Hybrid Electric Vehicle - MHEV

There are two main classifications of HEVs. The first criterion of the classification is the powertrain structure and the second classification criterion is the size of the battery pack and electric drive or in other terms the degree of hybridization. Regarding the first criterion, there are serial, parallel and serial-parallel hybrid powertrain architetures[6]. Regarding the second criterion, there are micro, mild, and full hybrid electric vehicles [7]. The focus of this thesis will be on the MHEV P2 parralel hybrid powertrain architecure. The P2 parralel architecture will be described in the next subsecton. Now the description of the main features of the MHEV vehicles follows. The average MHEVs electric motor power is about $10 - 20$ kW at the voltage of $100 - 200$ V (the voltage may vary, for example, 48 V voltage is very popular among MHEVs). The electric motor and the ICE engine are usually coupled in a parallel MHEV architecture. The electrical powertrain is designed to crank the engine and offer energy recuperation during vehicle braking. There are demands of high specific power and long service batteries in MHEVs [7]. The battery's charge and discharge power depend on its state of charge or SoC. The batteries in MHEVs typically operate between 40 and 70% of SoC. Comparing with a conventional vehicle, the MHEV can provide better fuel economy by $20 - 30\%$ [7]. Examples of MHEVs are Honda Insight Hybrid and Civic Hybrid [7]. There are also VW Golf GTE and Audi A3 Sportback e-tron(figure 1.1 [8]) [2].

Figure 1.1: Audi A3 Sportback e-tron

1.4 Parallel architecture

The main focus of this thesis will be on the parallel HEV powertrain architecture, and its subgroup the P2 parallel architecture.

1.4.1 General

In parallel architecture (figure 1.2) the torque of the ICE engine and the EM are summed up via mechanical torque 'summation element' [1]. The 'summation element' is usually a belt or a gear transmission that is joined together on a common power flow. The main advantage is that parallel architecture demands only one EM. Also the advantages are that there are no double energy conversions and the ICE engine and the EM provide the vehicle propulsion torque together, which enables the ICE engine downsizing. The main disadvantage of the parallel architecture is that ICE engine is not being decoupled from the rest of the drivetrain. Therefore, the optimal speed control of ICE engine cannot be carried out [2]. The following description will be about the P2 type of the parallel architecture and its properties.

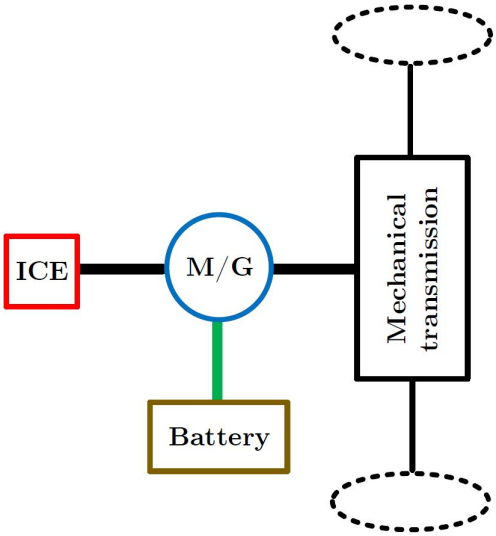

Figure 1.2: Paralel hybrid architeture

1.4.2 P2 architecture

The P2 architecture is the main topic of this thesis. The main property of P2 architecture is that it has an electric motor coupled with the ICE engine at the dual clutch transmission (DCT) input shaft. Also, an additional clutch is added between the ICE engine and the transmission so that the ICE can be decoupled from the rest of the drivetrain and therefore enable pure electric drive. Power flow in P2 architecture can be visualized via bond graph method (figure 1.3). Bond graph rules are given in the appendix.

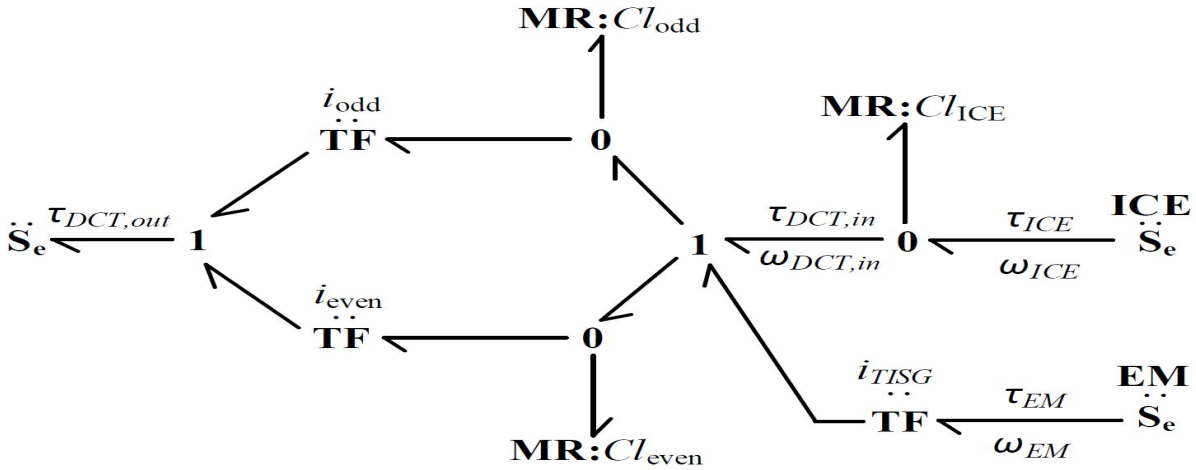

Figure 1.3: P2 architeture non-causal bond graph

Based on the design, the P2 architecture enables following hybrid functionalities [9]:

- Start-stop,
- E-Drive/E-Creep (figure 1.4),

- Regenerative braking (figure 1.5),
- Sailing (figure 1.4),
- Coasting (figure 1.5),
- Torque Assist (TA) (figure 1.6),
- E-Boost (figure 1.6),
- Load point moving (LPM) (figure 1.6),
- Load point shifting (LPS) (figure 1.6).

The first five functionalities are clarified in [10]. In this thesis, the focus will be on the TA, e-Boost, LPM and LPS functionalities, and each of them will be later described in detail. Figures 1.4 - 1.7 show the power flow in various functionalities that P2 architecture provides. The red arrows represent propulsion direction, and the blue arrows represent the regenerative charging direction. Thicker red arrows represent the power difference. Based on bond graphs, the main advantage of this architecture is the mechanical decoupling of the ICE engine thus the pure e-Drive. Next advantage is the EM placement in front of the DCT transmission whose gear shifting program allows for different torque gains provided by EM. Also, the EM helps to change gears in a way that it provides/takes additional torque for different gear shifting phases thus reducing inertia bumps and torque holes in gear shifting [2]. The disadvantages of the P2 architecture are the installation costs and relatively high control complexity [9]. On figures 1.6 and 1.7 the thicker red bonds represent the bigger power amount on these bonds.

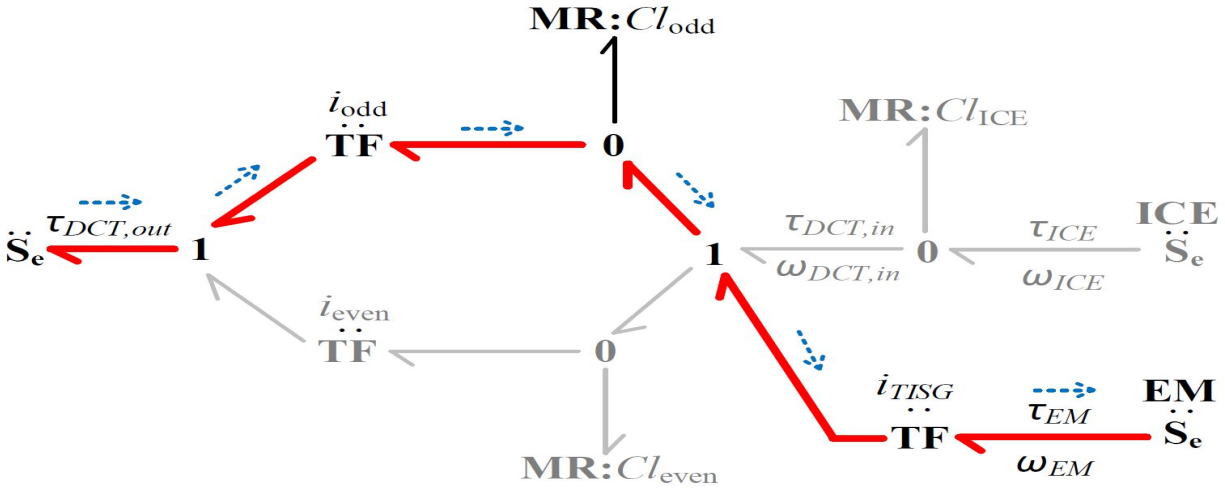

Figure 1.5: Regenerative braking/Coasting non causal bond graph

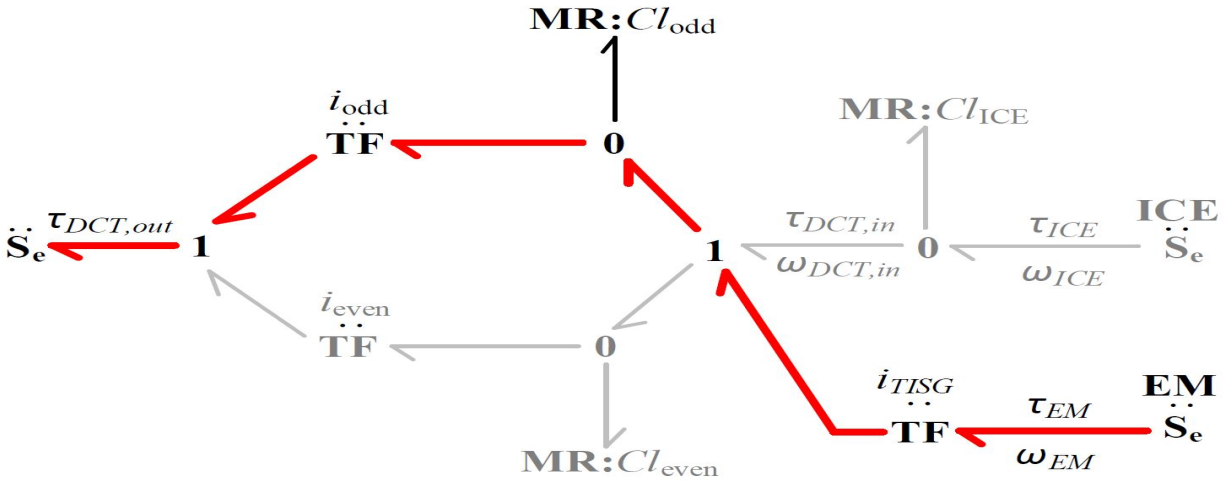

Figure 1.4: e-Drive/Sailing non causal bond graph

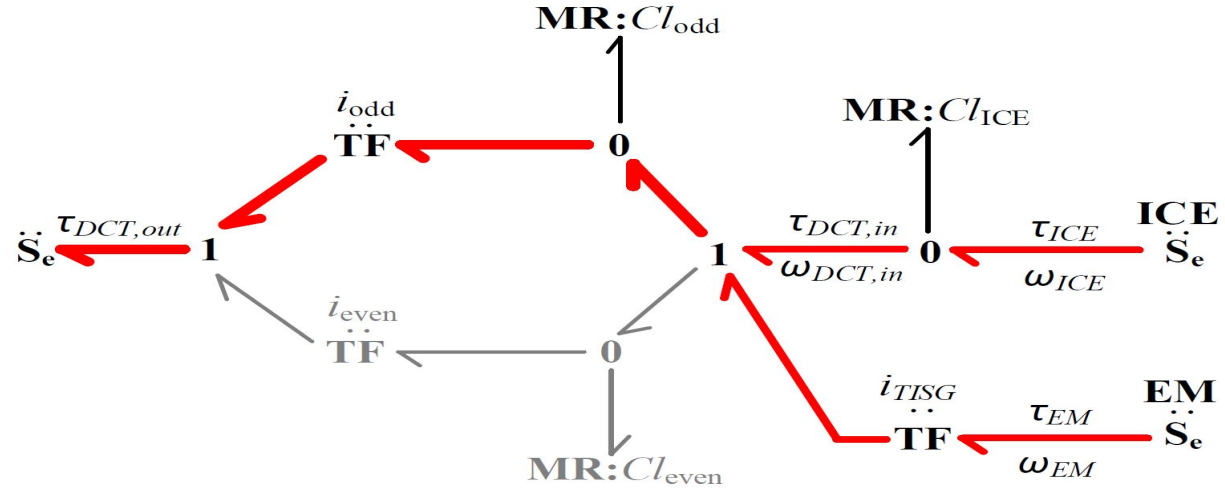

Figure 1.6: TA/e-Boost/LPM/LPS non causal bond graph

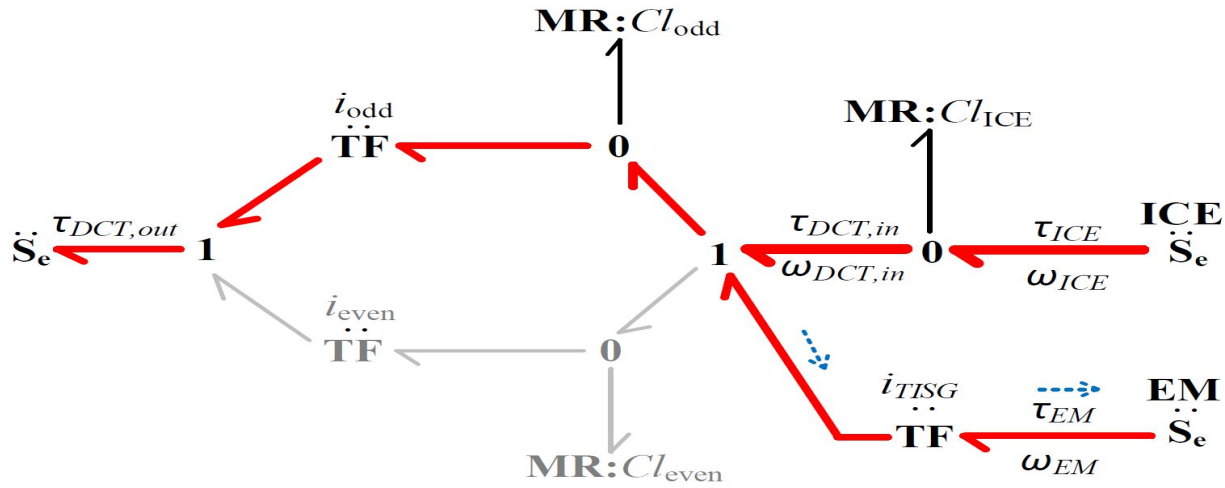

Figure 1.7: LPM/LPS non causal bond graph

Chapter 2

MHEV Mathematical Model

In this chapter, the MHEV powertrain mathematical model will be presented. First of all, a backward model or the so called quasi-static model will be described, and later the forward model or the dynamical model will be shown. In the backward model, the only state variable is the battery SoC, while powertrain transients considered based on the assumption that those transients are fast enough in comparison to the battery's SoC dynamics. The main reason for the backward model development is the calculation time reduction while optimizing the powertrain torque variables for the Load point moving functionality, as will be later explained in detail. The backward model was developed and implemented in MATLAB environment, while the forward model was built in AVL CRUISE ^{TM} environment.

2.1 Backward model

2.1.1 Dynamic battery model

The dynamic battery model comes from equivalent battery circuit equations. The battery's open circuit (figure 2.1, [11]) voltage characteristics, $U_{oc}(SoC)$ is a function of the battery's SoC. The internal resistance $R(SoC, i)$ is made dependent on the battery's SoC and the battery current i i.e. different values R_c and R_{dc} are used for charging and discharging respectively [11]. The assumption is that the battery current i is positive for discharging. The rated battery capacity is 10 Ah, while the minimal and maximal voltage are 37 and 54 V respectively.

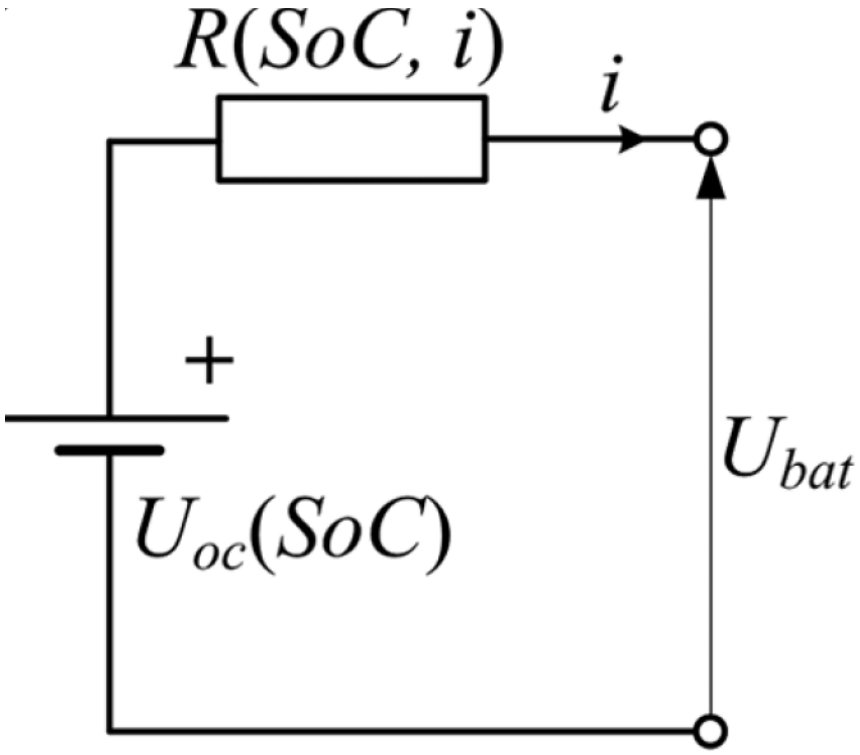

Figure 2.1: Equivalent battery's open circuit

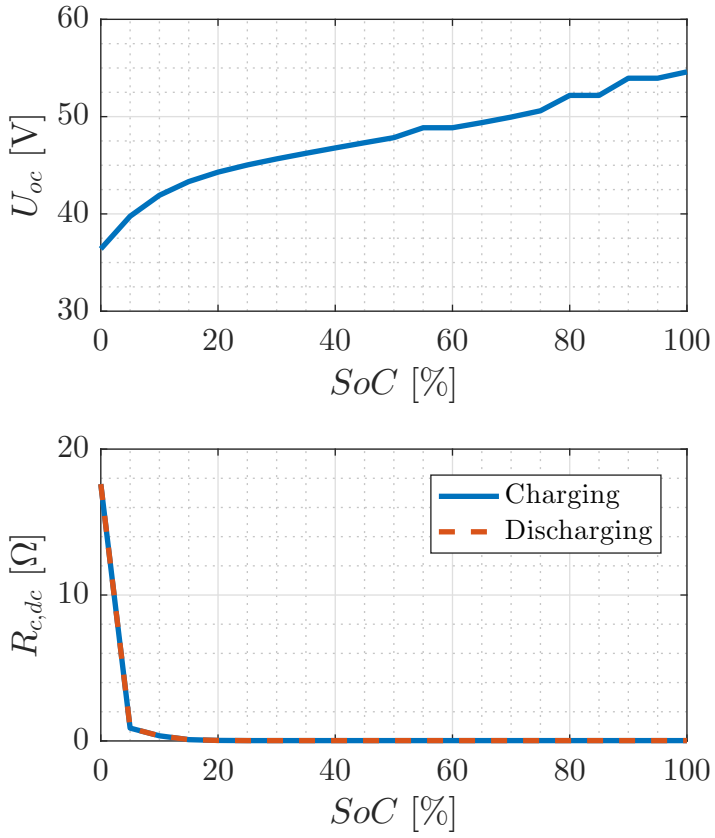

Figure 2.2: Open voltage and internal resistance characteristics

Battery's SoC dynamics is defined by the following equation:

$$\frac{dSoC}{dt} = \frac{-i}{Q_{max}}, \tag{2.1}$$

where the Q_{max} is the maximum battery charge. Current i in the equation 2.1 is defined from the battery power equation, P_{batt}, as follows:

$$P_{batt} = U_{oc}(SoC)i(t) - R(SoC, i)i^2(t). \tag{2.2}$$

Solving the above equation 2.2 by current and inclusion into the statement 2.1, the final equation of battery's SoC dynamics follows:

$$\frac{dSoC}{dt} = \frac{\sqrt{U_{oc}^2(SoC) - 4R(SoC, i)P_{batt}} - U_{oc}}{2Q_{max}R(SoC, i)}. \tag{2.3}$$

The battery power, P_{batt}, is defined from the EM power as follows:

$$P_{batt} = \eta_{em}^k \tau_{em} \omega_{em}, \tag{2.4}$$

where η_{em} is the EM efficiency, k the coefficient that equals $k = -1$ for the motor operating mode, and $k = 1$ for the generator operating mode. The ECMS approach, which will be explained later, requires knowledge of the efficiency of the battery, which is also determined from the dynamic battery model as shown above. The round-trip loss-related efficiency is used. In the case of discharging, the battery efficiency $\eta_{batt,dc}$ is calculated by the following statement [11]:

$$\eta_{batt,dc} = \frac{P_{batt}}{P_{batt} + i^2(t)R_{dc}}, \tag{2.5}$$

whereas, for charging, the straightforward battery efficiency expression $\eta_{batt,c}$ is as follows:

$$\eta_{batt,c} = \frac{U_{oc}(t) - R_{dc}|i(t)|}{U_{oc}(t) + R_c|i(t)|}. \tag{2.6}$$

2.1.2 Internal Combustion Engine (ICE)

MHEV's main propulsion system is based on of four-stroke, four-cylinder ICE with compression ignition (Diesel engine) with an effective volume of 1995 cm^3. Idle speed of the ICE equals 800 min^{-1}, while the maximum rotational speed is 5000 min^{-1}. The ICE maximum power equals 110 kW at 4000 min^{-1}, and the ICE maximum torque is 340 Nm at

2500 min^{-1}. As said above, the dynamic effects of electrical and mechanical transition events are not considered in the backward model i.e. the model uses only the static characteristic of the ICE. ICE static characteristic (figure 2.3) contains the brake specific fuel consumption map (BSFC), A_{ek}, and the ICE maximum torque curve.

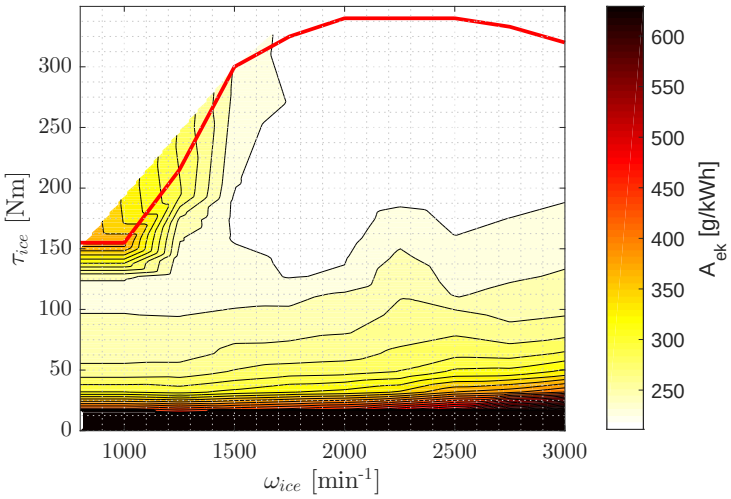

Figure 2.3: ICE static characteristic

2.1.3 Electrical motor (EM)

The MHEV auxiliary drive system is an asynchronous electric motor with a rated power of 10 kW and a nominal voltage of 48 V. The maximum EM speed is 20, 000 min $^{-1}$. Similar to ICE, for the EM only static characteristic is shown. The figure 2.4 shows the EM static characteristic in the motor and generator operating mode which contains the maximum torque curves and the EM efficiency map η_{em}.

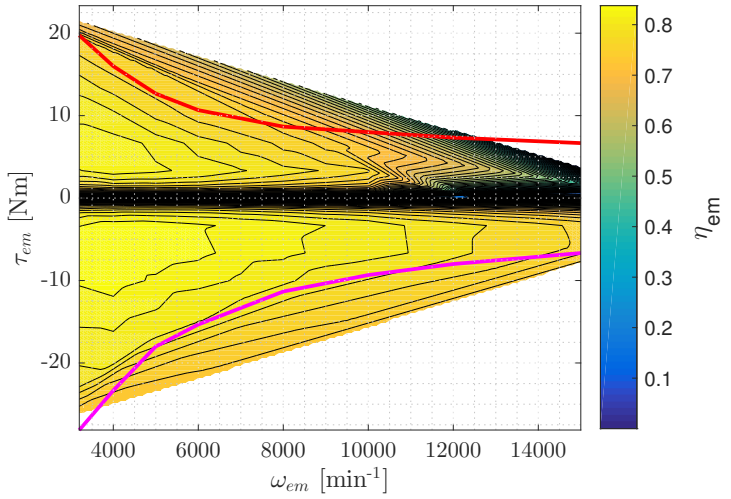

Figure 2.4: EM static characteristic

2.1.4 Equivalent consumption minimization strategy (ECMS)

For optimal powertrain control, the equivalent consumption minimization strategy (ECMS) is used. ECMS strategy represents a heuristic concept that the energy used to drive a vehicle ultimately comes from the ICE, and as such, the hybrid system serves only as an energy buffer [12]. In other words, the battery's electrical energy was somehow converted from the chemical energy of the fuel. Considering that the battery energy consumption and the fuel consumption are not directly comparable, an equivalent fuel consumption, $\dot{m}_{eq}$ is defined as follows:

$$\dot{m}_{eq} = \begin{cases} A_{ek}P_{ice} + A_{ek}\eta_{batt,c}P_{batt}, & P_{batt,c} < 0 \\ A_{ek}P_{ice} + \overline{A_{ek}}\eta_{batt,dc}^{-1}P_{batt}, & P_{batt,dc} > 0 \end{cases} \tag{2.7}$$

where P_{ice} is the power of ICE, $P_{batt,c}$ and $P_{batt,dc}$ are battery power values when charged and discharged respectively $\eta_{batt,c}$ and $\eta_{batt,dc}$ the battery efficiency when charging and discharging respectively, A_{ek} brake specific fuel consumption, $\overline{A_{ek}}$ average brake specific fuel consumption. The average brake specific fuel consumption of $\overline{A_{ek}}$, when discharging the battery, is defined as the mean value of the brake specific fuel consumption at the ICE maximum torque. It reflects the fact that the "price" of the current discharge power is associated with the unknown ICE efficiency during the charging interval in the past [2].

2.1.5 MATLAB environment

The backward model equation was implemented using MATLAB m.scripts and MATLAB Simulink environment. In figure 2.5 the implementation of EM static characteristic is shown. In figure 2.6 the implementation of ICE static characteristics is shown. In figure 2.7 the implementation of battery open voltage circuit is shown.

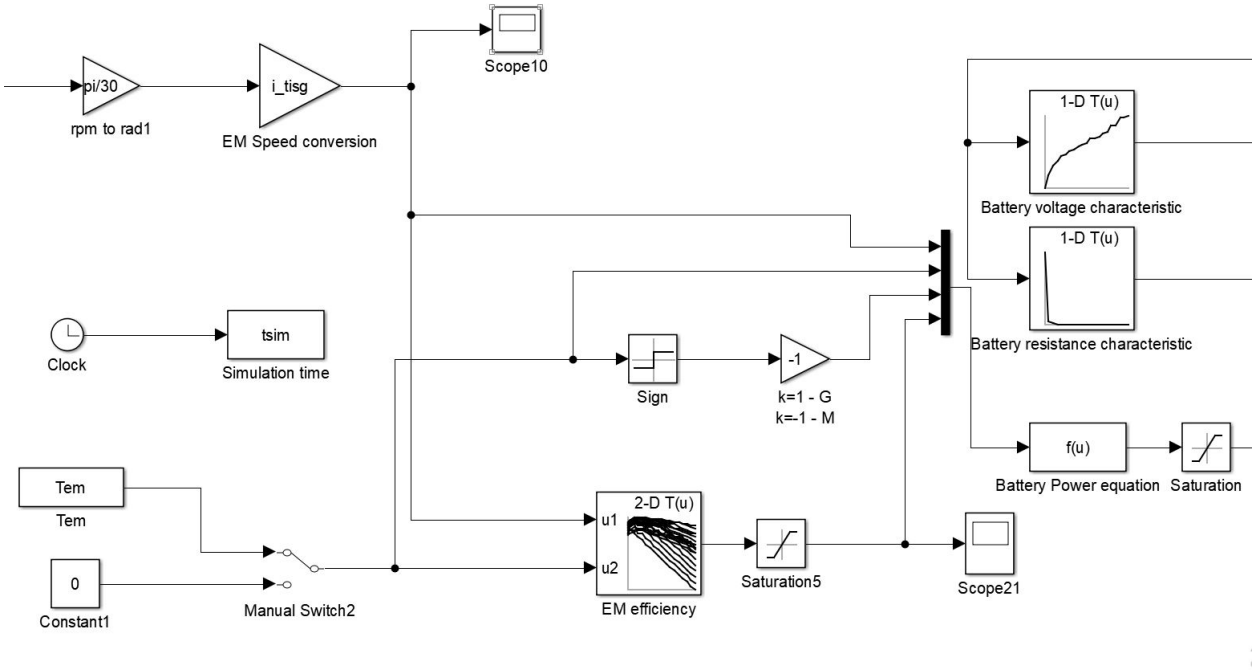

Figure 2.5: EM static characteristics - Simulink environment

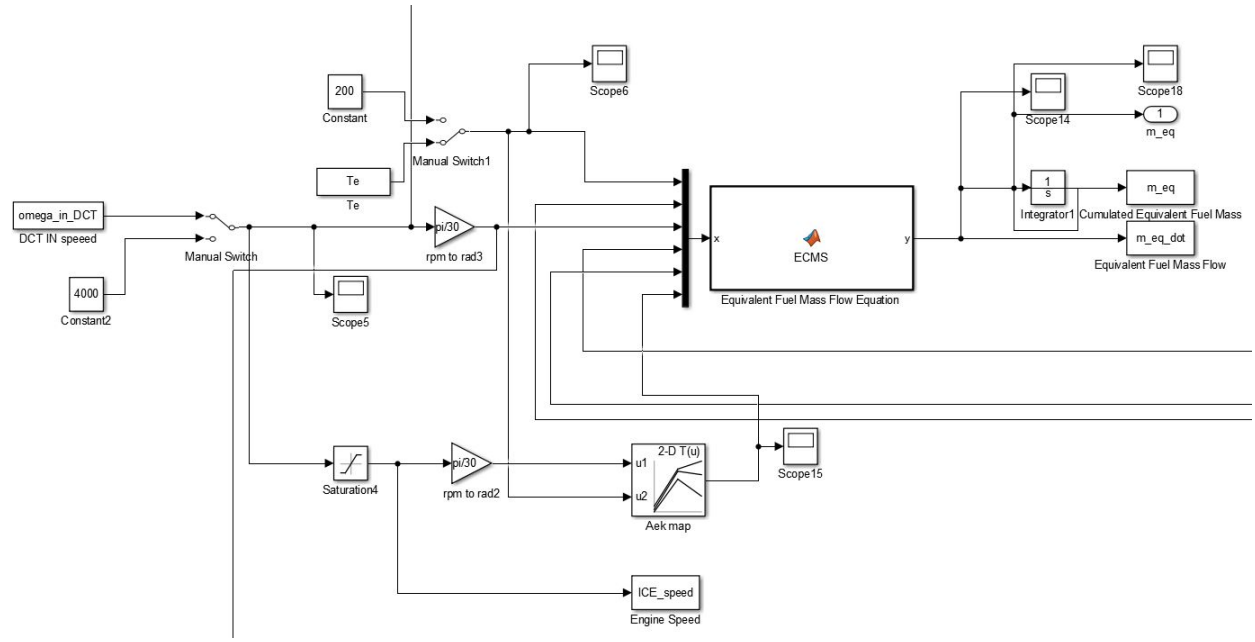

Figure 2.6: ICE static characteristics - Simulink environment

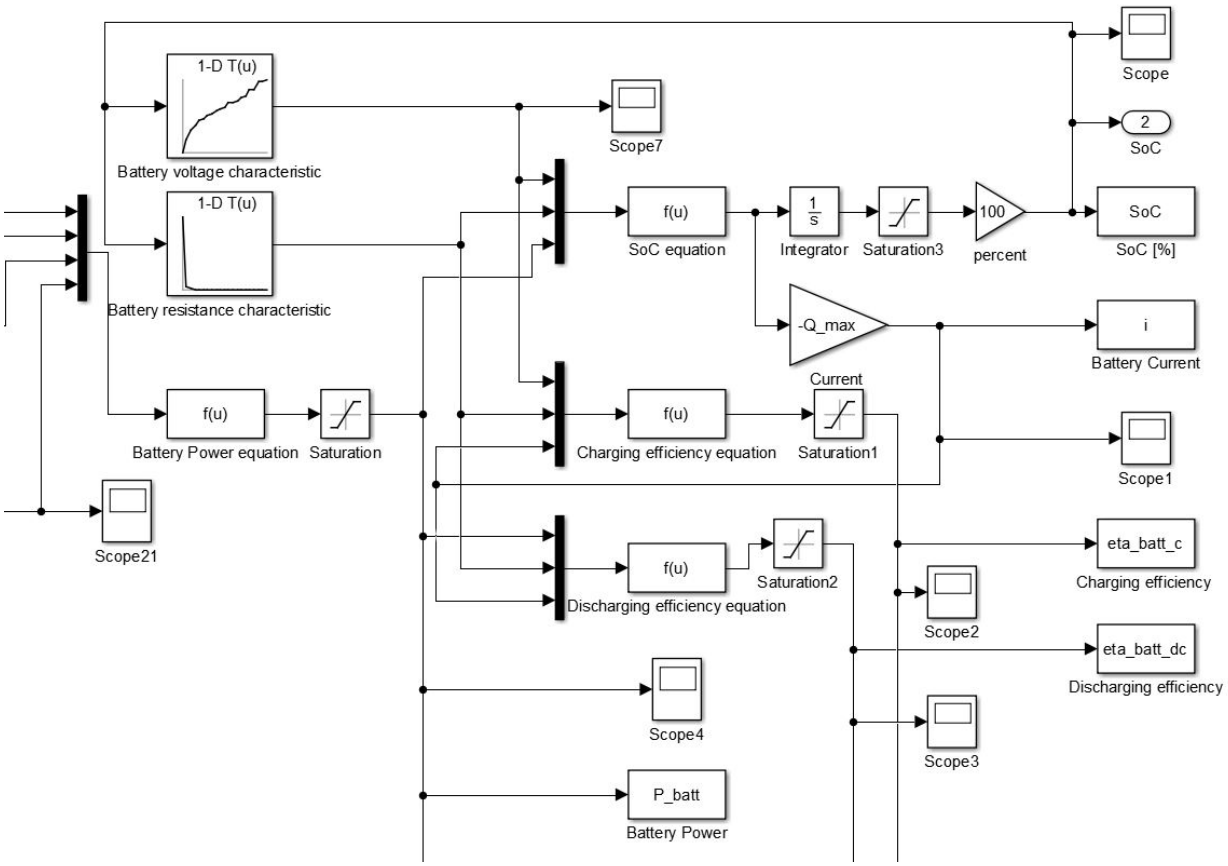

Figure 2.7: Battery open voltage circuit - Simulink environment

2.2 Forward model

The difference between the previously developed backward model and the forward model is that the forward model includes the dominant dynamic effects such as powertrain inertias. In figure 2.8 the causal bond graph of the P2 configuration is given. Analog to the shown bond graph, the MHEV AVL CRUISE^{TM} model (figure 2.9) was developed. In the following subsections, the forward model components will be described. Note that the ICE engine and EM models will not be described again because the only difference now is that both of the models have a inertia built in the blocks. The half shaft elasticity and damping are not considered in this model. In later chapters, a more detailed dynamic ICE engine model will be described.

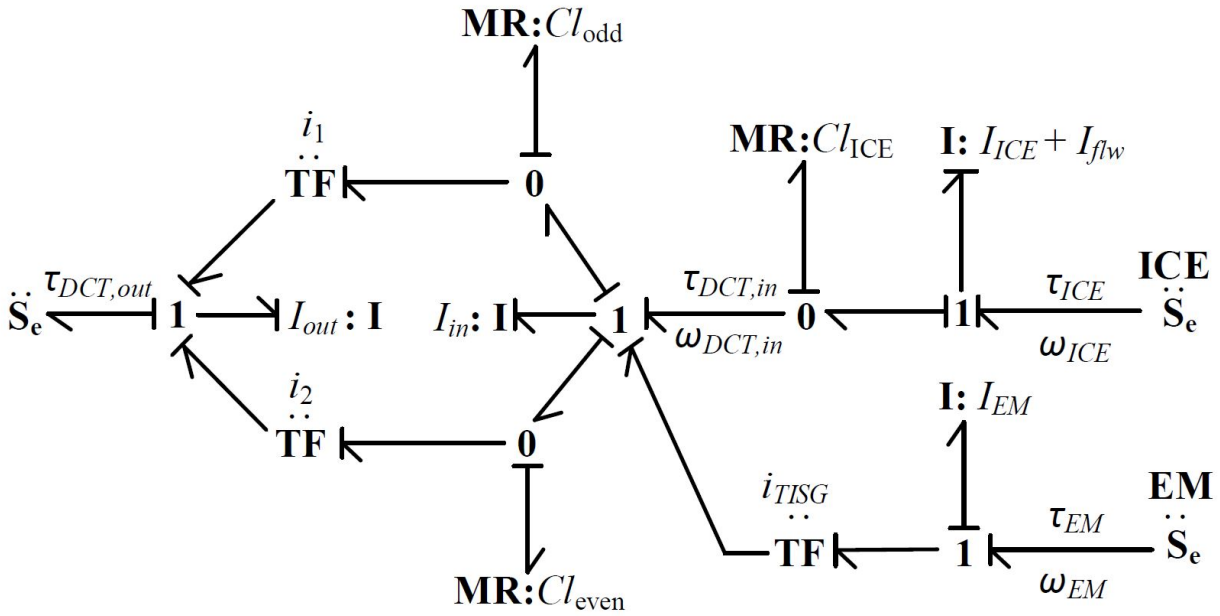

Figure 2.8: P2 causal bond graph

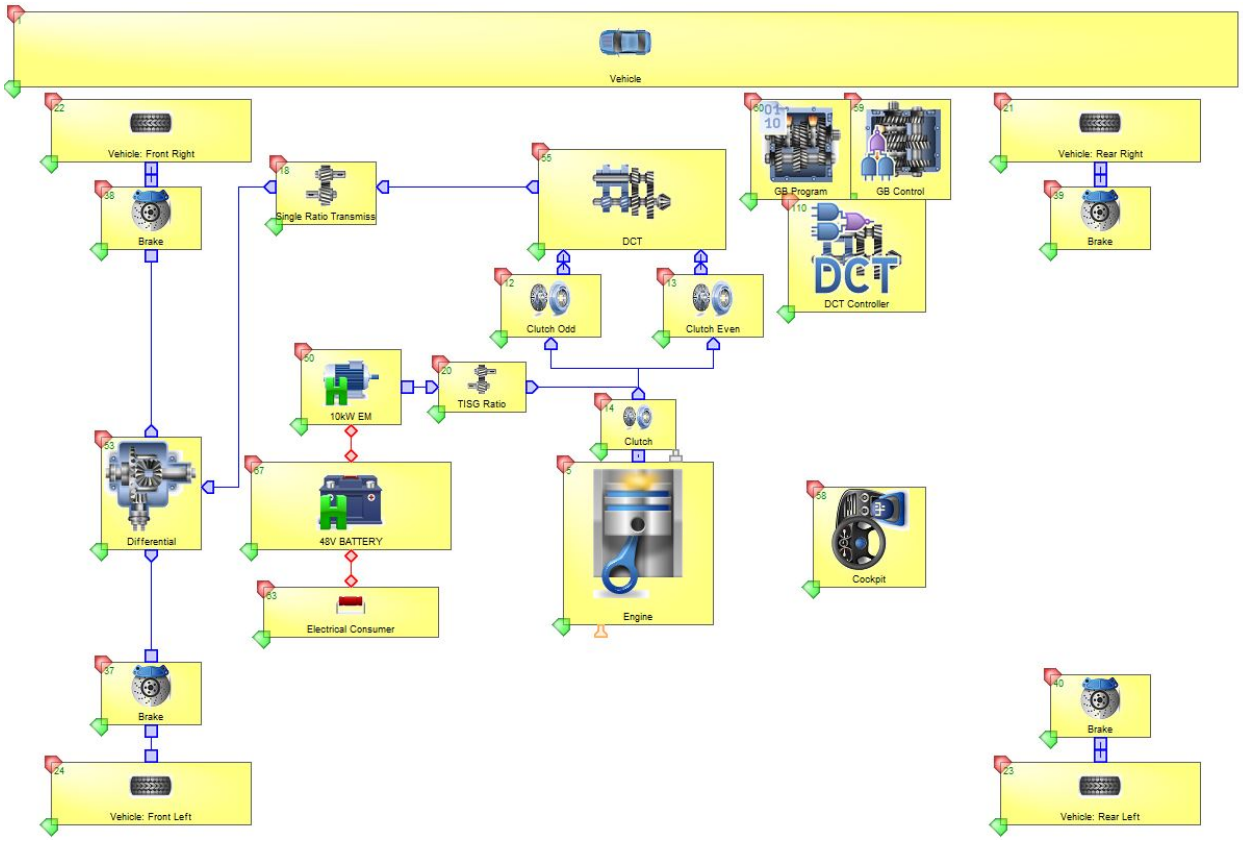

Figure 2.9: P2 MHEV model in AVL CRUISE ™ environment

2.2.1 ICE Clutch

ICE Clutch is modeled as a linear torque transmission element with inertia. Friction losses are not considered. Figure 2.10 represents the clutch actuation characteristics.

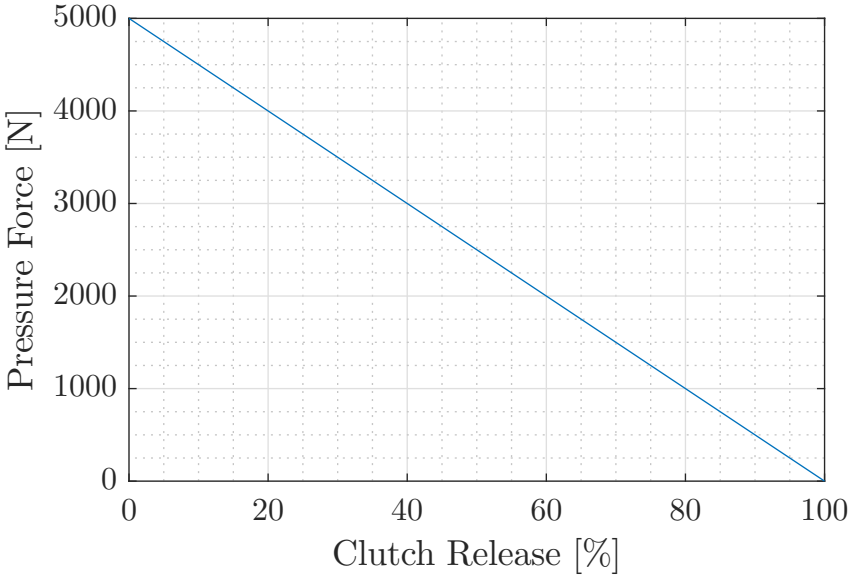

Figure 2.10: ICE clutch actuation characteristics

2.2.2 Transmission and differential

The DCT transmission is used to transmit the power from the engine and EM to the differential. The gear ratios and the gear teeth numbers are given in table 2.1. Differential transmission ratio is 3.37, and the transmission ratio between the EM and the DCT input shaft, i_{tisg} equals 4.0.

Gear	Gear ratio	Number of teeth input	Number of teeth output
1	3.91	11	43
2	2.11	19	40
3	1.39	31	43
4	1.02	43	44
5	0.81	43	35
6	0.67	46	31

Table 2.1: DCT transmision ratios

To control the DCT transmission, a shift scheduling algorithm needs to be defined. For this case, the gear shifting program was adopted from AVL CRUISE ™ and it was defined that the current gear is a function of the acceleration pedal travel and the vehicle velocity.

The gear shifting program curves are shown in figure 2.11. More detailed shift scheduling algorithm development can be found in [13].

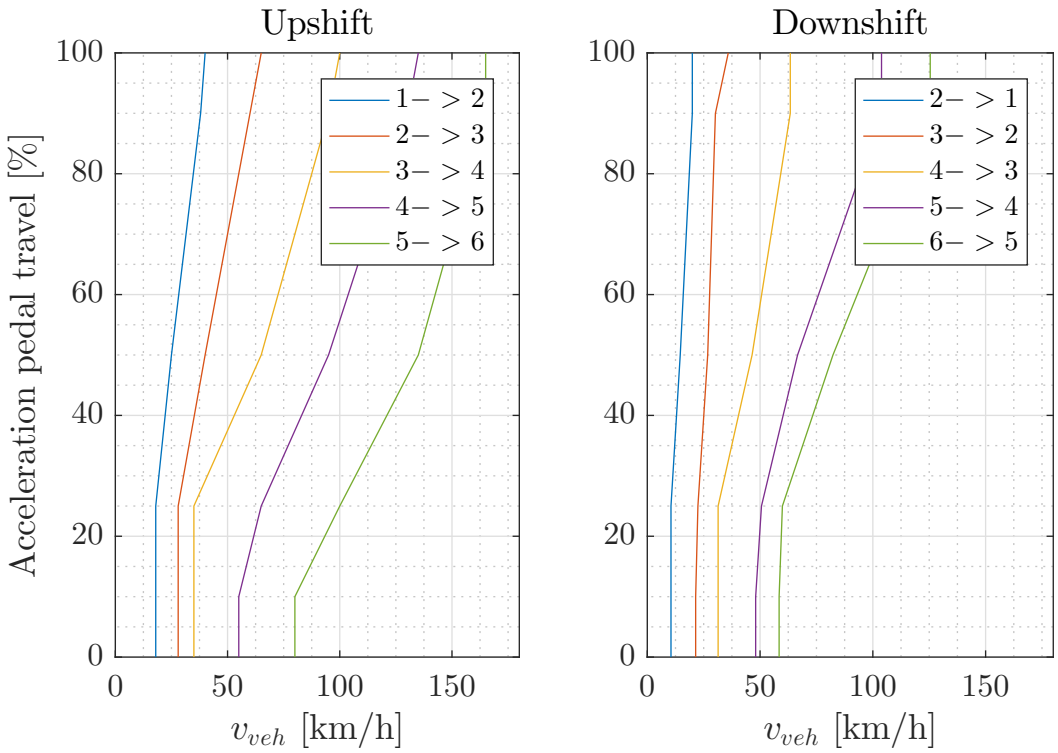

Figure 2.11: Gear shifting program for DCT transmission

2.2.3 Brakes and wheels

Brakes are modeled as friction disc brakes. Brake's effective friction radius is 130 mm, with the friction coefficient of 0.25, while the wheels friction coefficient is fixed and equals 0.95. Wheel's static and dynamic rolling radius equals 317.19 mm. Wheel's rolling resistance factor, R_0 is a function of the vehicle speed, and its characteristics is given in figure 2.12.

2.2.4 Control maps

In order to successfully implement hybrid functionalities, besides the powertrain elements characteristics, control maps are introduced. Their purpose is to limit the EM power, in several functionalities, in order to achieve SoC sustainability. The EM power limits i.e. the control maps are given in figure 2.13.

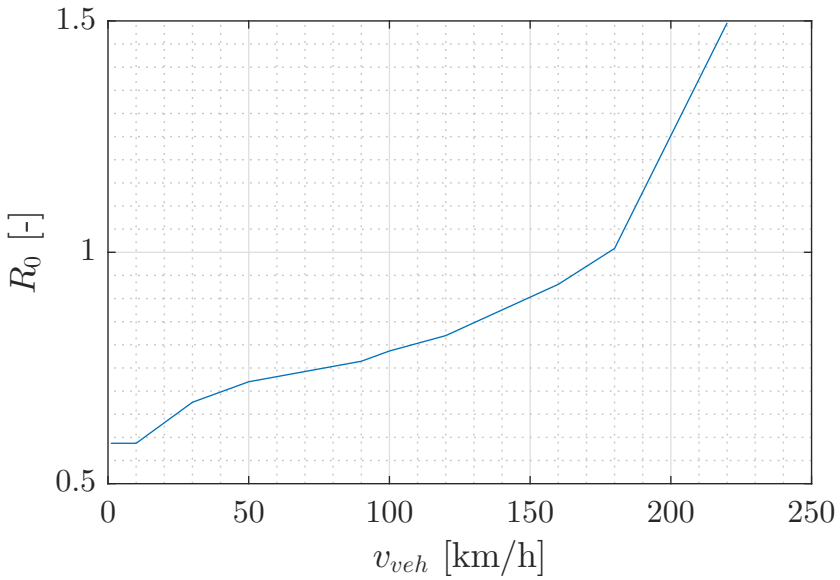

Figure 2.12: Rolling resistance factor

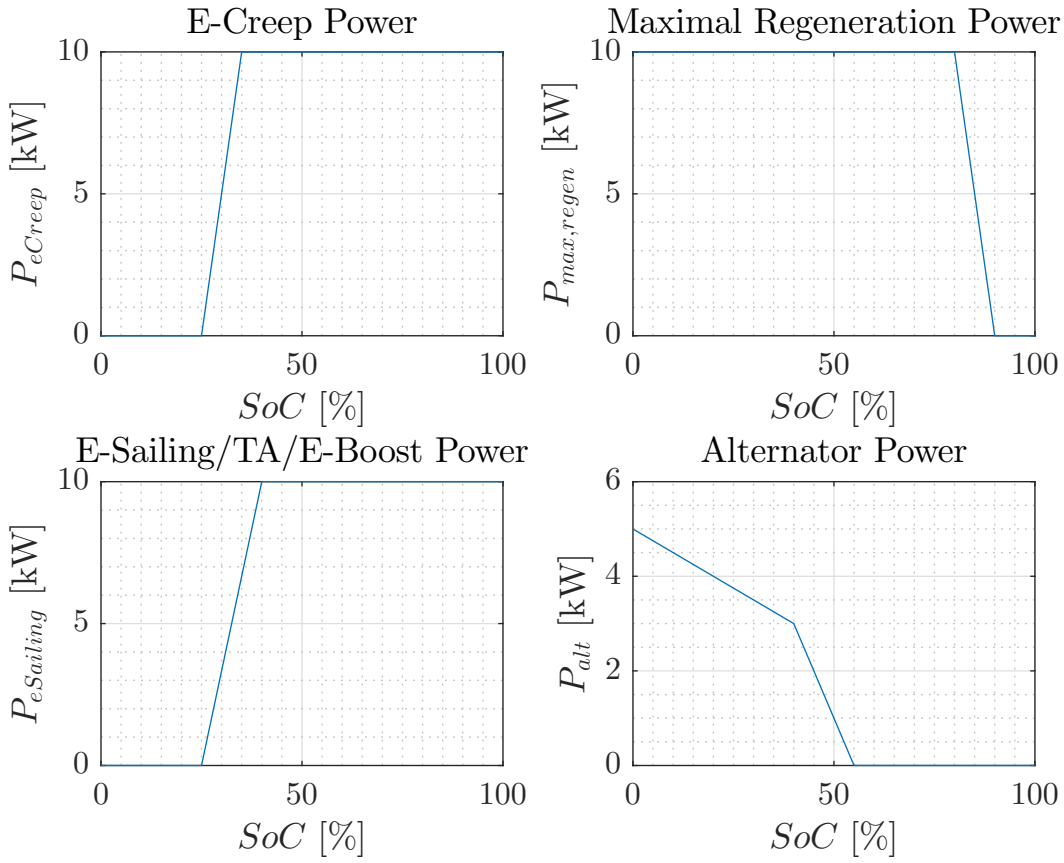

Figure 2.13: EM control maps

2.2.5 Auxiliary power consumers

Idle speed losses i.e. auxiliary power consumers are modeled as a power loss, $P_{el,cons}$. The characteristics of electrical consumers is shown in figure 2.14. The auxiliary power consumers include all of the auxiliary devices that are powered by the engines. That includes the A/C

system, steering servo pump, windshield wipers etc.

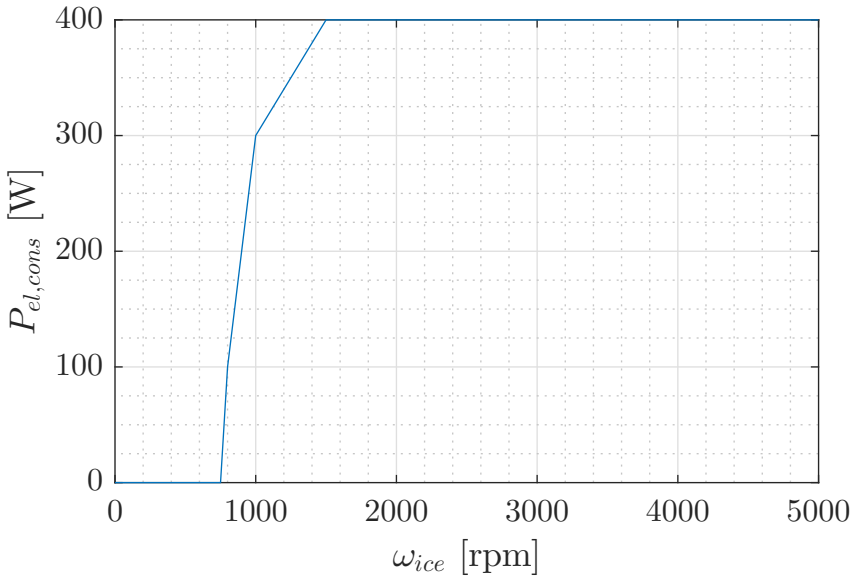

Figure 2.14: Auxiliary power consumer characteristics

In the next chapter, the MHEV control functionality development will be given and explained in detail.

Chapter 3

MHEV control functionalities development

In this chapter, the concept and development of several hybrid functionalities will be presented. Basic MHEV functionalities such as E-Creep, Sailing, Coasting and Regenerative braking have already been developed and described in [10]. Through this chapter, the Torque Assist, E-Boost, Load Point Moving, and Load Point Shifting will be described. Their main property is that they enroll and manipulate both of the power sources i.e. the ICE engine and the EM, thus gaining fuel economy and vehicle performances.

3.1 Torque Assist

3.1.1 Concept

ICE engines typically have low fuel economy at high engine speeds, at low average loads and at high dynamic responses [14]. Torque assist is implemented with the aim to run the ICE engine where it has the best efficiency [9]. In the torque-assist hybrid, the ICE engine and the EM are always mechanically linked [15]. So, the main concept of the Torque Assist functionality (figures 3.1 and 3.2) is to propel the vehicle from both of the power sources which means that in comparison with basic functionalities such as E-Drive or Sailing, which use only the EM in order to propel the vehicle, the powertrain is now in hybrid operating mode. What it does is that it shifts the ICE engine operating point to the optimal fuel economy operating point and assists the ICE engine with EM so that the EM provides the additional torque needed in order to satisfy the driver's torque request.

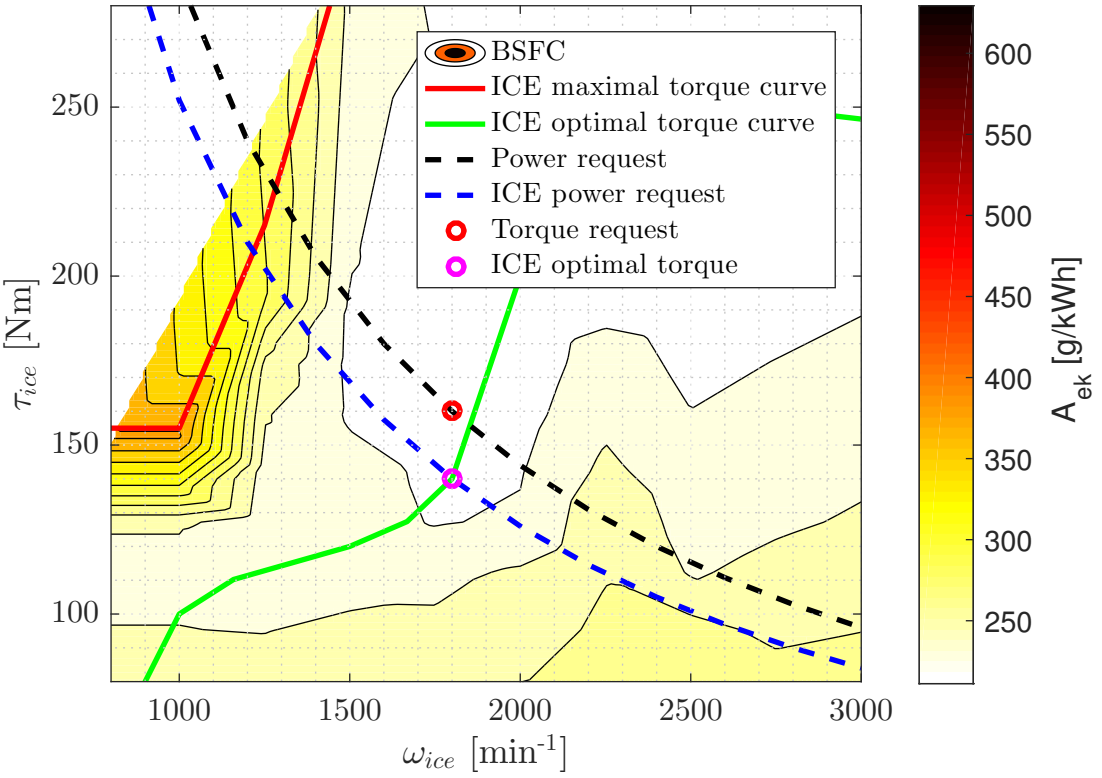

Figure 3.1: Torque Assist concept - ICE

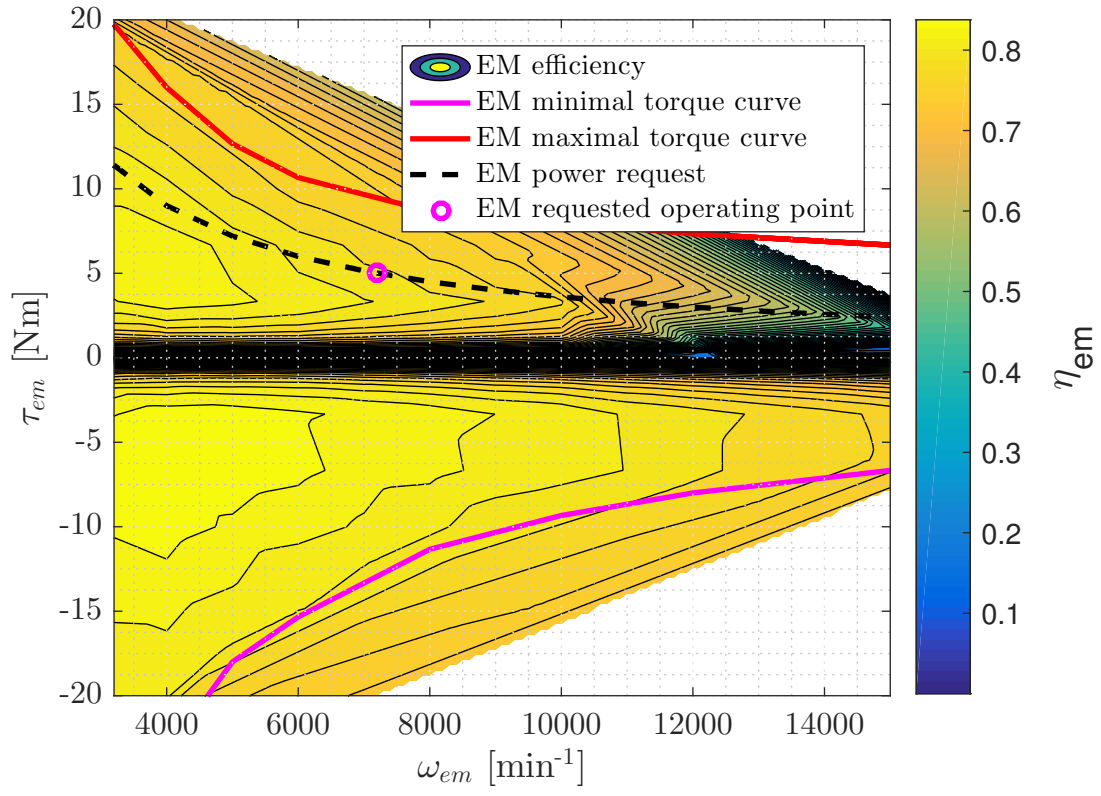

Figure 3.2: Torque Assist concept - EM

3.1.2 Implementation

On the driver's torque demand, the optimal ICE torque is being calculated. After that, the comparison between the driver's torque demand and the optimal ICE torque is carried out. If the demand torque is higher than the ICE optimal torque, then the ICE engine's operating point is shifted to the optimal operating point while the EM provides the additional torque. In that case, the EM draws the battery current and discharges the battery i.e. the battery SoC declines. The Torque Assist flowchart is shown in figure 3.3.

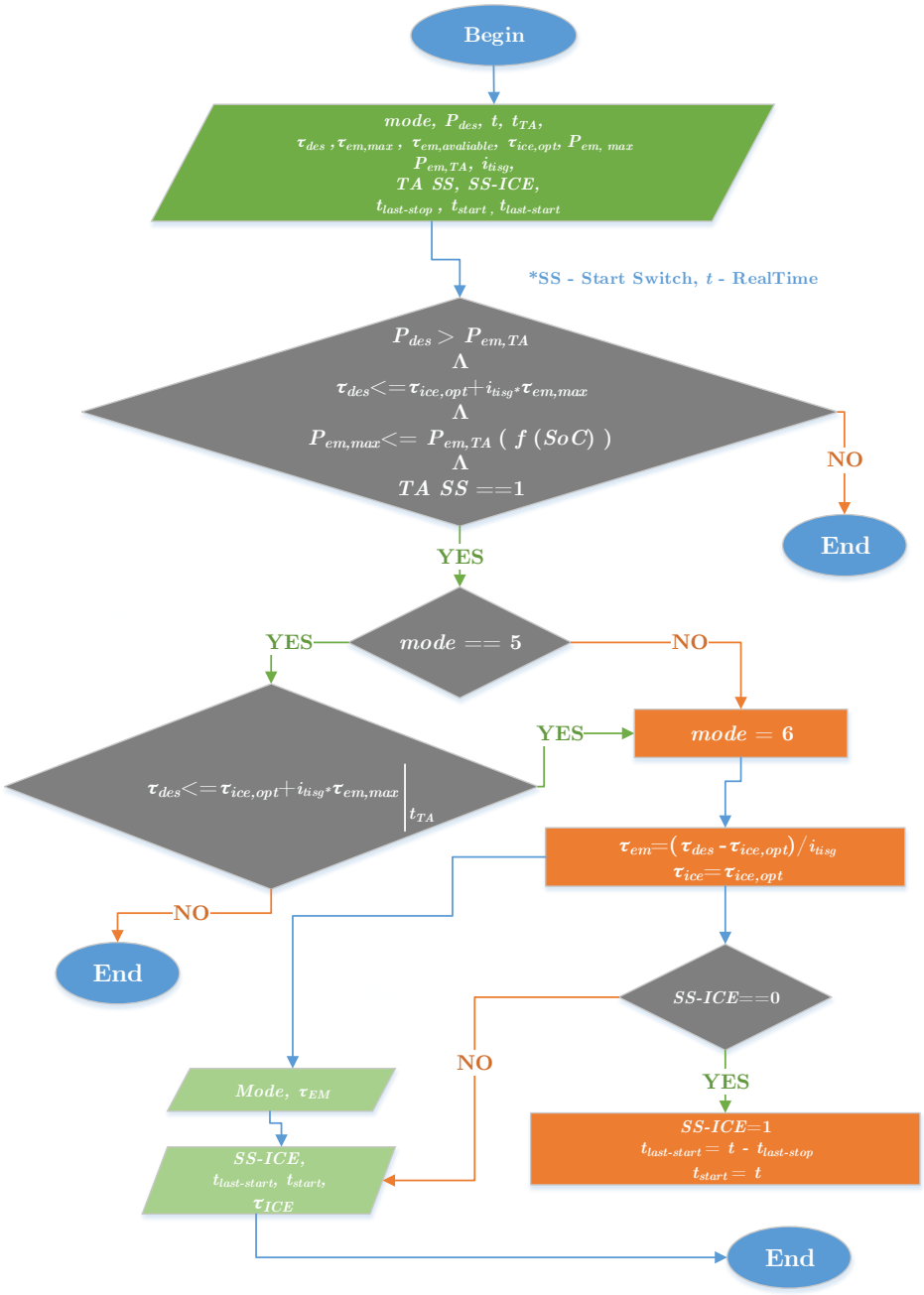

Figure 3.3: Torque Assist flowchart

Conditions that are needed to trigger TA functionality are as follows:

- desired power, P_{des} needs to be higher than the TA available power, $P_{em,TA}\,(SoC)$ (figure 2.13.c),
- desired torque, τ_{des} needs to be lower than the sum of ICE optimal torque, $\tau_{ice,opt}$ and the EM maximal torque available, $\tau_{em,max}$,
- maximal available EM power, $P_{em,max}$ must be equal or lower than the $P_{em,TA}\,(SoC)$,
- TA start switch must be active,
- and if the current mode[1] is conventional then the main TA condition must be true for at least 1 s.

After all the above conditions are satisfied, then the powertrain mode is set to:

$$mode = 6, \tag{3.1}$$

the ICE engine torque is set as follows:

$$\tau_{ice} = \tau_{ice,opt}, \tag{3.2}$$

while the EM torque is set to:

$$\tau_{em} = \frac{\tau_{des} - \tau_{ice,opt}}{i_{tisg}}. \tag{3.3}$$

In figures 3.4 and 3.5 the implementation of TA is shown. The figures show that the TA functionality is successfully implemented. At higher vehicle velocities, the ICE torque operating point is set to be optimal, while the EM provides the additional torque thus discharging the battery. Figure 3.4 also shows that the driveability is not violated because the current velocity matches the desired velocity.

[1]Mode numbers are given in table 4.1

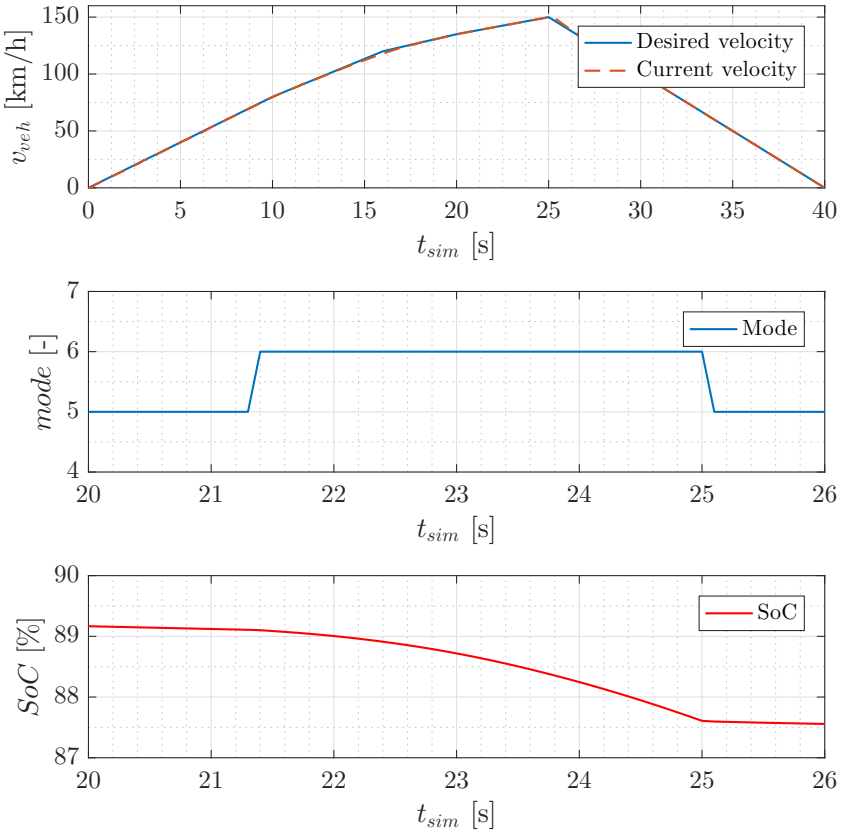

Figure 3.4: Torque Assist demonstration - Velocity, Mode and SoC

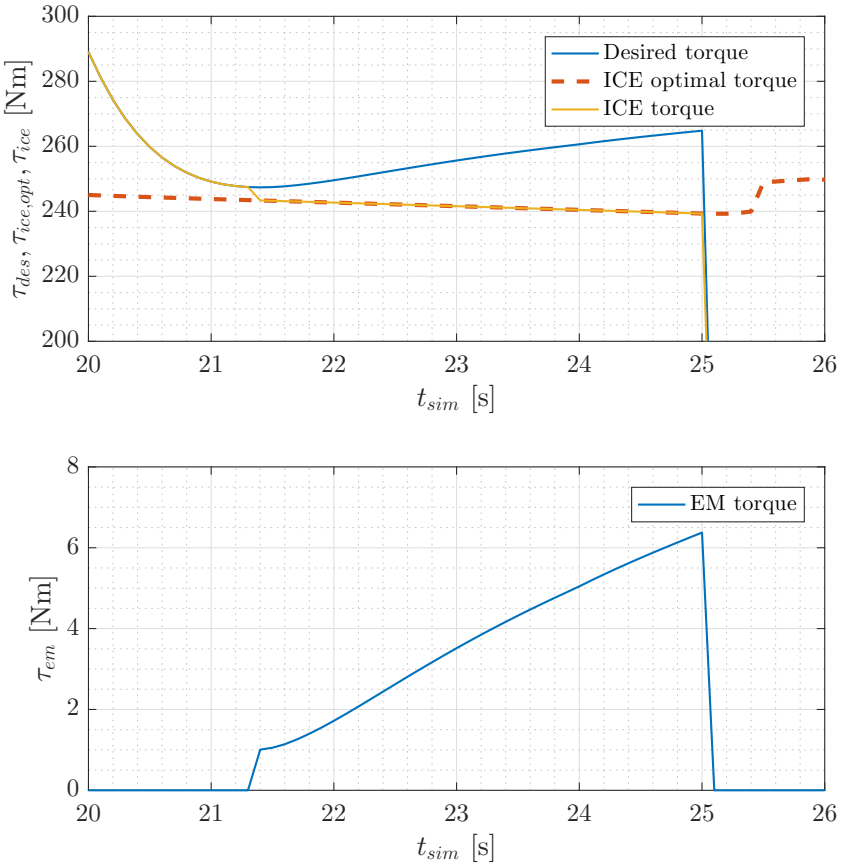

Figure 3.5: Torque Assist demonstration - Torques

3.2 E-Boost

3.2.1 Concept

Similar to TA, in the E-Boost functionality the EM assists the ICE engine, but this time not to achieve ICE optimal fuel economy. This time, E-Boost assists the ICE engine during sudden vehicle accelerations [7]. EM power is being added to the ICE engine full power. That enables a power boost and i.e at the end a ICE engine downsizing in static terms. On the other hand, dynamic transients of ICE torque response can be considered. ICE engine has a slow torque response (usually $\sim$ 200 ms), while the EM has a fast torque response (usually $\sim$ 10 ms). Because of the P2 configuration, and torque summation on the DCT input shaft, E-Boost allows faster torque response of the DCT input shaft and therefore faster vehicle velocity response (shown in figures later). The second important feature of E-boost is the better fuel economy because the ICE engine has small efficiency during fast dynamic responses [14].

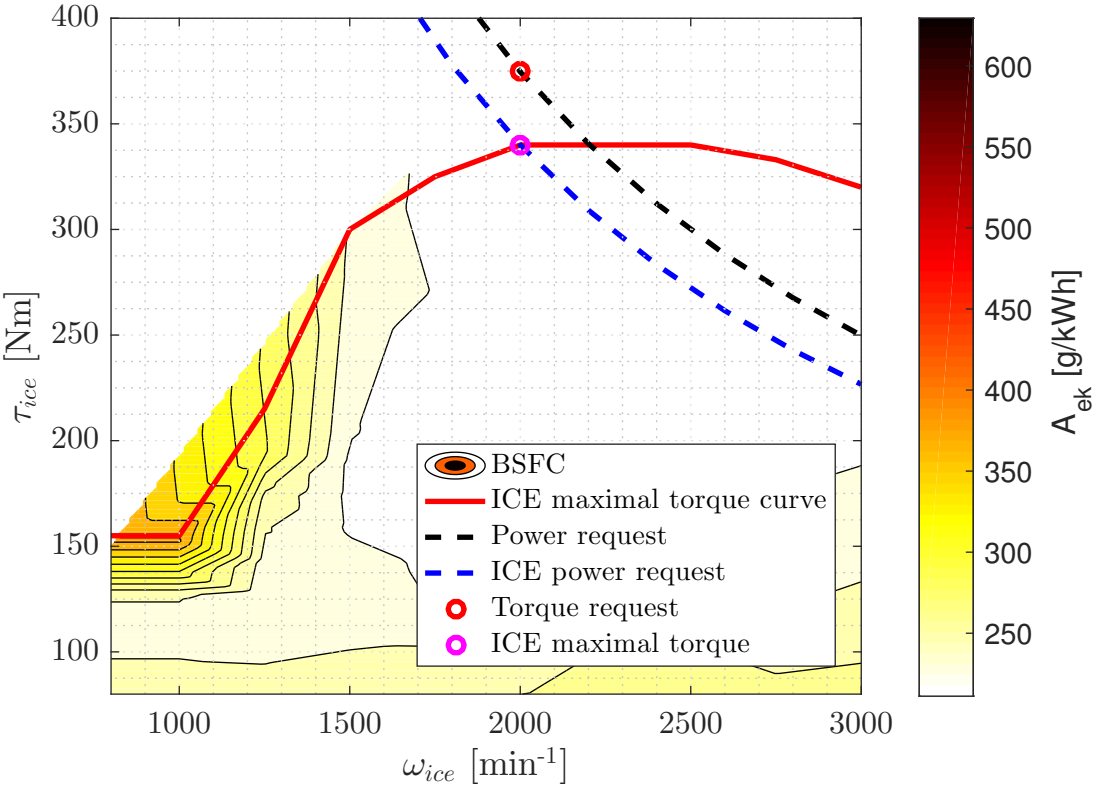

Figure 3.6: E-Boost concept - ICE

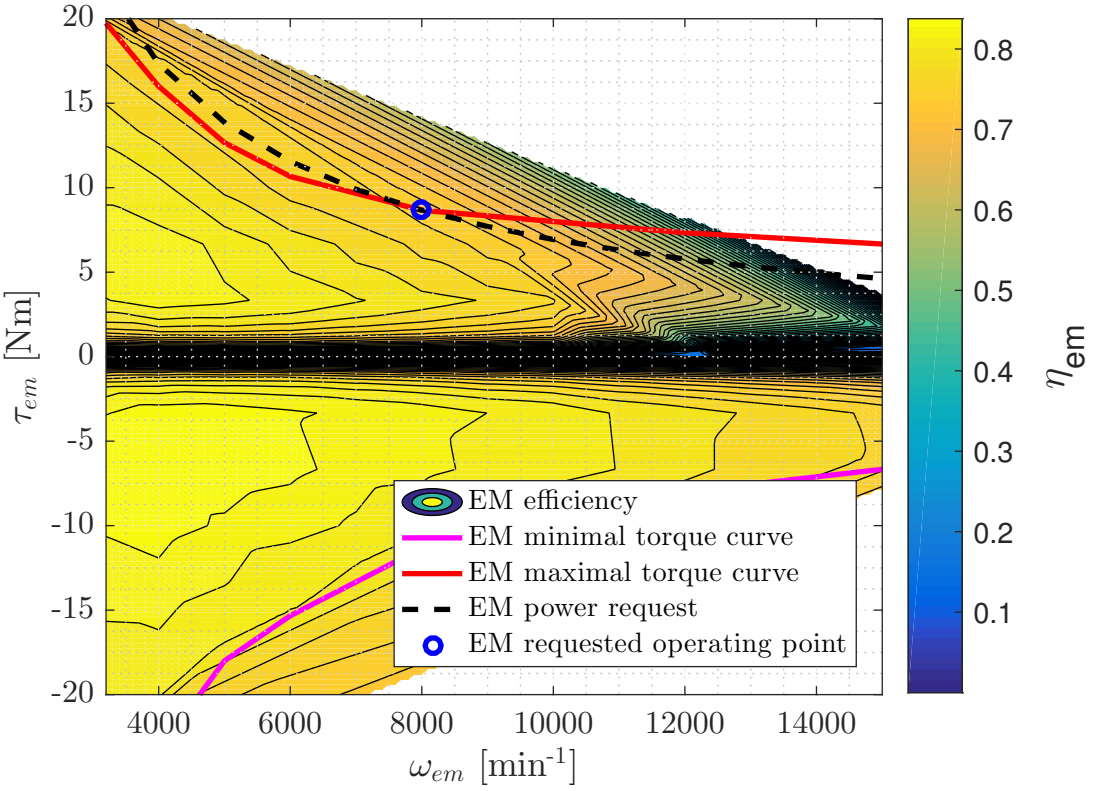

Figure 3.7: E-Boost concept - EM

3.2.2 Implementation

First of all the acceleration pedal travel is observed. If the derivation of acceleration pedal travel crosses a certain threshold, this could be the trigger for the E-Boost functionality activation. In the meantime, the desired torque is calculated. The E-Boost flowchart is shown in figure 3.8. Conditions that are needed to trigger E-Boost functionality are as follows:

- the desired power, P_{des} needs to be higher than the E-Boost available power, $P_{em,E-Boost}\,(SoC)$ (figure 2.13.c),
- derivation of the acceleration pedal travel must be greater than 200 [-] [2] or the acceleration pedal must be fully pressed,
- maximal available EM power must be equal or lower than the $P_{em,eBoost}\,(SoC)$,
- E-Boost start switch must be active.

[2]This threshold was determined empirically.

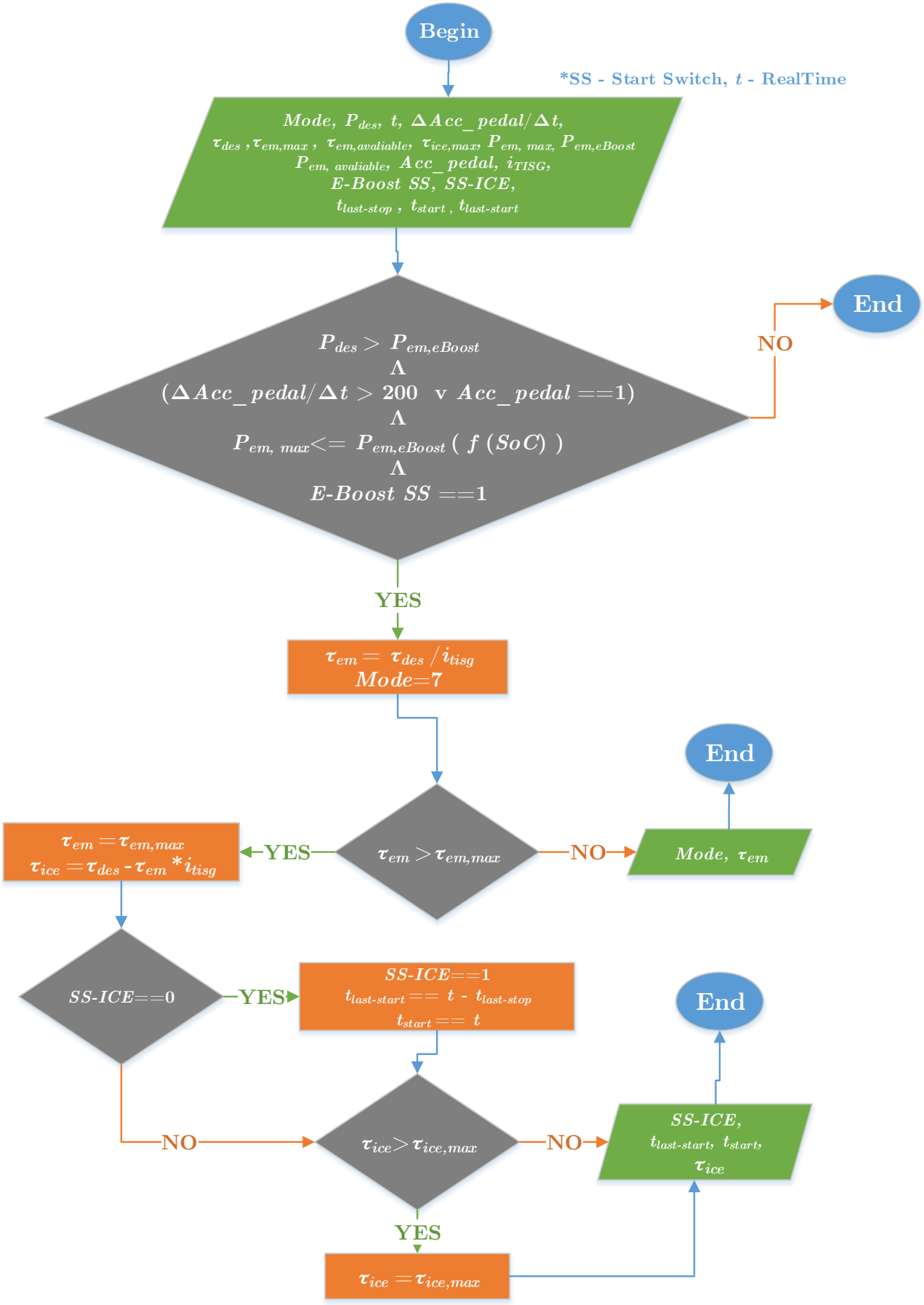

Figure 3.8: E-Boost flowchart

After all the above conditions are satisfied, the powertrain mode is set to:

$$mode = 7, \tag{3.4}$$

and the EM torque is set as follows:

$$\tau_{em} = \frac{\tau_{des}}{i_{tisg}}. \tag{3.5}$$

If the desired EM torque exceeds the EM maximal torque, then the EM torque is set to the EM maximal torque as follows:

$$\tau_{em} = \tau_{em,max}, \tag{3.6}$$

and the ICE torque is defined as follows:

$$\tau_{ice} = \tau_{des} - i_{tisg}\tau_{em}. \tag{3.7}$$

If the desired ICE torque exceeds the ICE maximal torque, then the ICE torque is set to the ICE maximal torque as follows:

$$\tau_{ice} = \tau_{ice,max}. \tag{3.8}$$

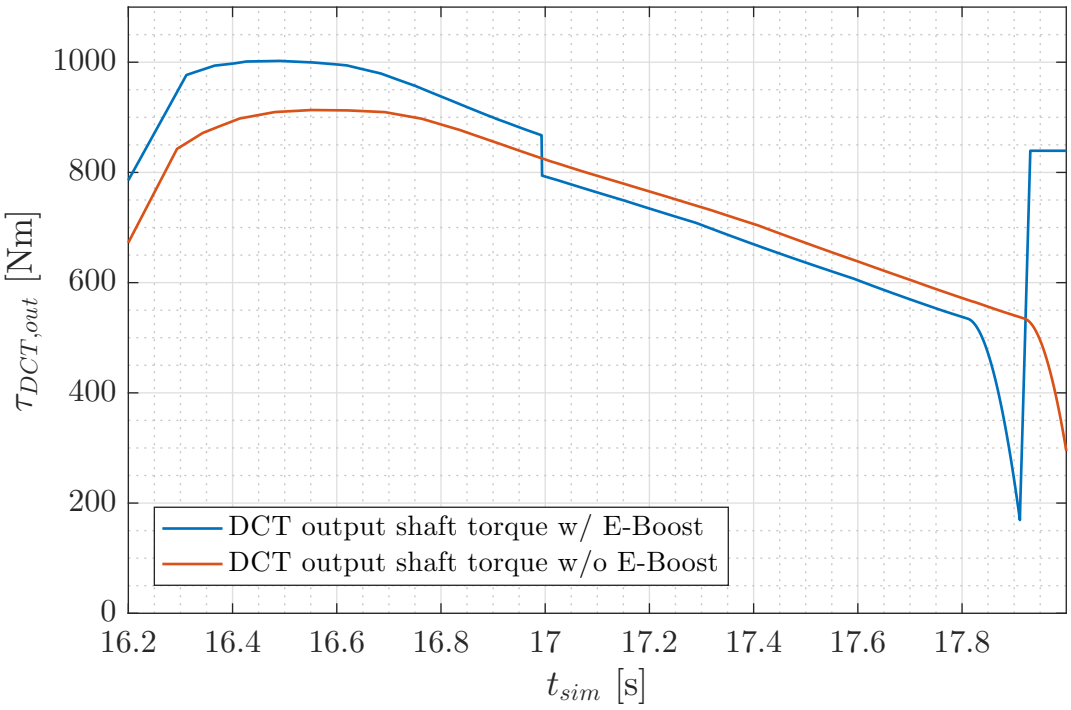

Figure 3.9: E-Boost demonstration - DCT output torque

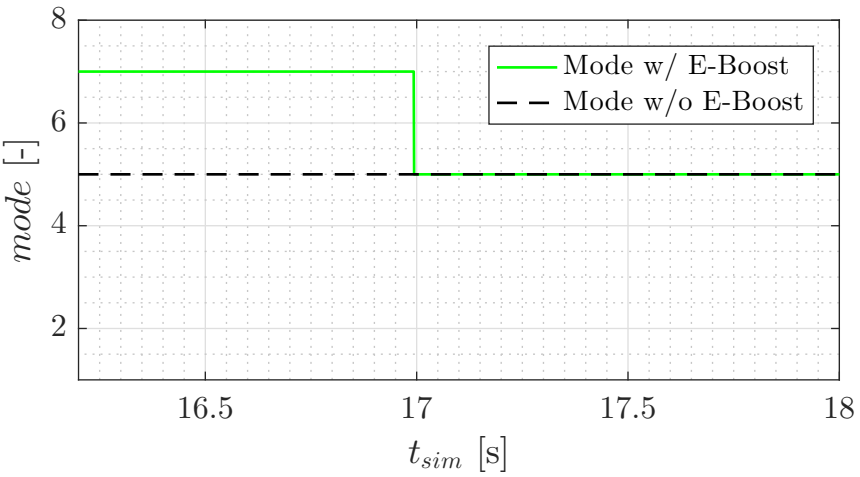

Figure 3.10: E-Boost demonstration - mode

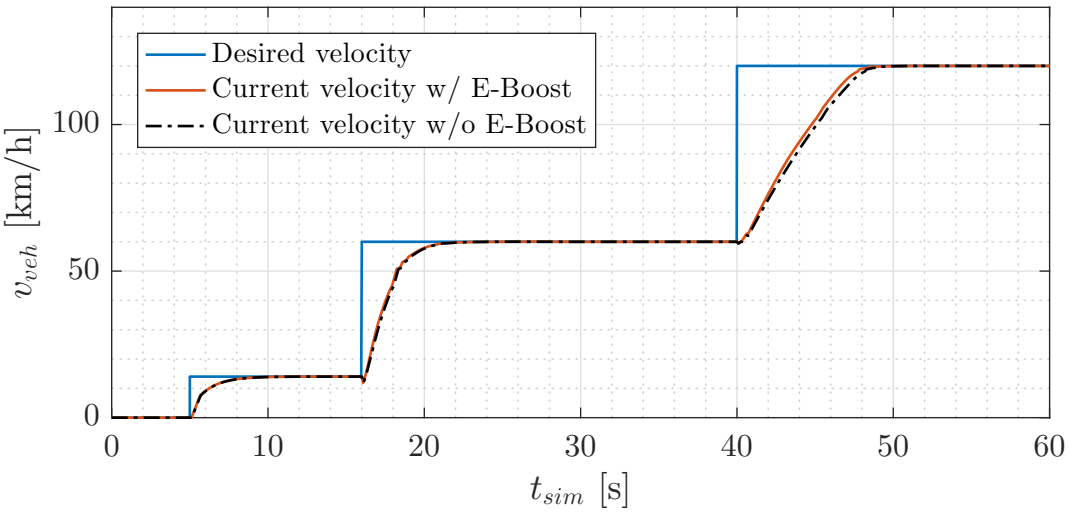

Figure 3.11: E-Boost demonstration - Velocity

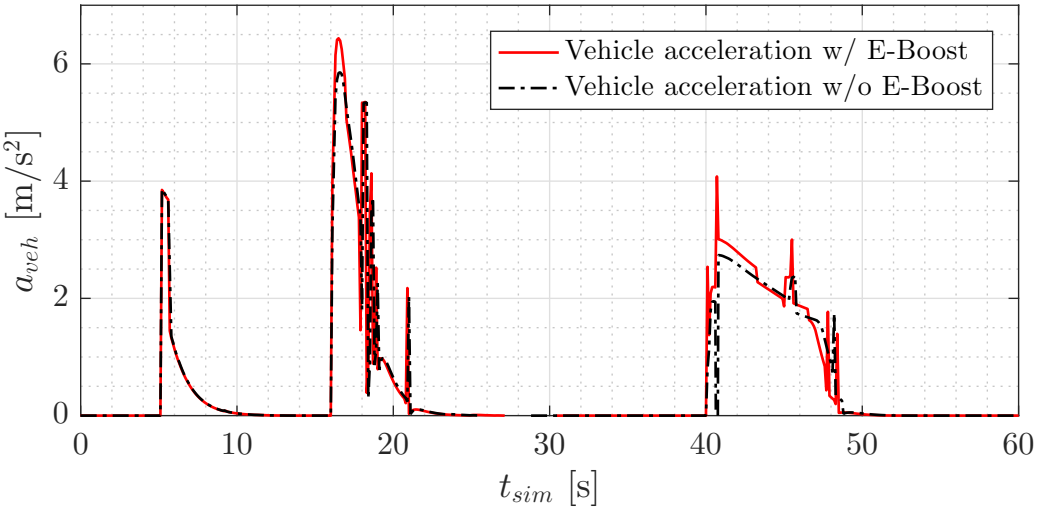

Figure 3.12: E-Boost demonstration - Acceleration

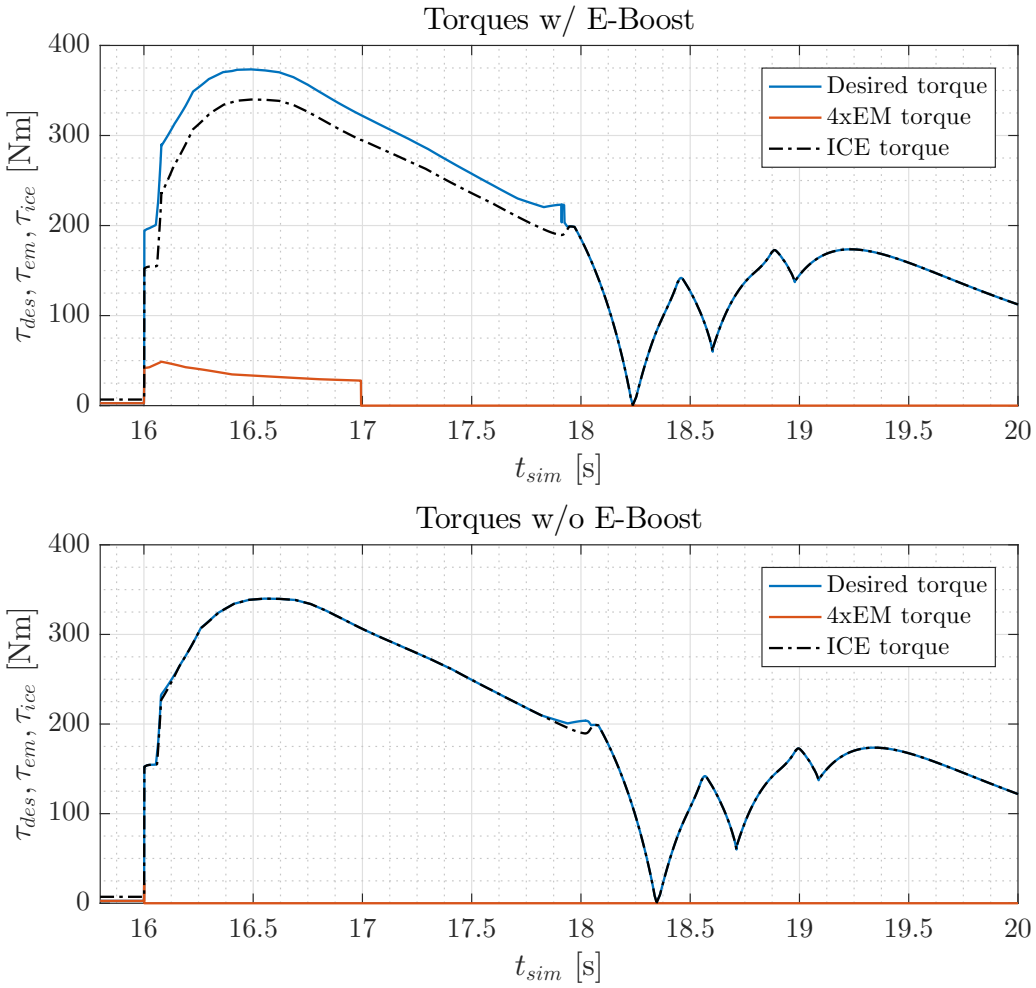

Figure 3.13: E-Boost demonstration - Torques

In figures 3.9 - 3.13 the E-Boost response on MHEV CRUISE ™ model is shown. The test was carried out using step desired velocity input. Figure 3.9 shows that E-Boost provides more torque on the DCT output shaft, in comparison with the case w/o E-Boost functionality, thus enabling the ICE downsizing. Figure 3.10 shows the E-Boost activation. Because of more torque being summed on the DCT input shaft, faster velocity response happens, as shown in the figure 3.11 and 3.12. On figure 3.13 engine torques comparison is given in the case w/ and w/o E-Boost functionality. The E-Boost functionality activates the EM which provides torque and assists the ICE engine in sudden vehicle acceleration (figure 3.12).

On the other hand, the E-Boost response (figures 3.14 - 3.18) was also tested on the Co-Simulation model [3], where the ICE engine has the dynamic transport delay modeled and other dynamic effects. DCT torque response (figure 3.14) is faster by around 180 ms, the exact same amount of time as it takes for ICE engine to provide torque. Similar to CRUISE

[3]The Co-simulation model will be explained later in detail

™ response, in the Co-Simulation model, vehicle velocity also has faster response w/ E-Boost then w/o E-Boost In comparison to CRUISE ™ model, Co-Simulation model shows an even bigger influence of the E-Boost functionality on the powertrain response, because of the dynamic ICE engine model and slower torque response as shown on figure 3.15.

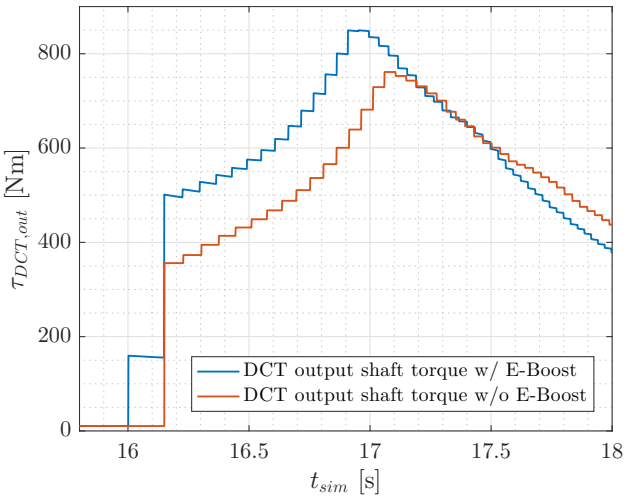

Figure 3.14: E-Boost demonstration - DCT output torque - CoSim

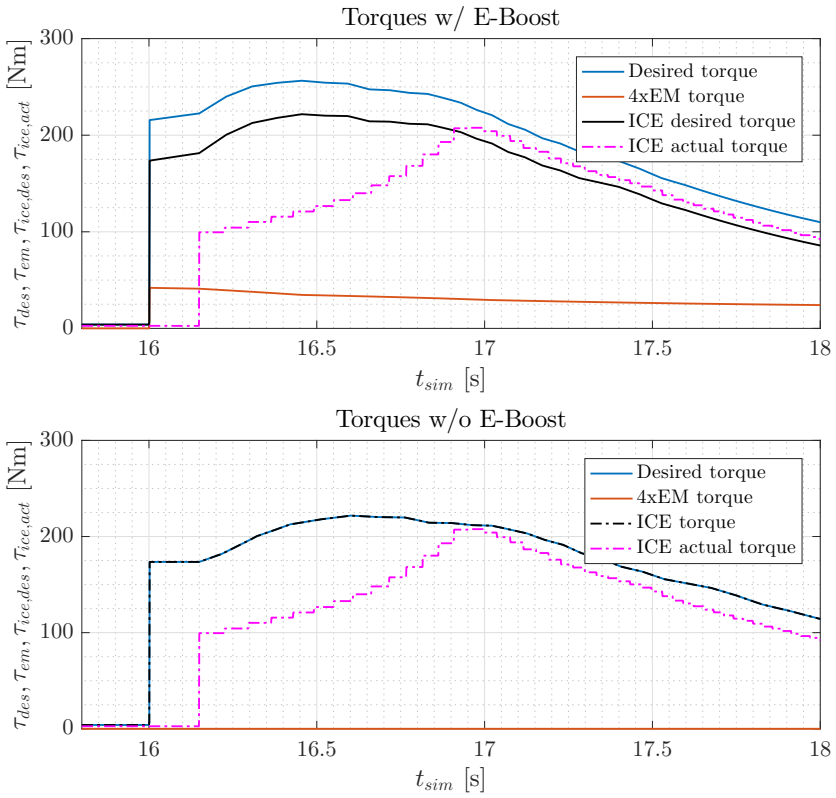

Figure 3.15: E-Boost demonstration - Torques - CoSim

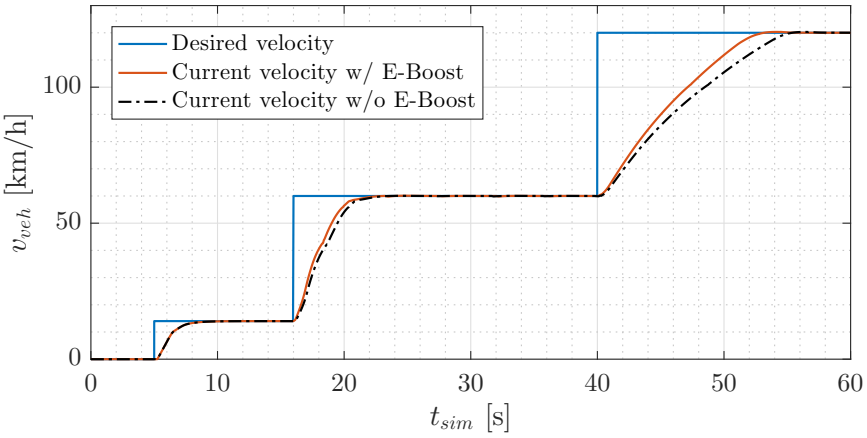

Figure 3.16: E-Boost demonstration - Velocity - CoSim

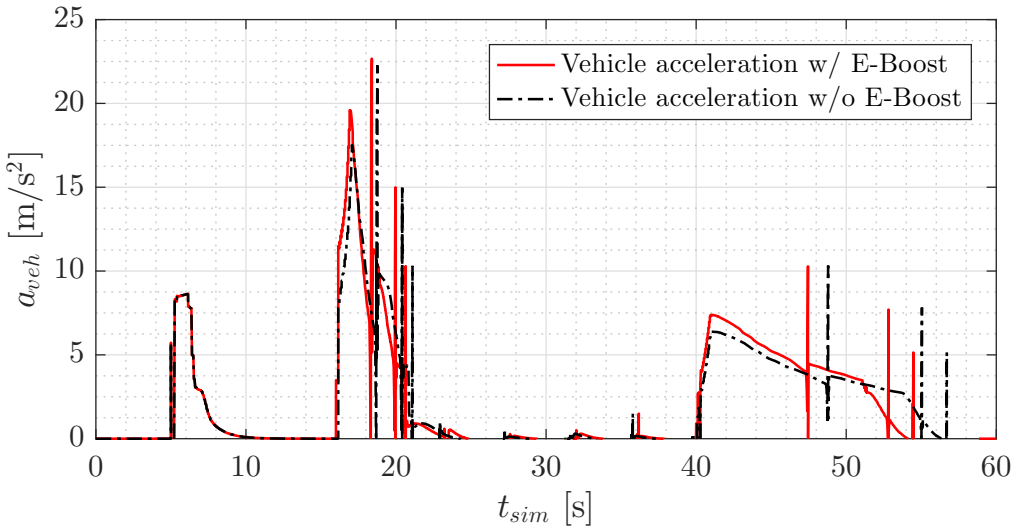

Figure 3.17: E-Boost demonstration - Acceleration - CoSim

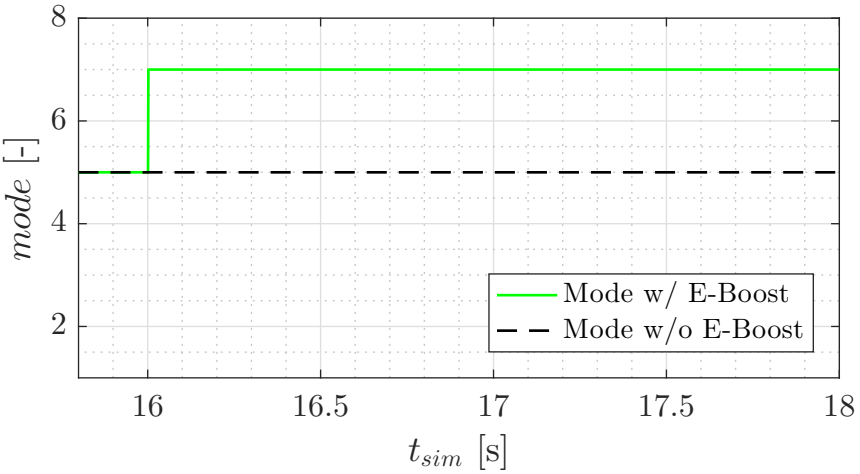

Figure 3.18: E-Boost demonstration - mode - CoSim

3.3 Load Point Moving (LPM)

3.3.1 Concept

Load point moving functionality, i.e. the possibility of moving a powertrain operating point in the torque axis is one of the possible functionalities of MHEV. LPM implies shifting the operating point of the ICE to the area of better efficiency using EM. The default operating point of the drive is achieved by the sum of the torques of ICE and EM with the aim of achieving minimal fuel consumption. With regard to the current operating point of the drive, the ICE operating point may move upwards in the area of better efficiency, whereby the ICE propels the vehicle and with the rest of the torque it charges the battery through the EM, which in this case operates as a generator. Also, the ICE operating point may also move downwards if in the lower areas the ICE has better efficiency, where the EM covers the difference between the required drive torque and ICE torque. Then EM works in motor mode and discharges the battery. This kind of approach is the engine centric control (figure 3.19 and 3.20), where only the ICE efficiency is considered.

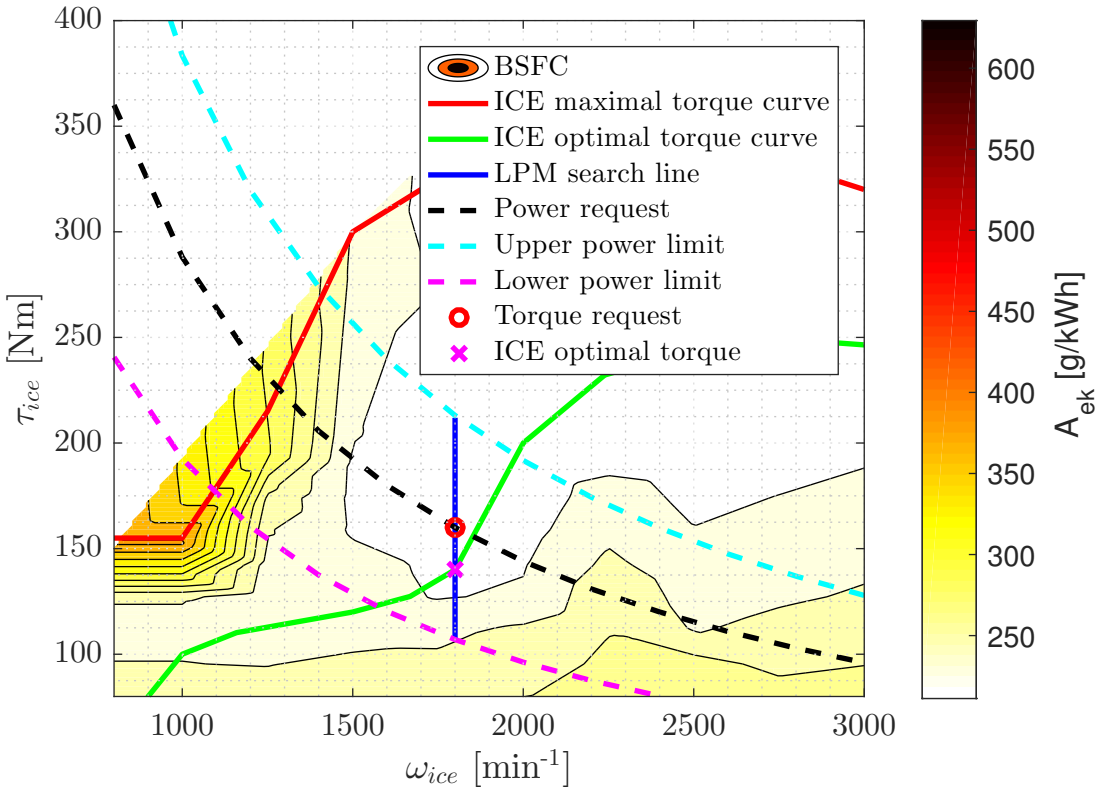

Figure 3.19: LPM engine centric control concept - ICE

In this thesis, the Load point moving will be implemented using the already mentioned

ECMS optimal control criteria (chapter 2.1.4.). In this case, the ICE operating point will not necessarily end up at the ICE optimal fuel consumption curve, but it can end up slightly above or below the ICE optimal fuel consumption operating point because the ECMS control concept considers also the efficiency of the EM.

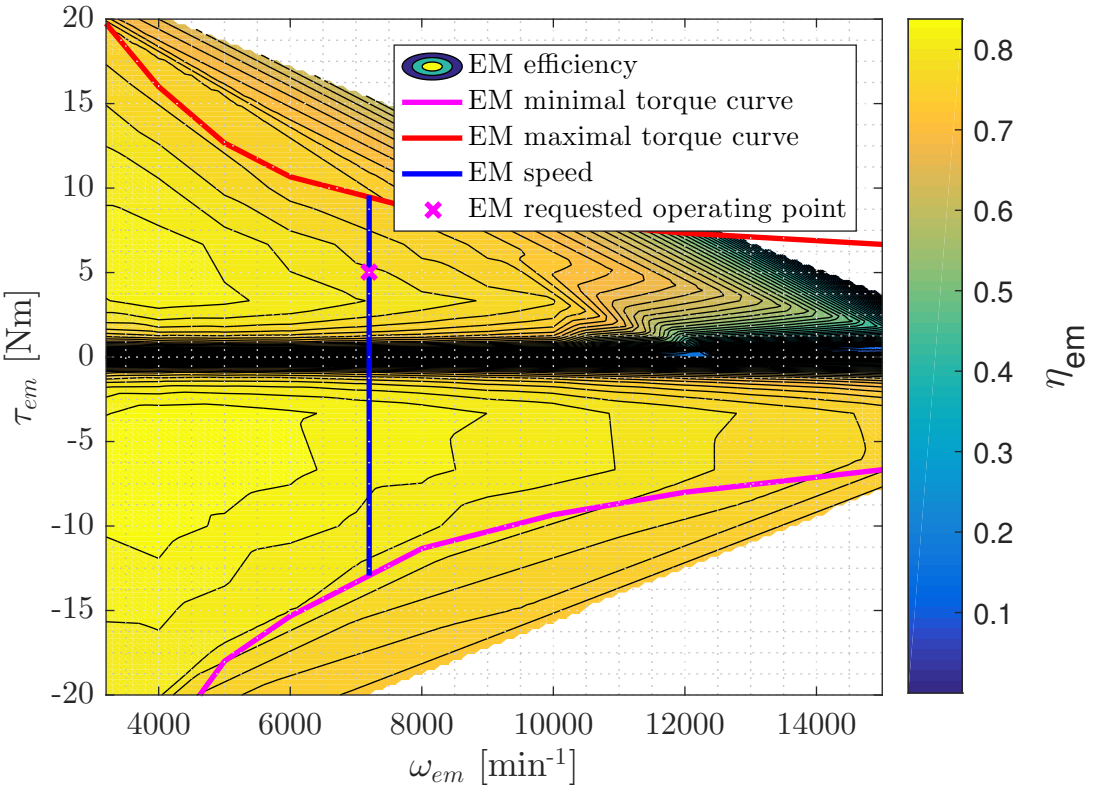

Figure 3.20: LPM engine centric control idea - EM

3.3.2 Off-line optimization implementation

In order to implement the Load point moving strategy on the MHEV model, the ECMS criterion function needs to be defined, and an off-line optimization needs to be carried out. As mentioned before, the optimization will be done based on the developed backward MHEV model. The optimization will be carried out w/o the explicit SoC controller. The explicit SoC controller will be added later.

ECMS criterion function and optimization constraints

Optimization task is to find the optimal ICE engine torque, τ_{ice} which will minimize the ECMS criterion function:

$$minJ = \int_{t_0}^{t_f} \dot{m}_{eq}\left(\mathbf{x}(t), \mathbf{u}(t)\right) dt, \tag{3.9}$$

where the state vector, $\mathbf{x}(t)$ is defined as follows:

$$\mathbf{x}(t) = [SoC(t)]^T, \tag{3.10}$$

and the control vector $\mathbf{u}(t)$ defined as:

$$\mathbf{u}(t) = [\tau_{ice}(t)]^T, \tag{3.11}$$

EM torque is kinematically bonded with the ICE engine torque with the following equation:

$$\tau_{em} = \frac{\tau_{DCT,in} - \tau_{ice}}{i_{tisg}}, \tag{3.12}$$

and the ICE clutch state, Cl_{ice} is defined as follows:

$$Cl_{ice} = \begin{cases} 1, & \tau_{ice} = 0 \\ 0, & \tau_{ice} > 0, \end{cases} \tag{3.13}$$

where the 1 stands for open state and 0 for the closed clutch state. Optimization constraints on the control vector $\mathbf{u}(t)$ are as follows:

$$0 \leq \tau_{ice} \leq \tau_{ice,max}, \tag{3.14}$$

$$\tau_{em,min} \leq \tau_{em} \leq \tau_{em,max}. \tag{3.15}$$

No explicit SoC controller was implemented, but search constraints are defined to ensure SoC sustainability as follows:

$$\tau_{ice} \geq \tau_{des}, \tag{3.16}$$

for SoC lower than 30%, and for SoC greater than 70% :

$$\tau_{ice} < \tau_{des}. \tag{3.17}$$

DIRECT algorithm and point cloud definition

DIRECT or Dividing Rectangle optimization algorithm is a sampling algorithm that requires no knowledge of the criterion function gradient [16]. Instead, the algorithm samples points in the search domain, and uses the information it has obtained to decide where to

search next [16]. A global search algorithm like DIRECT can be very useful when the objective function is a "black box" function or a simulation [16]. That's why this algorithm was chosen to be implemented on the MHEV backward model. For the implementation of

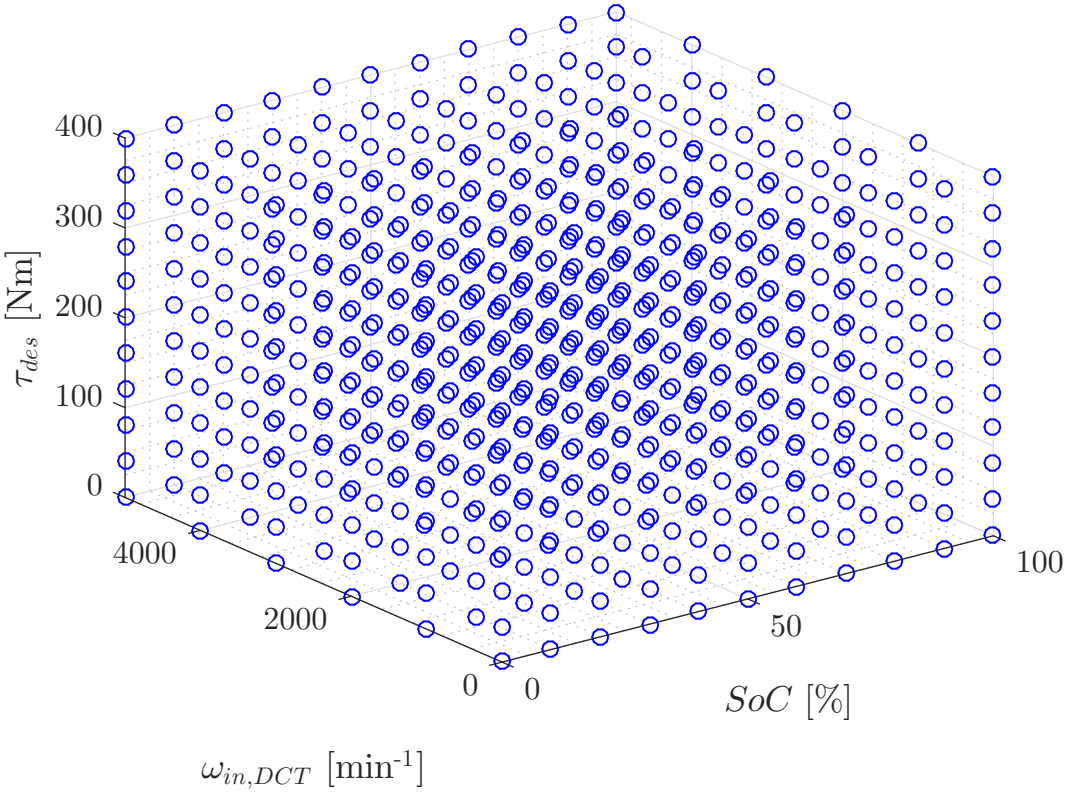

Figure 3.21: Point cloud

DIRECT algorithm, it was necessary to define a 3D point cloud (figure 3.21). For each point, the algorithm calculates the optimal ICE engine torque, τ_{ice}. Mentioned point cloud is a 3D grid that has battery SoC on the x axis, DCT transmission input speed, $\omega_{in,DCT}$ on the y axis and the desired torque, τ_{des} on the z axis. For the better view, a rare point cloud is shown on the figure. Used grid for optimizing purposes has a dimension of $40 \times 10 \times 20$ which makes 8000 points in total.

3.3.3 LPM w/o explicit SoC controller implementation

The result of the optimization is a 4D map that has three inputs, as defined in the point cloud subsection and three outputs. The 4D map scheme is given on figure 3.22. That map is now implemented in AVL CRUISE ^{TM} MHEV model as a "n-Dimensional" table block (figure 3.23).

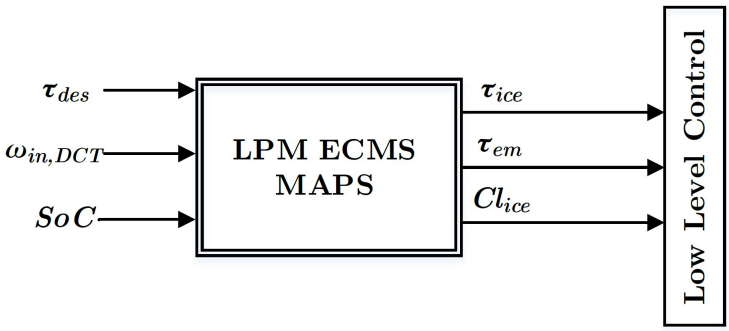

Figure 3.22: 4D map - block diagram

Figure 3.23: nD block in AVL CRUISE ™ environment

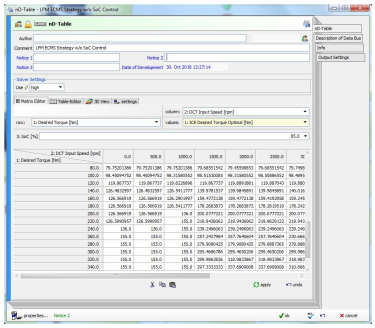

Figure 3.24: nD block properties in AVL CRUISE ™ environment

3.3.4 LPM w/ explicit SoC controller implementation

In the last subsection 3.3.3. , the implementation of LPM ECMS optimal control maps into AVL CRUISE ™ MHEV model. But this approach does not have an explicit SoC controller in the control strategy. The disadvantage of not having a explicit SoC controller is that the control strategy can't ensure the SoC sustainability on the end of the cycle. That's why next to the LPM ECMS maps an explicit proportional SoC controller (figure 3.25) with a dead zone is defined as follows [2, 17, 18]:

$$P_{batt} = \begin{cases} K_P e_{SoC}, & |e_{SoC}| > \Delta SoC \\ 0, & |e_{SoC}| \leq \Delta SoC \\ P_{batt,max}\,\text{sign}\,(e_{SoC}) & |K_P e_{SoC}| \geq P_{batt,max}, \end{cases} \tag{3.18}$$

where the P_{batt} is, in this case, the controller output i.e. the demanded battery power needed

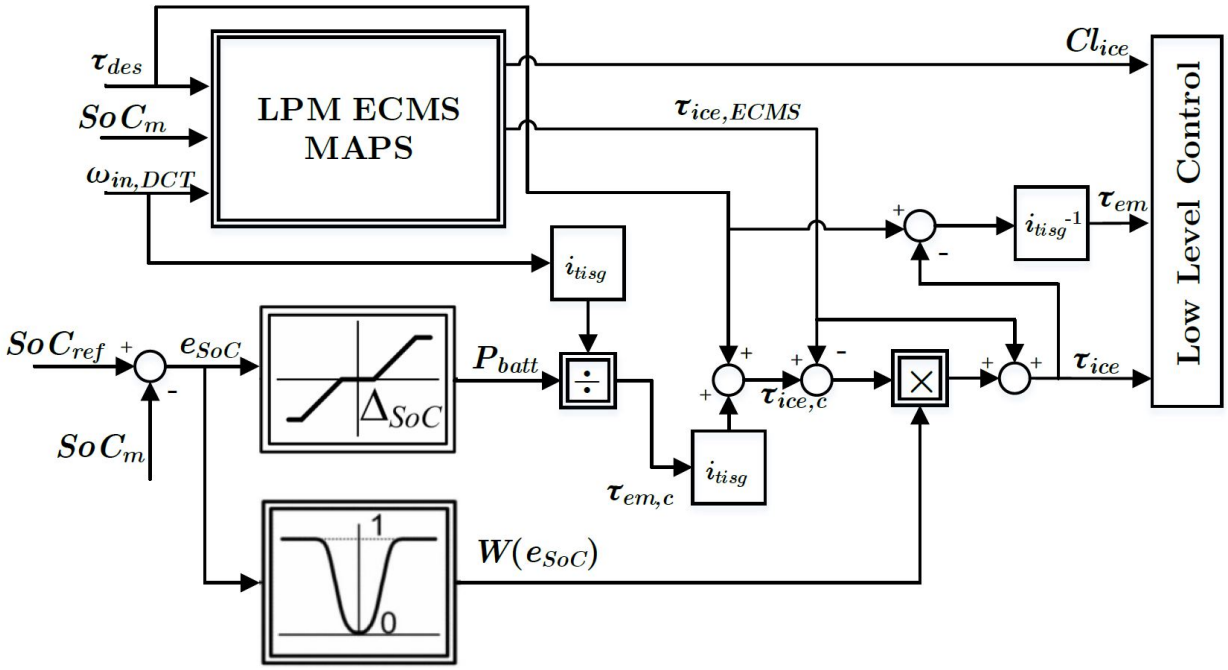

Figure 3.25: LPM w/ SoC controller block diagram

to correct the SoC control error, e_{SoC} is defined by the following equation:

$$e_{SoC} = SoC_{ref} - SoC_m, \tag{3.19}$$

where the SoC_{ref} is the desired battery SoC and in this thesis set to $SoC_{ref} = 50$ %, and the SoC_m is the current SoC. The controller proportional gain is set to $K_P = 500$ W/%, and the controller deadzone is set to relatively high value, $\Delta SoC = 15$ %, because of the relatively small battery capacity. Controller has a saturation that equals $P_{batt,max} = 10000$ W. From the P_{batt}, the desired EM control torque is calculated as follows:

$$\tau_{em,c} = \frac{P_{batt}}{\omega_{in,DCT} i_{tisg}}. \tag{3.20}$$

Next from the driver's desired torque, the desired control ICE torque is calculated:

$$\tau_{ice,c} = \tau_{des} + i_{tisg}\tau_{em,c}. \tag{3.21}$$

Because of the chattering [4] that happens between the SoC controller and the ECMS strategy, a weighting factor W is defined to smooth the transients between the two control strategies

[4] At the borders of SoC the chattering happens because the ECMS and the SoC controller are in conflict at these transient SoC boundary conditions

as follows [2, 17, 18]:

$$W = \begin{cases} |\tanh\left[b_w\left(e_{SoC} + \Delta SoC - \tanh\left(e_{SoC} + \Delta SoC\right)\right)\right]|, & e_{SoC} \leq \Delta SoC \\ 0, & |e_{SoC}| < \Delta SoC \\ |\tanh\left[b_w\left(e_{SoC} - \Delta SoC - \tanh\left(e_{SoC} - \Delta SoC\right)\right)\right]|, & e_{SoC} \geq \Delta SoC \end{cases} \tag{3.22}$$

where the b_w is the bandwidth of the weighting factor. With the implemented weighting

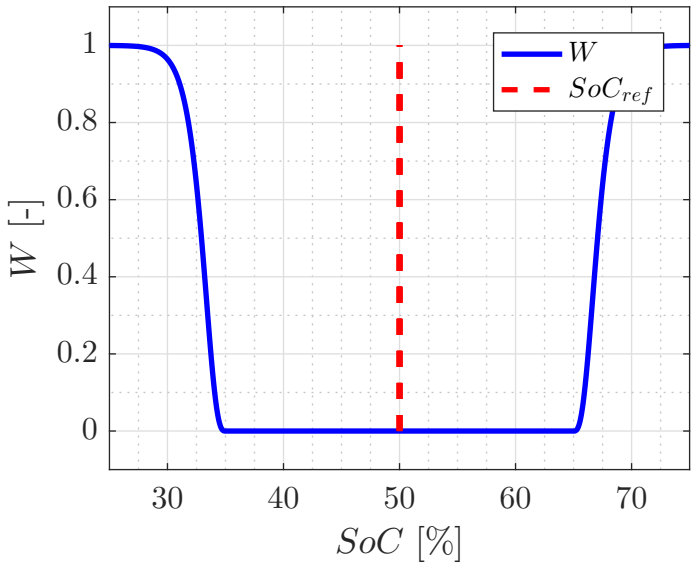

Figure 3.26: Desired SoC and weighting factor

factor, the final ICE torque τ_{ice} is calculated as follows:

$$\tau_{ice} = \tau_{ice,ECMS} + W\left(\tau_{ice,c} - \tau_{ice,ECMS}\right). \tag{3.23}$$

After the final ICE torque calculation, the final EM torque, τ_{em} is calculated the same as in statement 3.12. After all of the torque are calculated, they are saved into a LPM w/ explicit SoC controller "nDimensional" map, similar to the LPM ECMS w/o explicit SoC controller map, explained in the last subsection.

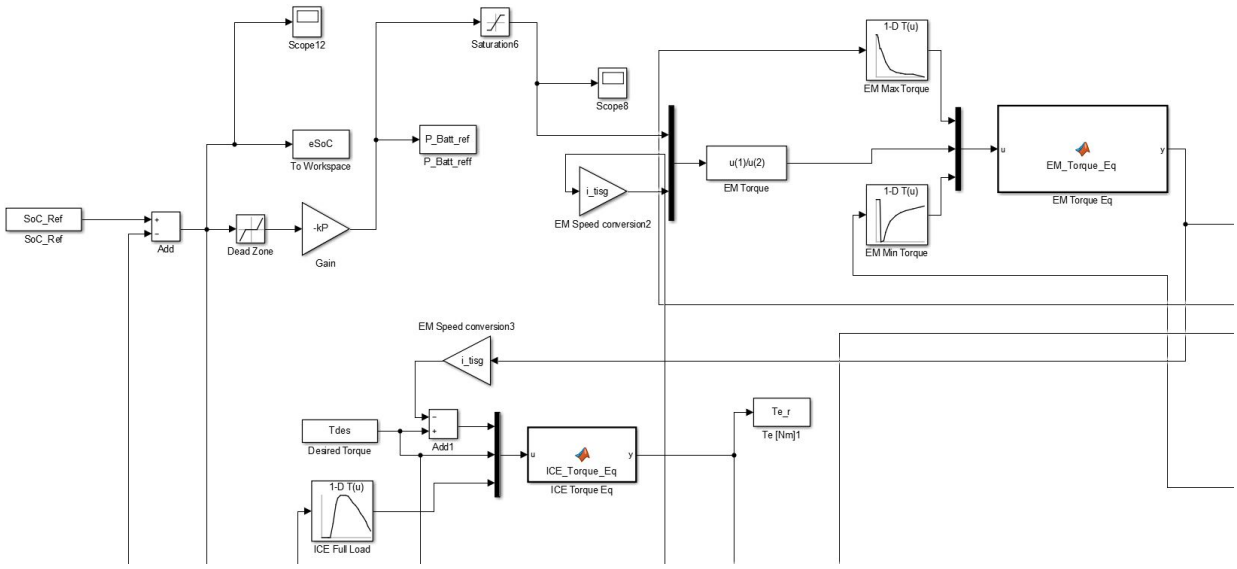

Figure 3.27: SoC controller - MATLAB environment

3.3.5 Demonstration and comparison of the LPM functionality w/ and w/o explicit SoC controller

In figure 3.28 a demonstration of the LPM functionality is shown. As explained before,

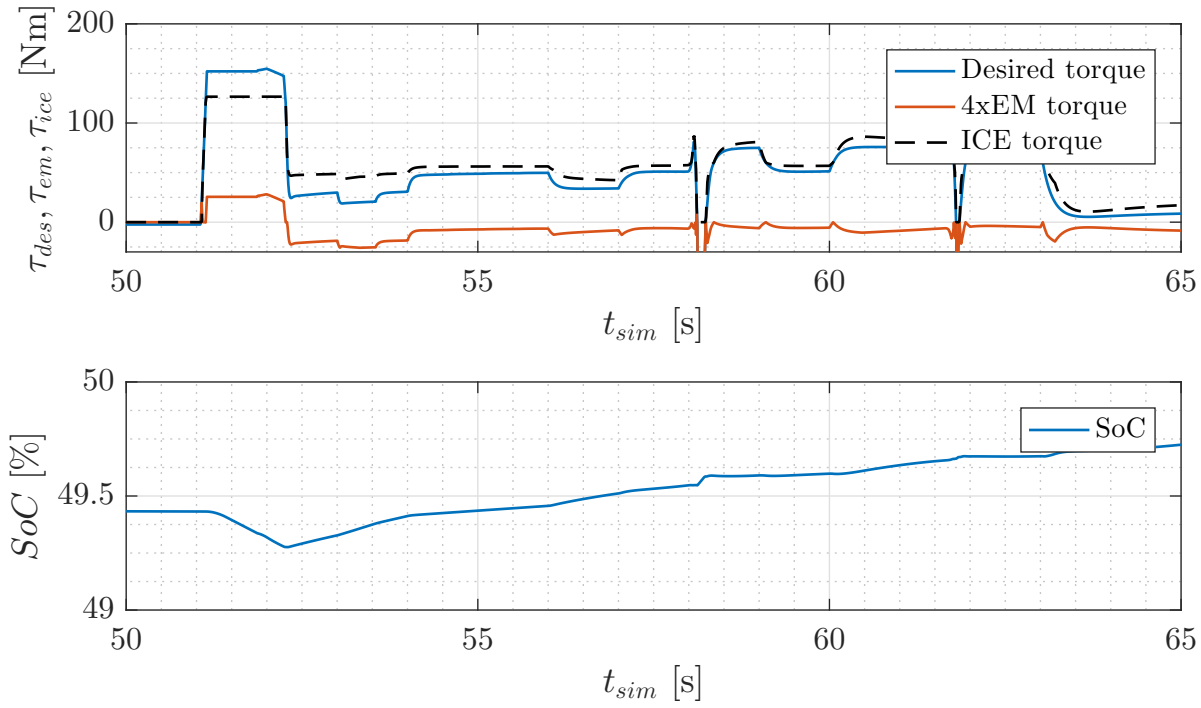

Figure 3.28: LPM demonstration - Torques and SoC

the ECMS strategy calculates the current optimal operating point of the powertrain. As

shown on the figure, at very high loads, the ECMS strategy moves the ICE engine load point to smaller values than demanded and activates the EM that assists the ICE engine in order to provide the torque needed to propel the vehicle. On the other hand, in the case of smaller vehicle loads, the ECMS strategy tends to move the ICE engine load point to higher values in order to provide more torque, so that the vehicle can be propelled and the battery can be charged through the EM, which now operates as a generator. Note that the SoC is around 50% so that the strategy w/ and w/o explicit SoC controller would behave the same. But if the current SoC is out of the dead zone boundaries, then the strategies behave

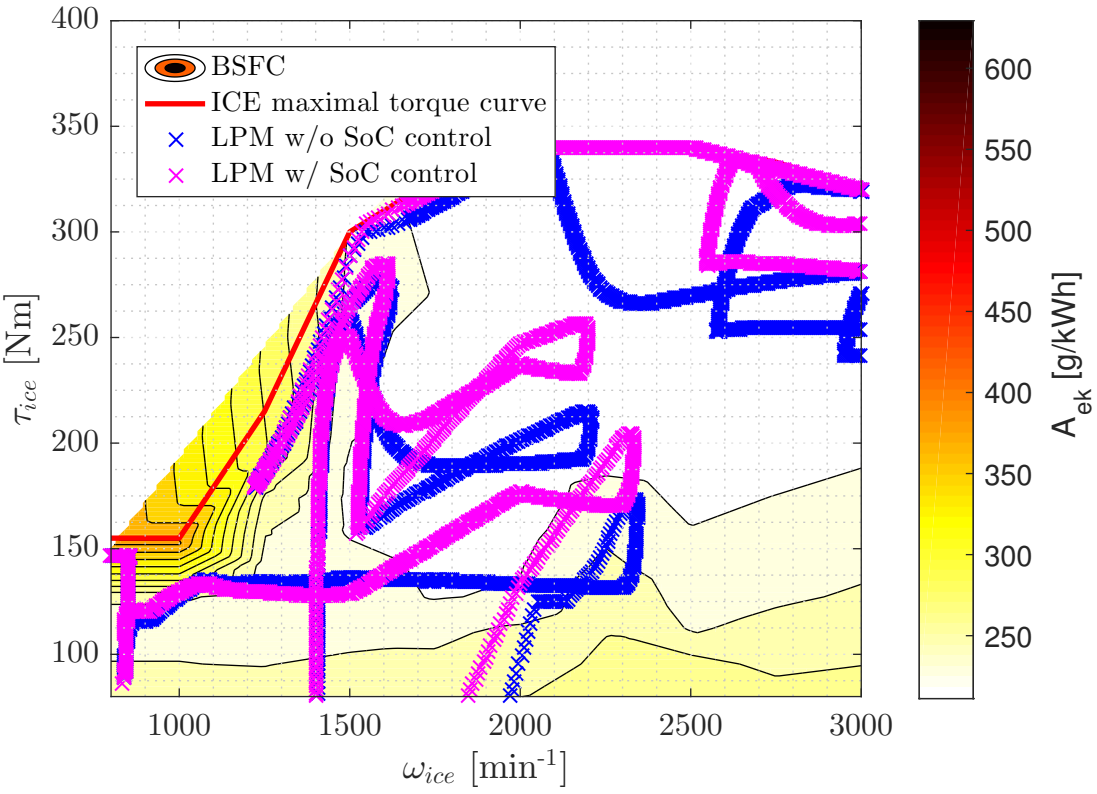

Figure 3.29: LPM comparison - ICE

differently. As shown on the figures 3.29 and 3.30 the comparison between two strategies is given. For this example, a initial SoC was set to 20%. For this simulation, the used cycle was custom defined in order to demonstrate the behavior difference. At very low SoC, the LPM w/o explicit SoC controller does not load the ICE engine a lot in order to recharge the battery as it is in the case w/ the SoC explicit controller. The main difference between those two strategies is that the strategy w/o explicit SoC controller always tends to minimize the ECMS criteria in order to propel the vehicle while the explicit SoC controller sees a large SoC control error and becomes dominant thus forcing the battery charging (figure 3.31).

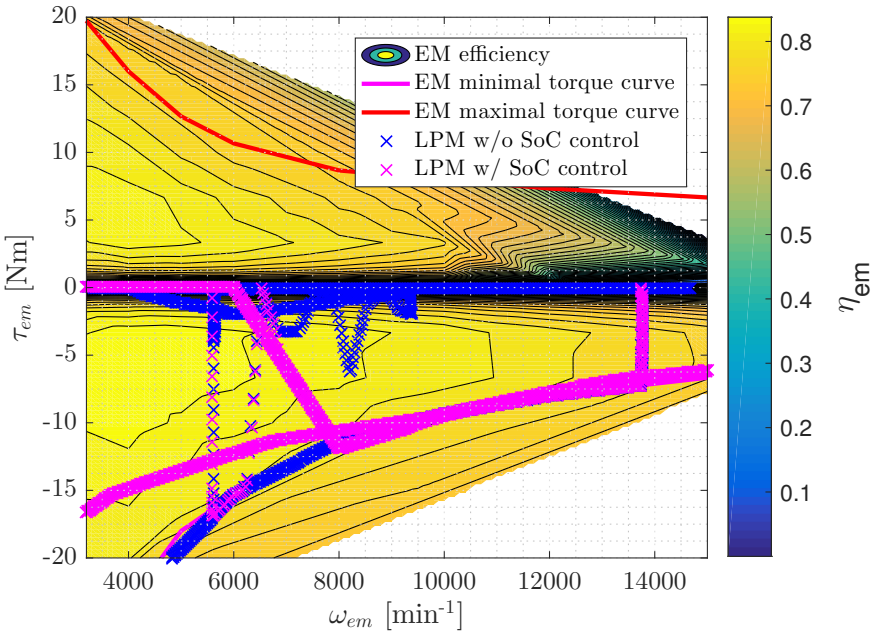

Figure 3.30: LPM comparison - EM

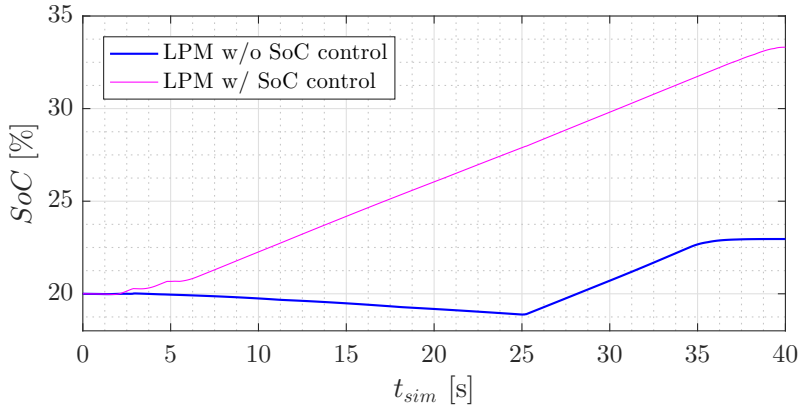

Figure 3.31: LPM comparison - SoC

The LPM functionality logic activation is shown on figure 3.35. The implementation in this thesis is that if the LPM functionality switch is active, then the LPM functionality is active if none of the other functionalities is active.

3.4 Load Point Shifting (LPS)

3.4.1 Concept

The Load Point Shifting functionality is the horizontal extension of the LPM functionality possible with the P2 configuration [2].

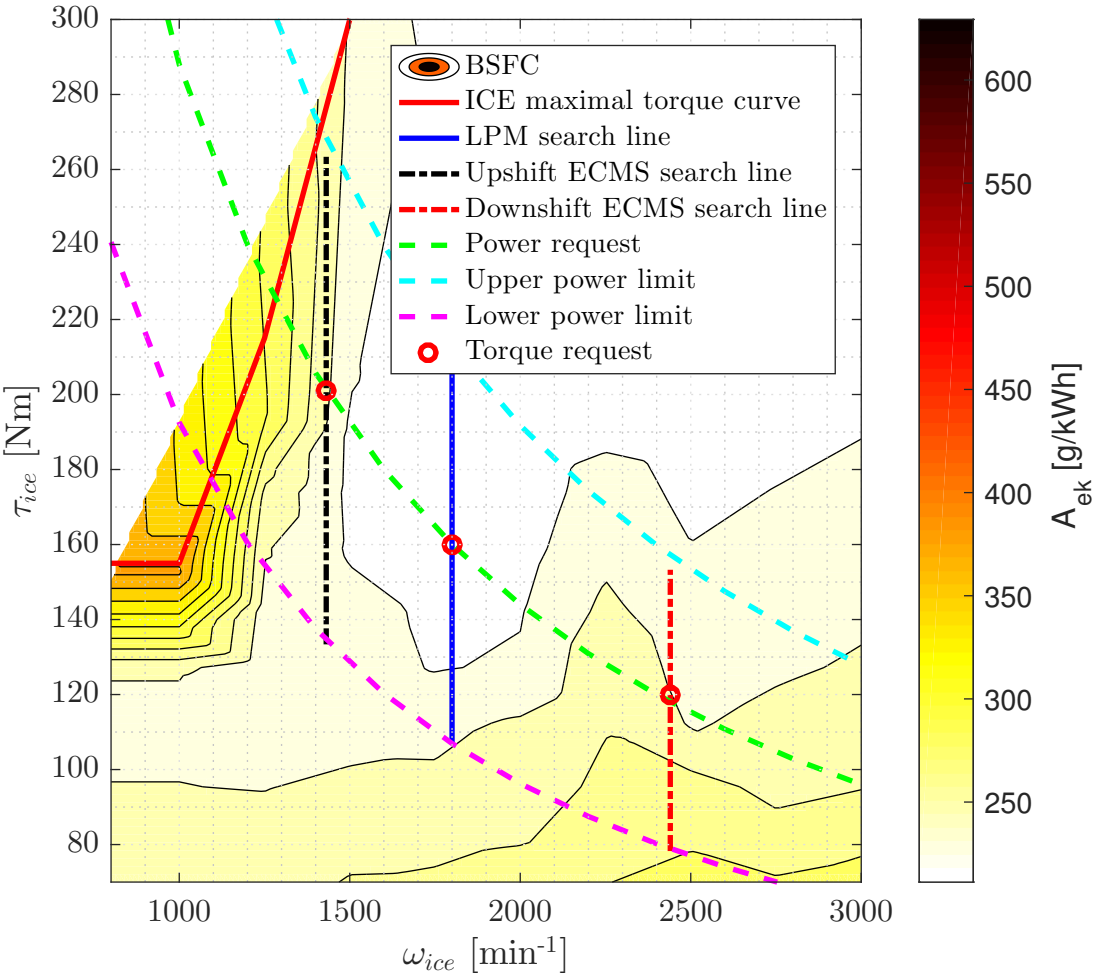

Figure 3.32: LPS concept - ICE

Manipulating the DCT transmission gear shifting program, it is possible to extend the LPM functionality (figure 3.32). By changing the DCT transmission ratio i.e. the current DCT transmission gear, for the same vehicle velocity it is possible to achieve different ICE and EM speeds. The main concept of the LPS functionality is to find the optimal gear ratio and therefore optimal ICE and EM torques in order to reduce fuel consumption.

3.4.2 Implementation

In order to implement the LPS functionality, the new powertrain speeds need to be calculated. First of all, the DCT transmission output shaft speed is defined as follows:

$$\omega_{out,DCT} = \frac{\omega_{in,DCT}}{i_{DCT,curr,gear}}, \tag{3.24}$$

where the $i_{DCT,curr,gear}$ is the current DCT transmission ratio. By changing the gears, the transmission output torque needs to stay the same i.e. the DCT output shaft speed can not be changed. For that reason, the formula for the new powertrain input speed is calculated by that condition. From that condition, the new powertrain input speed i.e. the new DCT transmission input speed is calculated as follows:

$$\omega_{in,DCT,new} = \omega_{in,DCT} \frac{i_{DCT,new,gear}}{i_{DCT,curr,gear}}, \tag{3.25}$$

where the $i_{DCTnew,gear}$ is the new DCT transmission ratio that was requested from the ECMS strategy. Besides that the DCT transmission output speed needs to be satisfied, the desired power can't be compromised. In comparison to LPM, for the implementation of LPS functionality, in the developed ECMS strategy maps, one additional column was added. That column is the equvialent fuel mass, m_{eq} data for every powertrain operating point. In order to fully implement the LPS on the MHEV powertrain model in every time

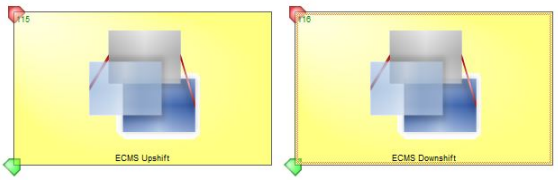

Figure 3.33: LPS nD maps in AVL CRUISE ™ environment

step the powertrain ICE engine torques, EM torques and the m_{eq}, for each ICE and EM ordered pair torques, are being calculated. In the mean time the gear shifting program decides which DCT gear will be next. For the LPS strategy to decide which gear will be next, all of the above mentioned data need to be available. The LPS strategy does the comparison between the current LPM m_{eq}, the ECMS upshift, $m_{eq,upshift}$ and the downshift, $m_{eq,downshift}$ and having in mind the decided gear from the gear shifting program, decides which gear will be next. In order to reduce frequent gear changes, the scaling factor C is introduced which multiplies the upshift and downshift, m_{eq} and only

when the m_{eq} for the upshift or downshift decision is acceptable then the LPS makes the change (figure 3.34). The scaling factor was set empirically to $C = 1.1$ and implemented

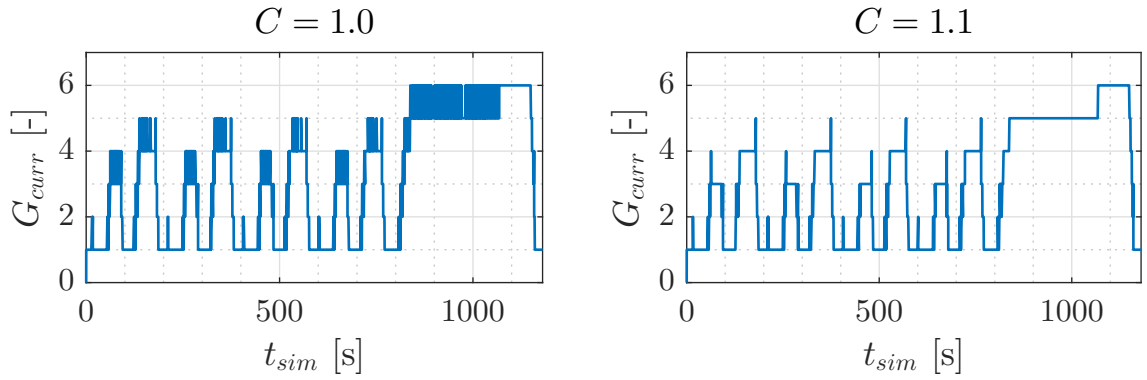

Figure 3.34: LPS scailing factor comparison

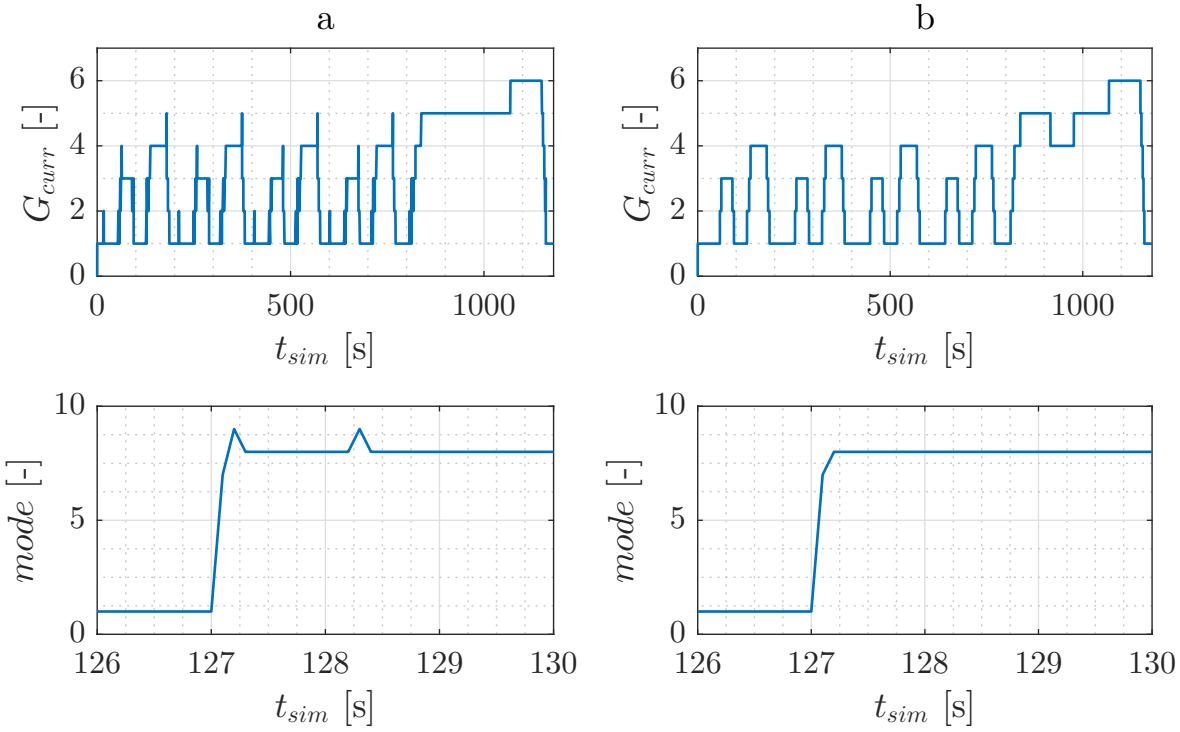

Figure 3.35: LPS (a) and LPM (b) demonstration

as follows:

$$G_{new} = \begin{cases} upshift & Cm_{eq,upshift} \leq m_{eq}, \\ curr & m_{eq} < Cm_{eq,upshift} and m_{eq} < Cm_{eq,downshift}, \\ downshift & Cm_{eq,downshift} \leq m_{eq} \end{cases} \tag{3.26}$$

where the G_{new} is the new desired gear from the LPS strategy. Since the LPS is the extension of the LPM functionality then it also decides the ICE desired torque as follows:

$$\tau_{ice} = f\left(\tau_{ice,ECMS}, G_{new}\right), \tag{3.27}$$

and analogue the EM torque:

$$\tau_{em} = f\left(\tau_{em,ECMS}, G_{new}\right). \tag{3.28}$$

In figure 3.36 the LPM and LPS flowchart is given. On the flowchart it is shown that the LPS functionality depends on the LPM start-switch functionality as well. If the LPM functionality switch is not active, then the LPS functionality can't be activated. Also on the flowchart is shown that if none of the before described functionalities are active, then regarding the LPM functionality start-switch the LPM is active. If the LPM start-switch is not active, then the powertrain is in the conventional mode, in other words, if the the LPM start-switch is active, then the powertrain's default mode becomes LPM as it replaces the conventional driving mode. The figure 3.35 shows the comparison between the LPS and the LPM functionality. The "a" side shows the desired gear change i.e. the activation of the LPS functionality.

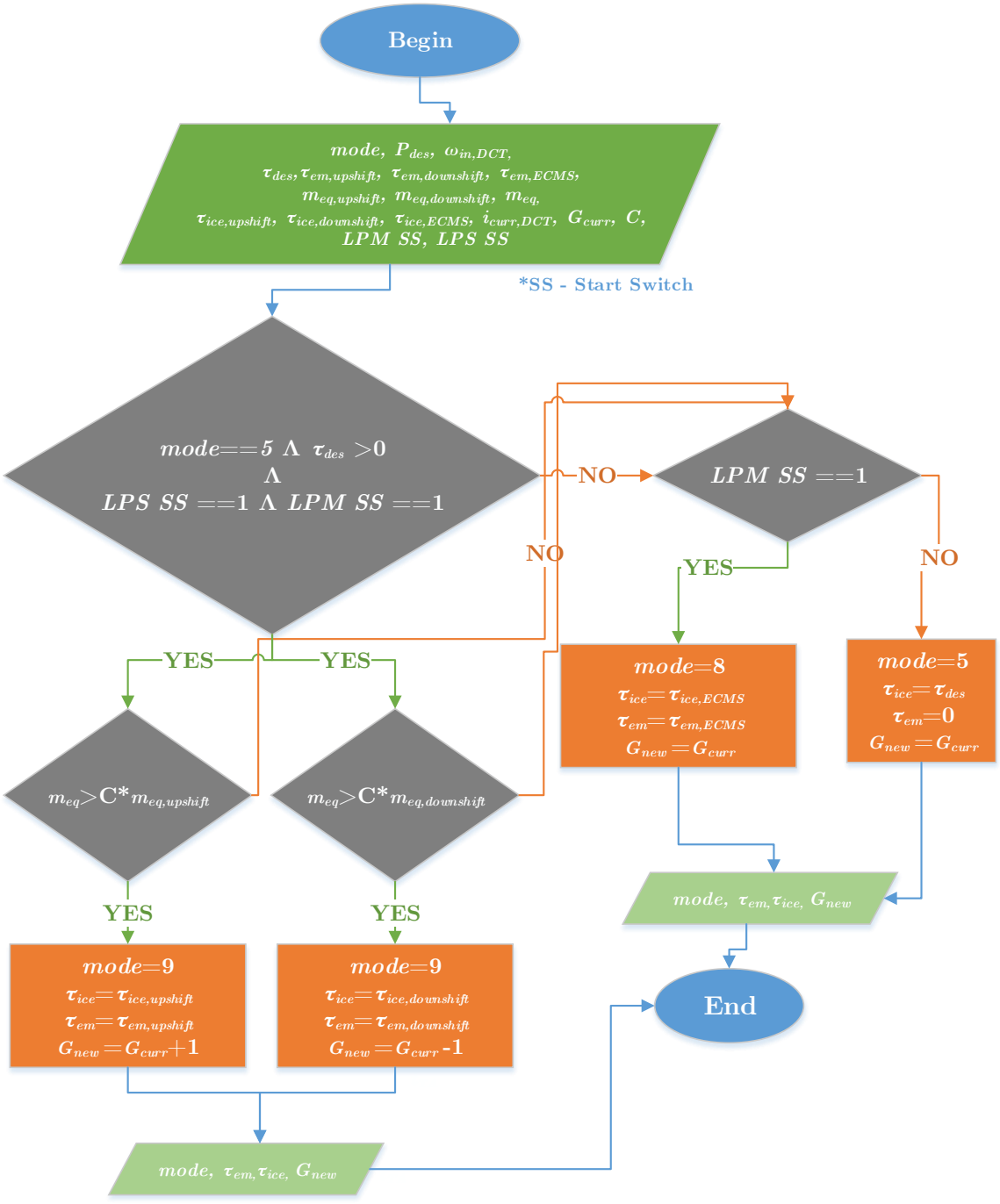

Figure 3.36: LPM and LPS flowchart

Chapter 4

Integration and control strategy validation

In this chapter, the MHEV CRUISE ™ model control strategies will be examined on several certification driving cycles where the overall fuel consumption and SoC will be calculated and compared between the active functionalities.

4.1 Control strategies integration

4.1.1 Individual functionality selection and integration

The previously described control strategies were developed and implemented separately into the MHEV model. Now the task is to integrate all of the developed functionalities into one strategy and examine their response on several certified driving cycles. Each of the functionality has its ID number, *mode* as shown on the table 4.1. The selection of active functionalities is also implemented. On figure 4.1 the functionality transition graph is

mode	Functionality
1	E-Creep
2	E-Sailing
3	E-Coasting
4	Regenerative Braking
5	Conventional mode
6	Torque Assist
7	E-Boost
8	Load Point Moving
9	Load Point Shifting

Table 4.1: Functionalities ID - mode

shows. More detailed flow charts of the each functionality activation conditions were given in previous chapter 3.

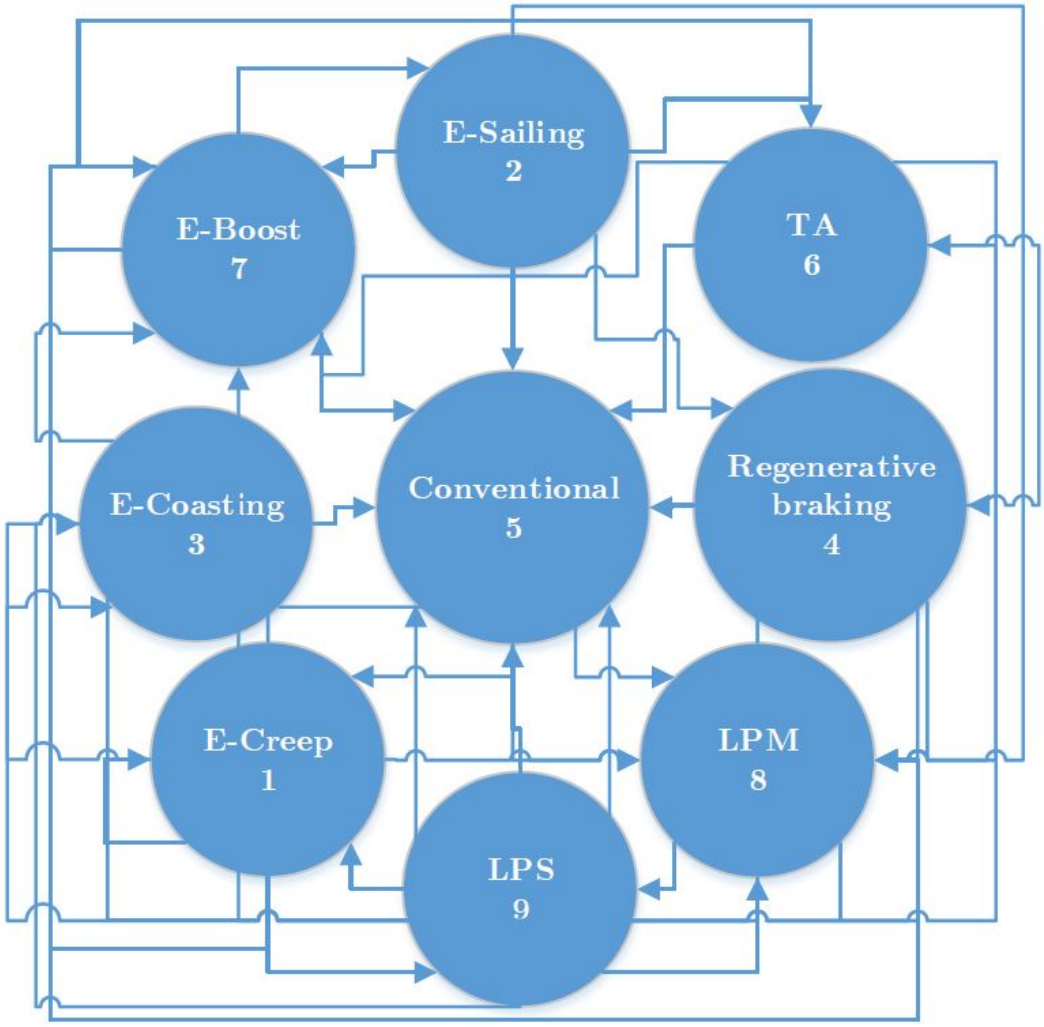

Figure 4.1: Functionalites transitions graph

4.1.2 'Compact' strategy

In addition to the developed functionalities and their integration, a 'compact' strategy was developed in order to test if the separated functionalities with switcher activation behave better or worse than the one strategy that compactly has several functionalites blended into one n-Dimensional map. That strategy has LPM functionality as a base. The strategy also includes Regenerative braking, E-Drive and the newly developed start-stop functionality through a 'Rule-based' controller platform. As before two models are developed,w/ and w/o explicit SoC controller respectively. Next subsection covers the logic for the 'Rule-based' start-stop functionality that differs from the E-Creep in the means of start-stop rules.

For example, the E-Creep functionality start-stop has a current gear and ICE temperature condition that doesn't allow the engine shut down.

Start-Stop development

The start-stop functionality is a developed 'Rule-based' controller that goes with the 'compact' n-Dimensional map. The start-stop functionality follows these rules:

- desired power,P_{des} must be smaller than $P_{min} = 9000$ W,
- SoC must be over 20%,
- acceleration pedal must be unpressed and the brake pedal must be pressed,
- vehicle velocity, v_{veh} must be zero,

for engine stopping, but for starting the rules are:

- desired power, P_{des} must be larger than the $P_{max} = 11000$ W,
- vehicle velocity, v_{veh} must be larger than zero
- current gear, G_{curr} must be greater than one or the current gear, G_{curr} can be equal to 1, but the acceleration pedal travel must be greater than 0.8
- brake pedal must be unpressed.

The fuel consumption comparison between the 'compact' strategies and the separately developed functionalities will be given in the following subsections.

4.2 Fuel consumption correction

In order to account for variations in final battery SoC when comparing performance of different control strategies, a fuel consumption correction is introduced [13]. That kind of fuel consumption definition gives the more realistic result of comparison between the conventional control strategy and the developed hybrid control strategies. Fuel consumption correction is carried out in a way that the initial SoC, $SoC_{initial}$ and the final SoC, SoC_{final} were calculated and subtracted for different driving cycles and different SoC initial conditions. From that comparison, a interpolation line between the calculated fuel consumption for every case was calculated. On figure 4.2 the actual fuel consumption difference is shown. From that

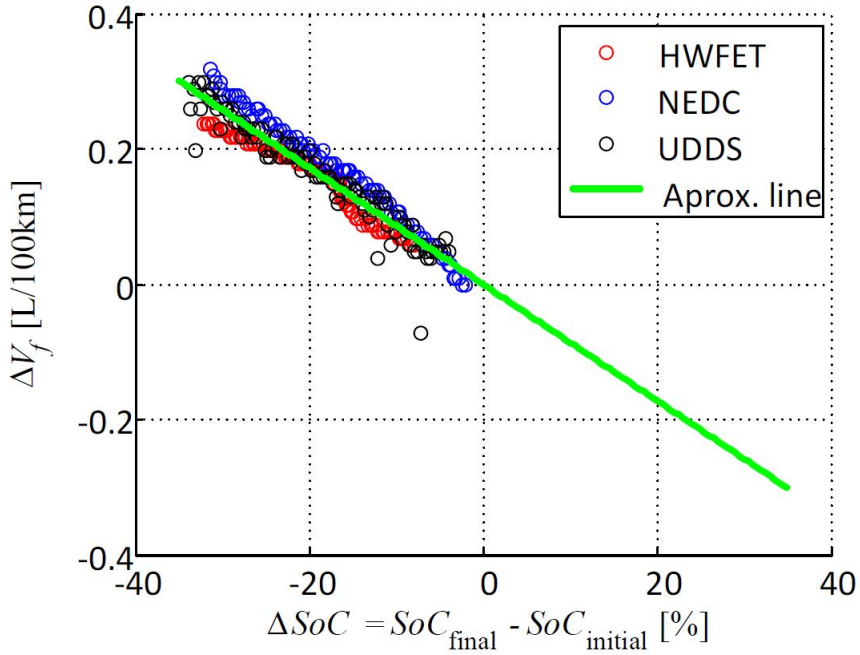

Figure 4.2: SoC variation dependecy on actual fuel consumption difference

interpolation a scaling factor, $k = 0.0087$ was produced. The corrected fuel consumption, $V_{f,corr}$ is defined as follows:

$$V_{f,corr} = V_f - k\,(SoC_{final} - SoC_{initial})\,, \tag{4.1}$$

where the V_f is the actual fuel consumption.

4.3 Certified driving cycles

A driving cycle commonly represents a set of desired vehicle velocites in function of time [19]. It is used to assess fuel consumption and emissions of a vehicle, so that different vehicles can be compared and analysed [19]. When the real vehicle is developed, the driving cycle is performed on a chassis dynamometer, where tailpipes emissions of the vehicle are collected and analyzed to assess the emissions rates [19]. In this thesis the gas emissions and fuel consumption will be simulated and tested on these driving cycles (figure 4.3) :

- NEDC - New European Driving Cycle (a)
- WLTP - Worldwide Harmonised Light Vehicle Test Procedure (b)
- US06 - Supplemental Federal Test Procedure (c)

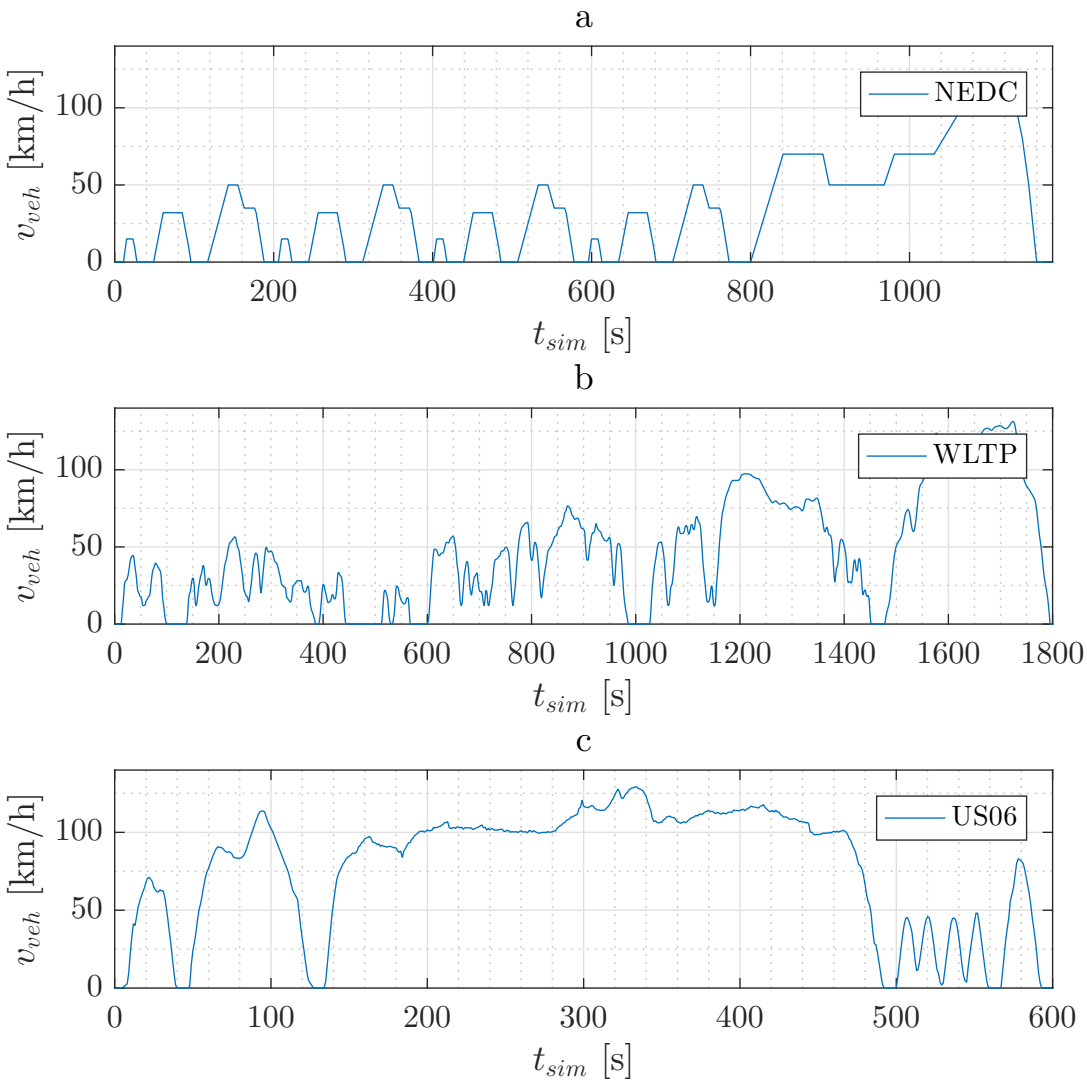

Figure 4.3: Certified driving cycles

In the following sections the fuel consumption analysis will be shown. The vehicle mass equals 1779 kg.

4.4 NEDC driving cycle

The NEDC is used as reference cycle for homologating vehicles until Euro6 norm in Europe and some other countries [19]. This cycle is criticized by many experts because it does not represent real life driving conditions. There are a lot of stopping and constant speed cruising. Also, accelerations are not that steep. That's why it is impossible to obtain certified values with the NEDC cycle when driving with the vehicle in real conditions [19]. For those reasons, a solution to replace the NEDC is being explored by European authorities [19]. The WLTP will probably appear for the upcoming norm Euro7 [19]. Regardless of that, the NEDC cycle is still valid and its purpose is to test the fuel consumption and gas

emissions. That's why the results for this cycle will be shown. Now the simulation results for NEDC cycle follow. Strategies were simulated for three initial battery SoC values:

- $SoC_{initial} = 30\%$
- $SoC_{initial} = 50\%$
- $SoC_{initial} = 90\%$

4.4.1 NEDC - $SoC_{initial} = 30\%$

Vehicle response with the Overall hybrid strategy (E-Creep + Sailing + Coasting + TA + E-Boost + LPM + LPS) including the explicit SoC controller will be shown on few following figures. On figure 4.4 the vehicle velocity response is shown. The figure shows that the drivability with the Overall hybrid strategy was not compromised. Figure 4.5

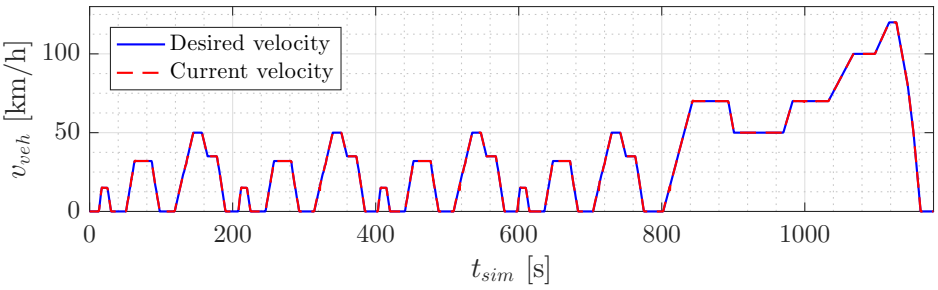

Figure 4.4: Overall strategy response - Velocity - $SoC_{initial} = 30\%$ - NEDC

shows that the vehicle for the most part of the cycle operates in the LPM functionality. Also a lot E-Creeping is noticed throughout the cycle because there are a lot of vehicle stops defined in the cycle. Figure 4.6 shows the battery SoC throughout the cycle. The

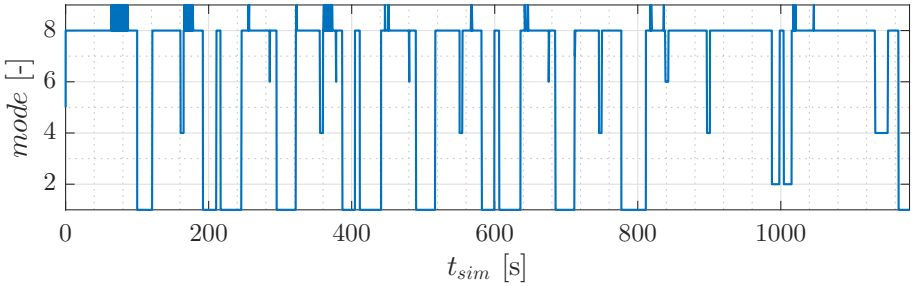

Figure 4.5: Overall strategy response - Modes - $SoC_{initial} = 30\%$ - NEDC

battery SoC was rising through almost the whole cycle because the LPM tends to charge the battery because of the SoC control error. But at the end of the cycle when the battery

SoC reaches the allowed SoC dead zone and the high vehicle velocity becomes constant, the Sailing functionality gets activated and discharges the battery, but the Regenerative braking functionality charges the battery at the end of the cycle so that the final SoC equals 48.43%. In the figure 4.7 is shown that the activation of the TA functionality. In the

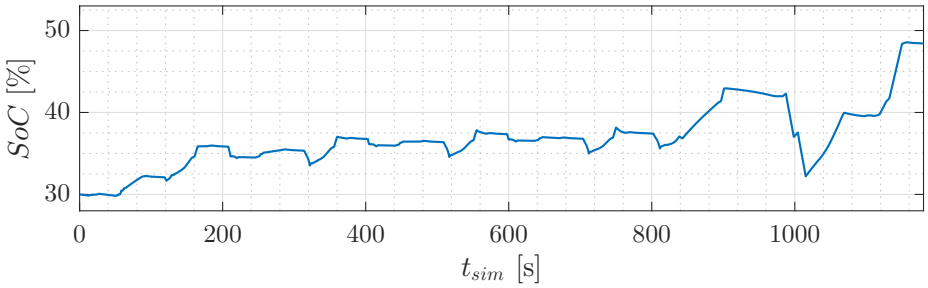

Figure 4.6: Overall strategy response - SoC - $SoC_{initial} = 30\%$ - NEDC

figure is shown that the TA functionality doesn't last very long due to the small load requests by the NEDC cycle. The figure 4.8 shows the activation of the LPS functionality.

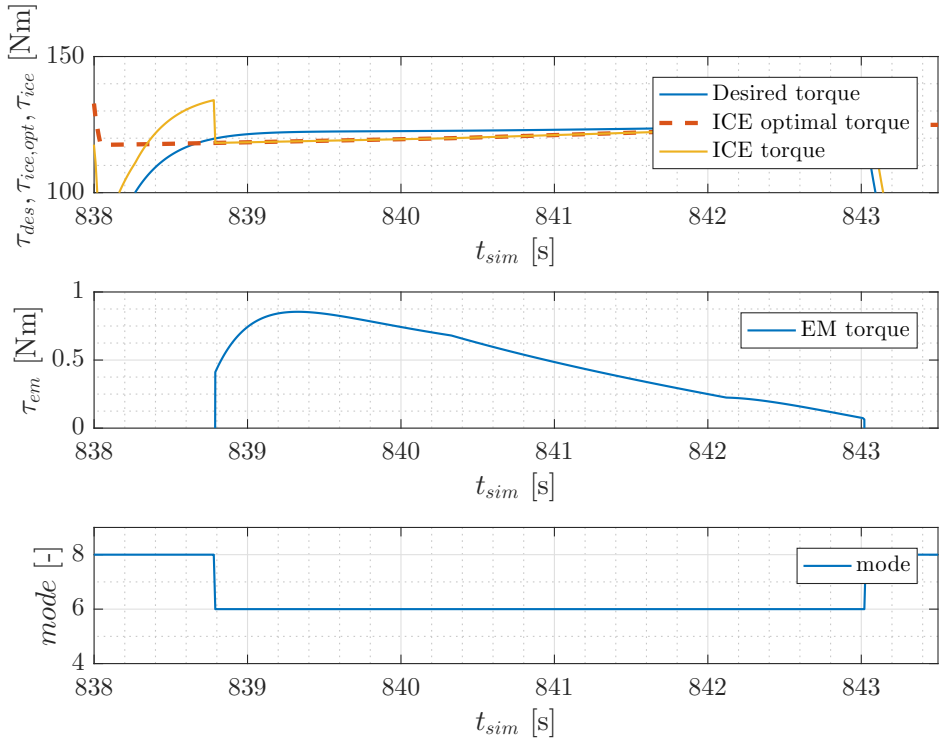

Figure 4.7: Overall strategy response - TA activation- $SoC_{initial} = 30\%$ - NEDC

The current gear is downshifted from the third to second gear in order to reduce the ECMS criteria. As shown on the figure 4.5 that functionality appear often on smaller vehicle velocities and on the acceleration parts of the cycle.

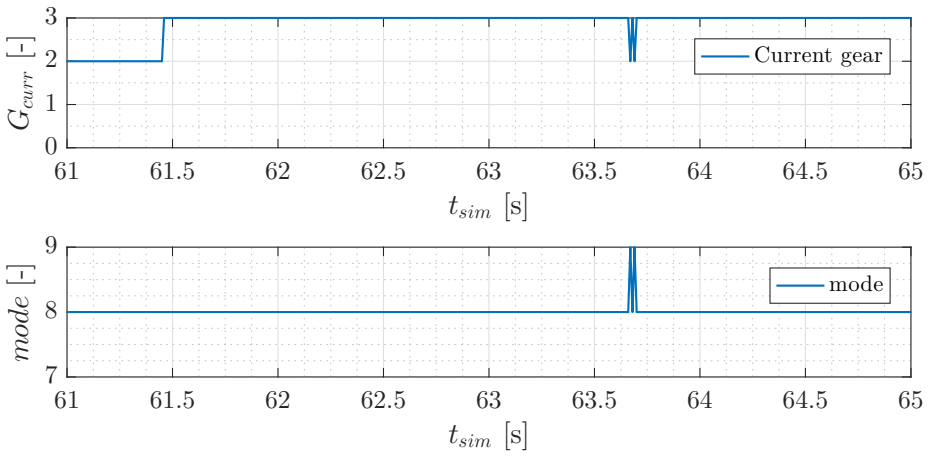

Figure 4.8: Overall strategy response - LPS activation- $SoC_{initial} = 30\%$ - NEDC

Table 4.2 presents the comparison between the developed control strategies. The integration of all the developed functionalities doesn't enhance the fuel economy in comparison with basic developed functionalities (E-Sailing, E-Coasting and E-Creep), but in comparison with the baseline strategy it shows fuel economy enhancement of 7.62%. The basic developed functionalities with TA doesn't show improvement of the fuel economy in comparison to basic functionality. The best fuel economy provides the 'Compact' strategy w/ explicit SoC controller. The fuel economy improvement in comparison with the baseline strategy is 18.01%. That's because the 'Rule-based' start-stop that is a part of the 'Compact' strategy has much more freedom in shutting down the ICE engine than the E-Creep rolling start-stop. The best example is that during the regenerative braking, the ICE engine gets shut-off by the 'Compact' strategy while in the case of the Overall hybrid strategy during regenerative braking, the functionality active is Regenerative braking that doesn't shuts-off the ICE engine. Obviously that has a lot of impact on the fuel economy increase.

Strategy	V_f[l/100km]	$V_{f,corr}$ [l/100km]	SoC_{final} [%]	ΔV[%]
Baseline	5.25	-	-	-
E-Sailing+E-Coast.+E-Creep	4.96	4.73	57.01	-9.90
E-Sailing+E-Coast.+E-Creep+TA	4.97	4.76	53.23	-9.33
'Compact' w/o expl. SoC contr.	4.85	4.72	44.73	-10.01
'Compact' w/ expl. SoC contr.	4.67	4.30	72.02	-18.01
Overall w/o expl. SoC contr.	5.16	5.03	44.87	-4.19
Overall w/ expl. SoC contr.	5.01	4.85	48.43	-7.62

Table 4.2: Fuel consumption comparison - $SoC_{initial} = 30\%$ - NEDC

4.4.2 NEDC - $SoC_{initial} = 50\%$

In figure 4.9 the vehicle velocity response is shown. Similar as before the drivability with Overall hybrid strategy was not compromised. Figure 4.10 shows that the vehicle for

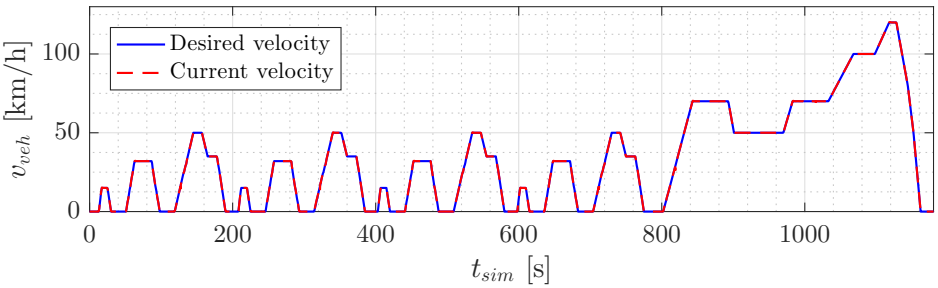

Figure 4.9: Overall strategy response - Velocity - $SoC_{initial} = 50\%$ - NEDC

the most part of the cycle operates in the LPM functionality, as it was with the previous case. This time more E-Creeping is noticed due to the larger initial SoC that enables the E-Creep functionality to be activated. Figure 4.11 shows the battery SoC throughout the

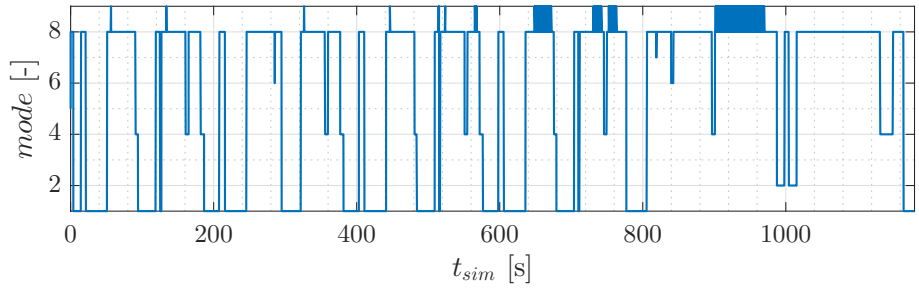

Figure 4.10: Overall strategy response - Modes - $SoC_{initial} = 50\%$ - NEDC

cycle. The battery SoC was now within the dead zone the whole cycle which means that the SoC controller was not active in this case. Similar to last case the sailing functionality gets activated on the end of the cycle thus discharging the battery, and the regenerative braking charges it back as before so that the final SoC equals 62.82%. Table 4.3 presents the comparison between the developed control strategies. In comparison with the previous case, the Overall strategy w/o explicit controller shows the improvement in fuel economy with the basic functionalities. In comparison with the baseline strategy, the Overall strategy w/o explicit SoC controller shows improvement in fuel economy by 10.67% and the Overall strategy w/ explicit SoC controller shows improvement in fuel economy by 10.29%. But the largest fuel economy increase shows the 'Compact' w/ explicit SoC controller, in comparison with the baseline strategy it equals 20.41%.

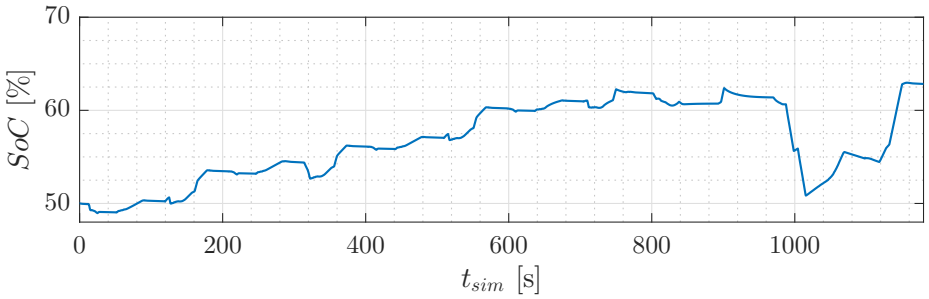

Figure 4.11: Overall strategy response - SoC - $SoC_{initial} = 50\%$ - NEDC

Strategy	V_f[l/100km]	$V_{f,corr}$ [l/100km]	SoC_{final} [%]	ΔV[%]
Baseline	5.25	-	-	-
E-Sailing+E-Coast.+E-Creep	4.77	4.70	57.72	-10.48
E-Sailing+E-Coast.+E-Creep+TA	4.77	4.69	58.08	-10.66
'Compact' w/o expl. SoC contr.	4.71	4.72	44.73	-10.01
'Compact' w/ expl. SoC contr.	4.37	4.18	72.02	-20.41
Overall w/o expl. SoC contr.	4.73	4.67	56.94	-10.67
Overall w/ expl. SoC contr.	4.81	4.69	62.83	-10.29

Table 4.3: Fuel consumption comparison - $SoC_{initial} = 50\%$ - NEDC

4.4.3 NEDC - $SoC_{initial} = 90\%$

On figure 4.12 the vehicle velocity response is shown. Similar as before the drivability with Overall hybrid strategy was not compromised. Figure 4.13 shows that there is no big

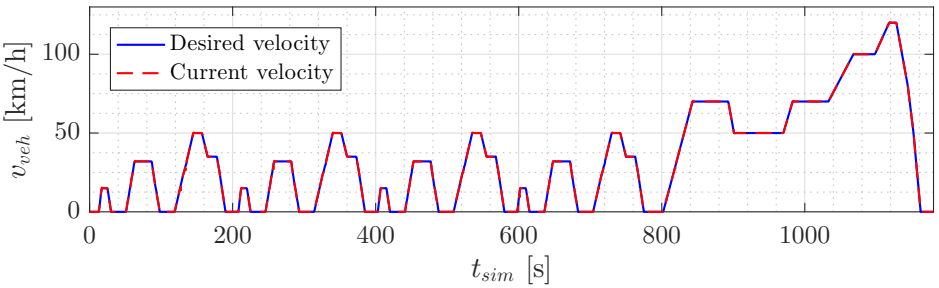

Figure 4.12: Overall strategy response - Velocity - $SoC_{initial} = 90\%$ - NEDC

of a difference between this case and the last case. Figure 4.14 shows the battery SoC throughout the cycle. The battery initial SoC was now set to a high value, in which case the explicit SoC controller tends to discharge the battery until it reaches the SoC dead zone. The rest of the SoC trajectory seems similar as with the one in previous case. Table 4.4 presents the comparison between the developed control strategies. This time the biggest influence on the fuel economy reduction is obvious. This time the Overall strategy in both

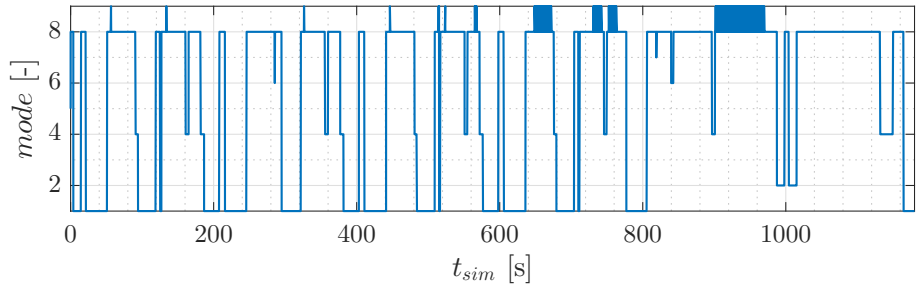

Figure 4.13: Overall strategy response - Modes - $SoC_{initial} = 90\%$ - NEDC

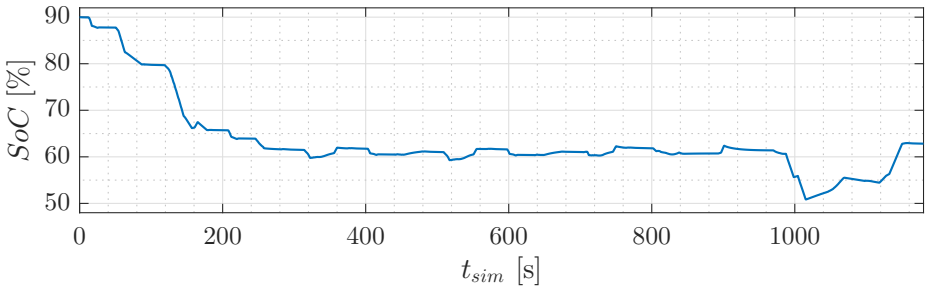

Figure 4.14: Overall strategy response - SoC - $SoC_{initial} = 90\%$ - NEDC

cases (w/ and w/o) show worse fuel economy in comparison with the basic functionality. The basic functionalities with TA shows fuel economy improvement of 12.57%. As it was the case before, 'Compact' w/ explicit SoC controller shows the best fuel economy enhancement in comparison with other strategies. The fuel economy improvement in this case equals 22.16%. On figure 4.15 the SoC trajectory comparison and 4.16 the cumulative fuel mass, m_f are shown for different hybrid control strategies. On these figure it is shown what an impact different hybrid control strategies have on fuel consumption and SoC trajectories. For example, the Overall startegy and 'Compact' strategy w/ explicit SoC controller tend to force the battery discharge at high battery SoC, while with other strategies that is not the case. Consequently at this point, the cumulative fuel consumption gets reduced.

Strategy	V_f[l/100km]	$V_{f,corr}$ [l/100km]	SoC_{final} [%]	ΔV[%]
Baseline	5.25	-	-	-
E-Sailing+E-Coast.+E-Creep	4.38	4.63	60.36	-11.81
E-Sailing+E-Coast.+E-Creep+TA	4.40	4.59	61.77	-12.57
'Compact' w/o expl. SoC contr.	4.31	4.61	55.98	-12.27
'Compact' w/ expl. SoC contr.	3.93	4.09	72.02	-22.16
Overall w/o expl. SoC contr.	4.37	4.65	57.14	-11.42
Overall w/ expl. SoC contr.	4.48	4.71	62.82	-10.28

Table 4.4: Fuel consumption comparison - $SoC_{initial} = 90\%$ - NEDC

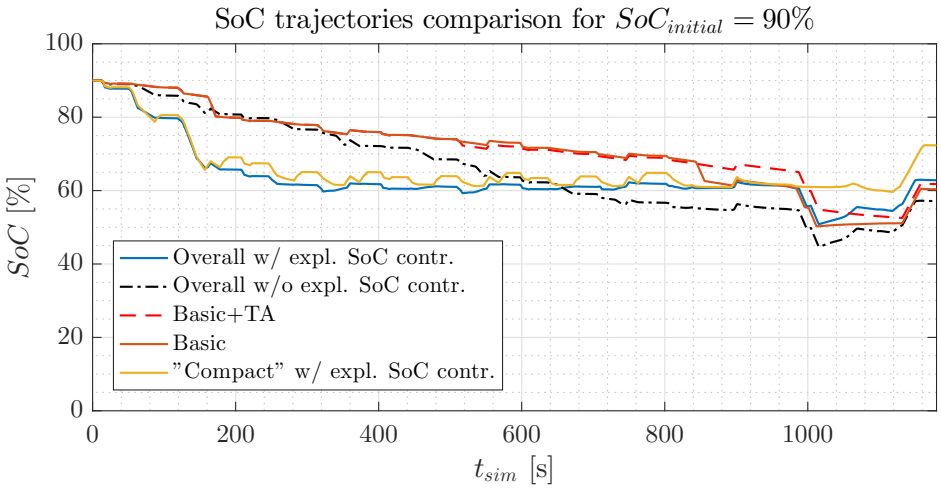

Figure 4.15: SoC trajectories comparison - NEDC

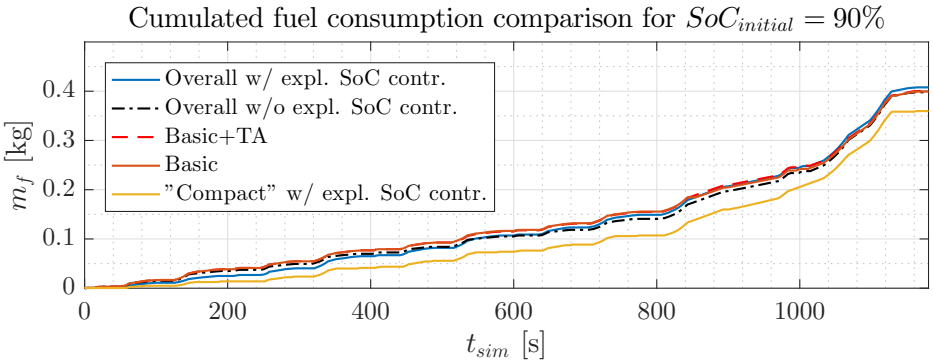

Figure 4.16: Fuel consumption comparison - NEDC

4.5 WLTP driving cycle

WLTP was developed with the aim of being used as a global test cycle across different world regions and as a replacement for NEDC, so pollutant and CO_2 emissions as well as fuel consumption values would be comparable worldwide [20]. It has a lot more dynamic included in comparison with the NEDC thus it represents the real-life driving conditions more truly. For this case, only the results for the initial SoC, $SoC_{intial} = 90\%$ will be given in detail, and for the other initial conditions, detail tables will be given in appendix. Figure 4.17 shows the vehicle velocity response for the Overall control strategy w/ explicit SoC controller. Figure 4.18 shows the strategy functionalities that have been active throughout the cycle. On the figure it is shown that the control strategy changes the functionalities a lot during the cycle. That is because the WLTP cycle has a influenced dynamics that requires different hybrid functionalities. Figure 4.19 shows the SoC trajectory throughout the cycle.

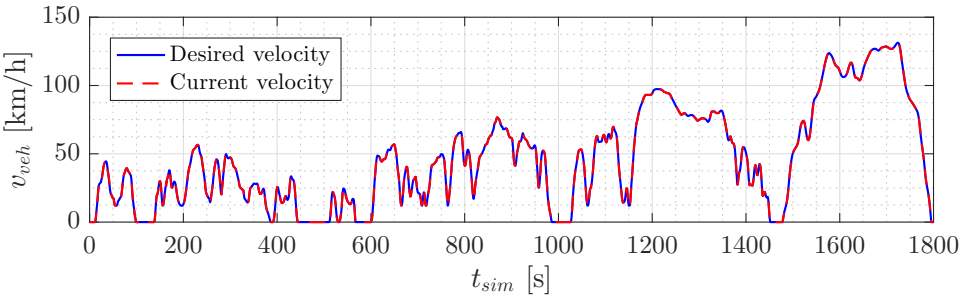

Figure 4.17: Overall strategy response - Velocity - $SoC_{initial} = 90\%$ - WLTP

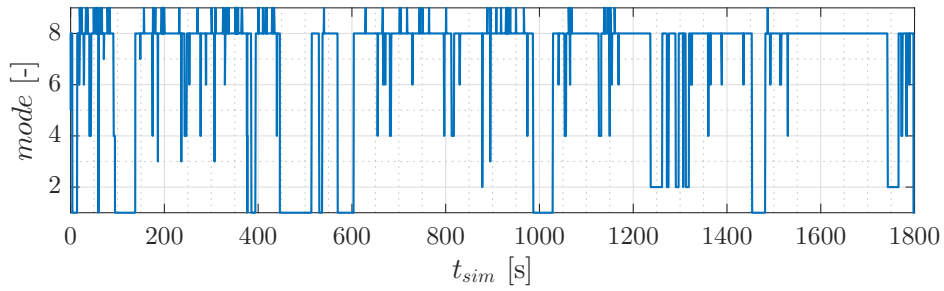

Figure 4.18: Overall strategy response - Modes - $SoC_{initial} = 90\%$ - WLTP

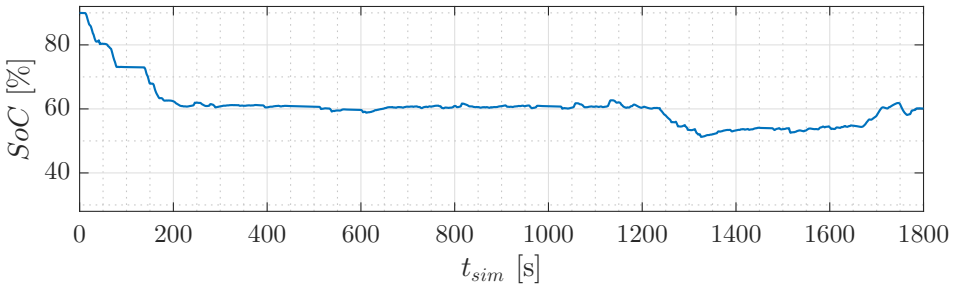

Figure 4.19: Overall strategy response - SoC - $SoC_{initial} = 90\%$ - WLTP

SoC trajectory stays flat for the most part of the cycle because of the SoC controller and because the ICE engine is loaded enough due to the high cycle dynamics, and doesn't need high EM torque intervention. Next the fuel consumption comparison for initial SoC of 90% will be given.

Strategy	V_f[l/100km]	$V_{f,corr}$ [l/100km]	SoC_{final} [%]	ΔV[%]
Baseline	5.32	-	-	-
E-Sailing+E-Coast.+E-Creep	4.82	5.16	50.06	-3.00
E-Sailing+E-Coast.+E-Creep+TA	4.82	5.17	49.89	-2.82
'Compact' w/o expl. SoC contr.	4.54	4.82	57.32	-9.73
'Compact' w/ expl. SoC contr.	4.43	4.60	71.02	-13.86
Overall w/o expl. SoC contr.	4.84	5.15	53.93	-3.73
Overall w/ expl. SoC contr.	4.91	5.16	60.16	-2.82

Table 4.5: Fuel consumption comparison - $SoC_{initial} = 90\%$ - WLTP

In table 4.5 fuel consumption comparison is shown. In this case the Overall hybrid control strategy w/o explicit SoC controller does show minimal improvement in the fuel economy in comparison with the basic hybrid control strategy (E-Sailing+E-Coast.+E-Creep). The reason why the fuel economy increase isn't larger is probably because the LPS functionality tends to often change gears, in which case the additional inertia losses are happening. The Overall hybrid control strategy w/o explicit SoC controller shows improvement of 3.73% in fuel economy in comparison with the baseline control. But as it was the case before, the 'Compact' w/ explicit SoC controller shows the best performance and fuel economy. In the case the fuel economy enhancement is up to 13.86%.

4.6 US06 driving cycle

The US06 cycle was developed to address to represent aggressive, high speed and high acceleration driving behavior, rapid speed fluctuations, and driving behavior following startup [21]. Similar as for WLTP, only the results for the initial SoC, $SoC_{intial} = 90\%$ will be given in detail, and for the other initial conditions, detail tables will be given in appendix. Figure 4.20 shows the vehicle velocity response for the Overall control strategy

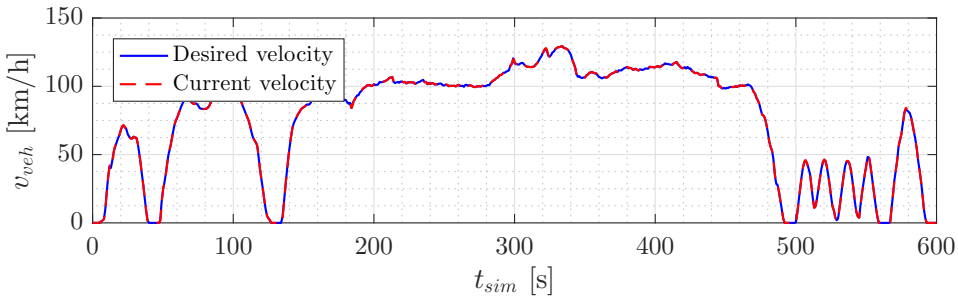

Figure 4.20: Overall strategy response - Velocity - $SoC_{initial} = 90\%$ - US06

w/ explicit SoC controller. Figure 4.21 shows the strategy functionalities that have been

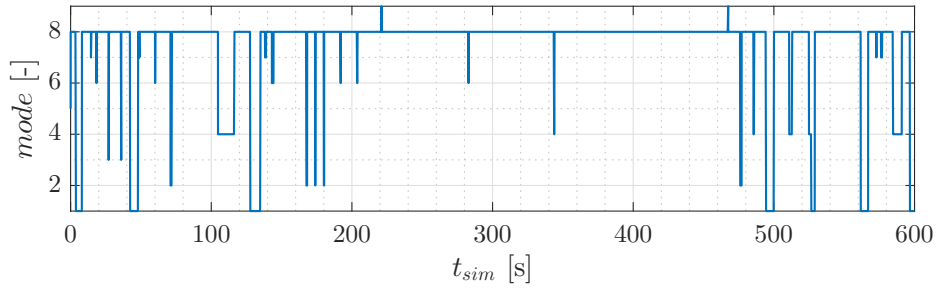

Figure 4.21: Overall strategy response - Modes - $SoC_{initial} = 90\%$ - US06

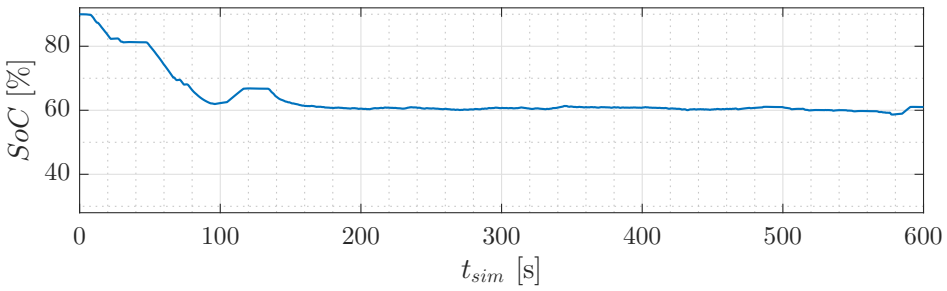

Figure 4.22: Overall strategy response - SoC - $SoC_{initial} = 90\%$ - US06

active throughout the cycle. For the good part of the cycle, the powertrain was in the LPM mode. Figure 4.22 shows the SoC trajectory throughout the cycle. SoC trajectory stays flat for the most part of the cycle because of the SoC controller and because the ICE engine is loaded enough due to the high cycle dynamics, very similar to the WLTP cycle results.

Strategy	V_f[l/100km]	$V_{f,corr}$ [l/100km]	SoC_{final} [%]	ΔV[%]
Baseline	6.27	-	-	-
E-Sailing+E-Coast.+E-Creep	5.87	6.07	67.36	-3.19
E-Sailing+E-Coast.+E-Creep+TA	5.87	6.07	67.13	-3.19
'Compact' w/o expl. SoC contr.	5.67	5.77	78.00	-7.90
'Compact' w/ expl. SoC contr.	5.44	5.63	67.09	-10.59
Overall w/o expl. SoC contr.	5.82	6.09	59.22	-2.87
Overall w/ expl. SoC contr.	5.79	6.04	61.01	-3.69

Table 4.6: Fuel consumption comparison - $SoC_{initial} = 90\%$ - US06

Table 4.6 shows comparison of the fuel consumption between the strategies. In the case of US06 cycle, the Overall hybrid control w/ explicit SoC controller strategy shows improvement in fuel economy in comparison with the baseline model and the basic functionalities. In comparison with the baseline model, the Overall strategy shows fuel economy increase of 3.69%. At the end, as it was the case in all examined cycles, the 'Compact' w/o explicit SoC controller control strategy shows the best fuel economy increase of 10.59% at initial

SoC, $SoC_{initial} = 90\%$ in comparison with baseline control strategy. In the next chapter the dynamic model of ICE engine will be introduced, and the Co-Simulation model development, so that the strategies can be validated on that more realistic powertrain model.

Chapter 5

MHEV Co-Simulation model development

In this chapter, the MHEV Co-Simulation model will be presented. The MHEV driveline with the EM is still modeled in the AVL CRUISE ™, but the ICE engine in CRUISE ™ is replaced with the more complex model in CRUISE ™ M environment. The coupling between those two models is done in AVL Model.CONNECT ™ environment, where the Co-Simulation model is built. First of all the description of the AVL CRUISE ™ M ICE engine model will be presented and then the Co-Simulation model will be shown. For completion purposes, the short description of the AVL Model.CONNECT ™ will be given.

5.1 AVL CRUISE ™ M ICE model

For this thesis, the ICE model was taken from one of the AVL CRUISE ™ M example ICE engine models. This engine is a four-stroke turbocharged compression combustion engine (aka Diesel engine) with the operating volume of 1495 cm^3. Idle speed equals 800 min^{-1}, while the maximal speed equals 4000 min^{-1}. The engine reaches the torque peak of 221.73 Nm at 2000 min^{-1}. Maximal engine power is 60.18 kW. The output shaft inertia equals 0.17 kgm^2. Within the CRUISE ™ M ICE engine, the modeled physical processes are:

- intake manifold dynamics,
- fuel injector dynamics,
- combustion dynamics,
- exhaust manifold and turbocharging dynamics.

Within this model, the signals are taken as Mean Value i.e. this model represents the so known MVEM (Mean Value Engine Model). For the control strategy purposes, the static and the BSFC characteristics (figure 5.1) needed to be calculated. The calculation was done so that the engine was loaded in the load signal normalized spectrum from 0 - 1 and through the engine speeds spectrum from 0-4000 min^{-1}. The difference between the CRUISE ™ and the CRUISE ™ M engine model is that the CRUISE ™ engine model can be controlled directly via the engine desired torque, and the CRUISE M engine model not. In order to control the CRUISE ™ M engine model the engine desired torque needs to be transformed into engine's load signal i.e. the electronic throttle angle. That's why the CRUISE ™ M engine's static characteristics needed to be inverted so that the characteristics output from desired engine speed and torque is the equivalent load signal. This example model is a so known N/Alpha Engine model. From the causality perspective that means that the mathematical input in the model is the current engine speed ('N') and the output of the model is the engine torque ('T'). The CRUISE ™ M engine model in the environment is shown in figure 5.5.

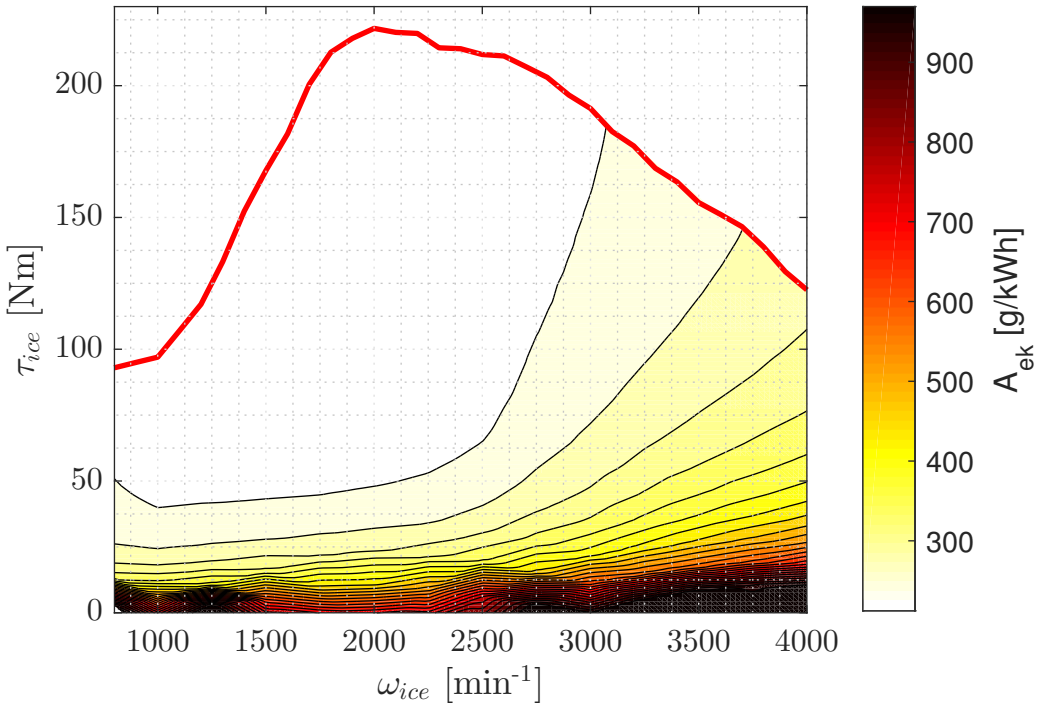

Figure 5.1: ICE static characteristic - CRUISE ™ M example model

5.2 MHEV Co-Simulation model

5.2.1 About AVL Model.CONNECT ™

Model.CONNECT ™ is model integration and co-simulation platform, that can connect virtual and real components [22]. Models can be integrated based on standardized interfaces (Functional Mockup Interface, FMI) as well as based on specific interfaces to a wide range of well-known simulation tools [22]. The idea of Model.CONNECT™ is to develop complex multi-disciplinary simulation models into one Co-Simulation model. After the simulation models are well defined, the simulation model components can be changed with the real model components. The Model.CONNECT ™ environment is shown in figure 5.2.

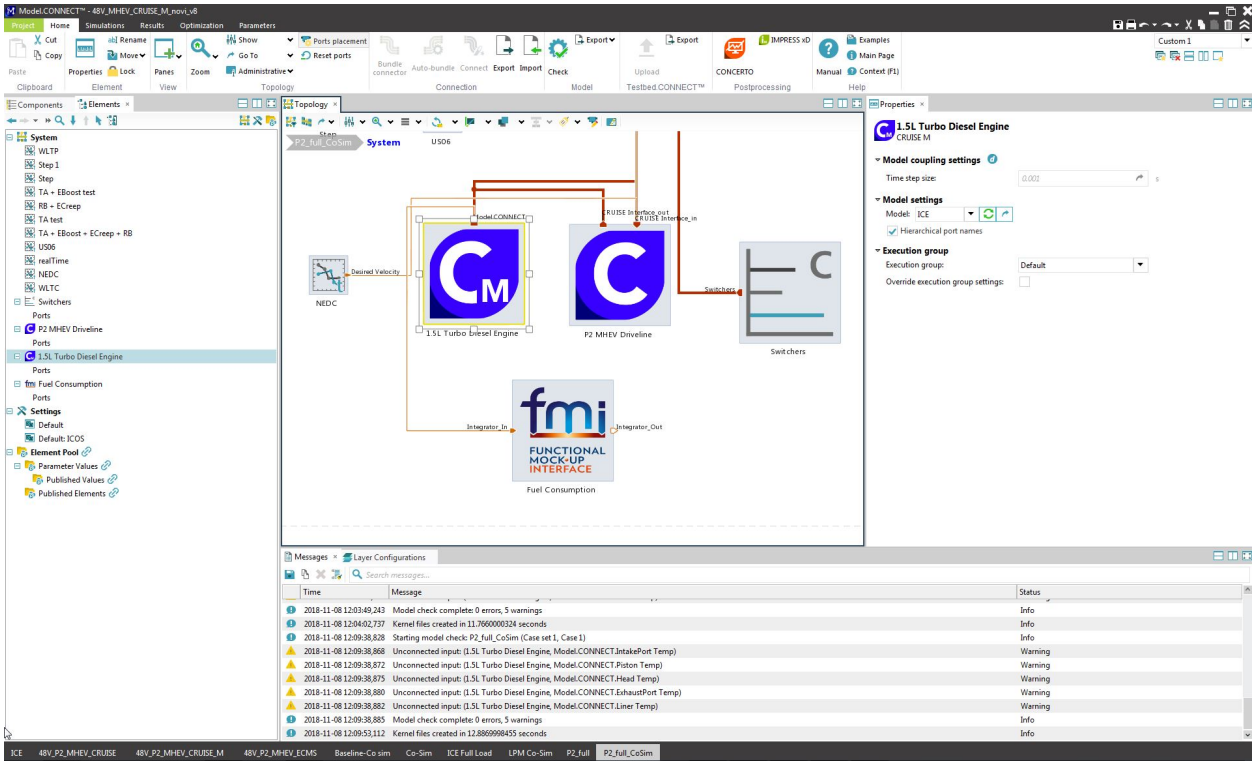

Figure 5.2: AVL Model.CONNECT ™ environment

5.2.2 Co-Simulation model development

For the purposes of the Co-Simulation model development an interface between two models needs to be defined. The main link between the ICE engine CRUISE ™ M model and the drivetrain model in CRUISE ™ is a flange. The flange in both of the models connects physically those two models. As mentioned before, the CRUISE ™ M engine model is an N/Alpha model so it needs a speed as an input, that's why the flange in CRUISE ™ M

model is defined in "speed" control, while the flange in CRUISE ™ model needs to be set in "torque" control mode. As said, in order to define the Co-Simulation model, an interface needs to be defined. An interface represents the signal exchange between the models. The interface between the CRUISE ™ and CRUISE ™ M model is shown in figure 5.3. The CRUISE ™ M signal inputs through the interface are as follows:

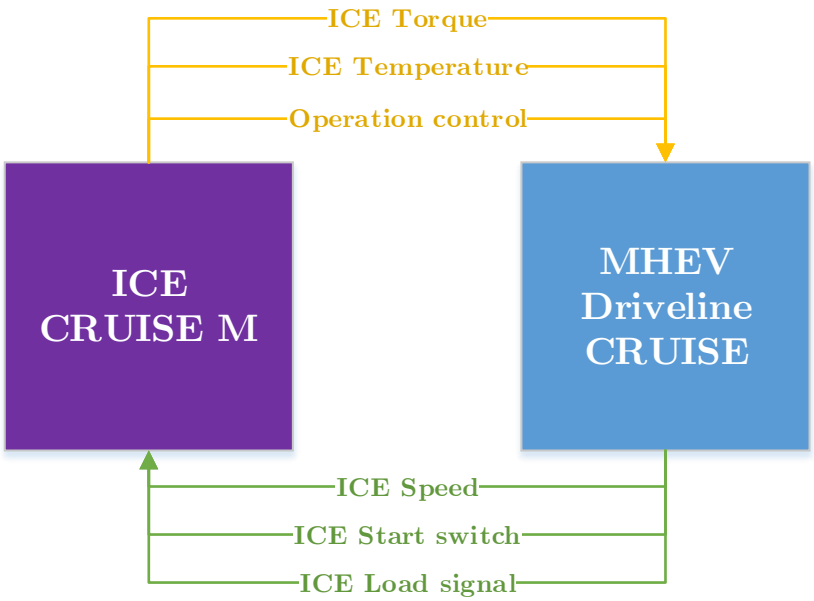

Figure 5.3: Co-Simualation signal exchange

- ICE speed,
- ICE load signal,
- ICE start-switch,

while the inputs signal to the CRUISE ™ model are as follows:

- ICE torque,
- ICE temperature,
- Operation control.

Besides the CRUISE ™ MHEV powertrain model and the CRUISE ™ M model, an MATLAB FMU integrator is implemented in order to integrate the current fuel mass flow

from the CRUISE ™ M engine. Also the constant block was added into the Co-Simulation model that contains switchers that can activate/deactivate hybrid functionalities. Last but not least, in order to fully define the Co-Simulation model, a coupling time step needs to be defined. In this case the coupling time step, $t_{coupling}$ is set to 1 ms. Now in the next chapter, the results of the Co-Simulation model response will be shown on the focus with the emphasis of the fuel economy gains with the already developed hybrid control strategies.

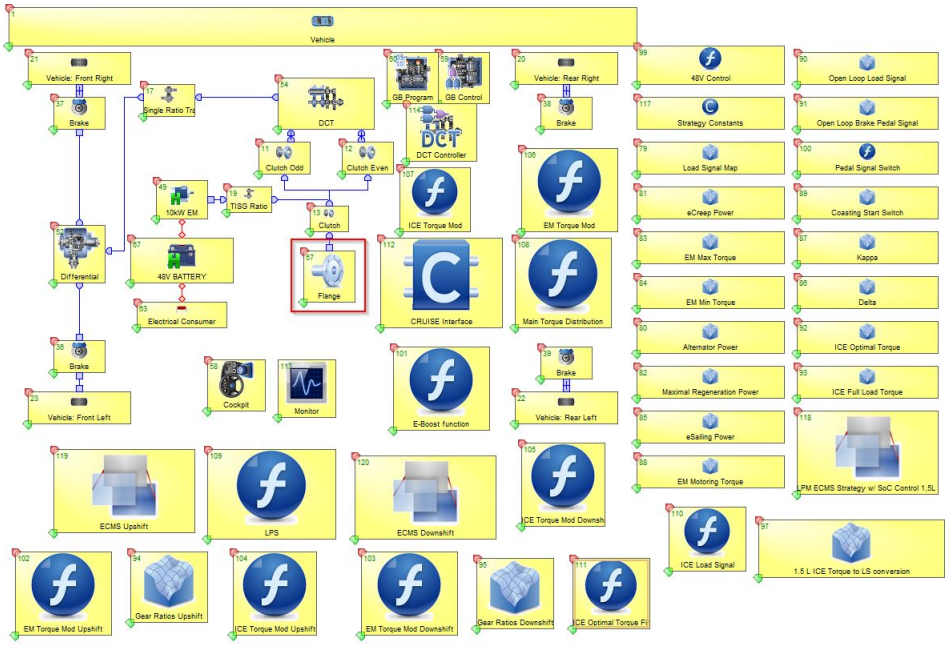

Figure 5.4: AVL CRUISE ™ environment - Flange

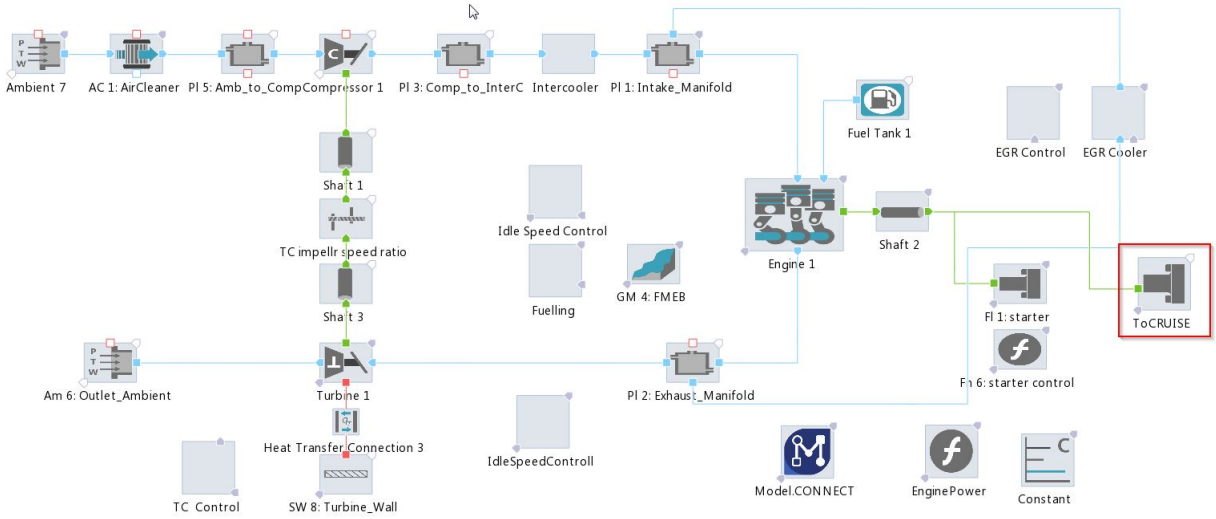

Figure 5.5: AVL CRUISE ™ M environment - Flange

Chapter 6

Control strategy validation on MHEV Co-Simulation model

In this chapter the control strategy validation for MHEV Co-Simulation model was done the same as for the MHEV CRUISE ™ model. The same strategies were developed and implemented for this model and tested for the certified driving cycles as it was the case before. In the following sections the fuel consumption analysis will be shown.

6.1 Fuel consumption calculation

In comparison with the MHEV CRUISE ™ model in the Co-Simulation model, there is no cumulative mass flow signal from the ICE engine component like in MHEV CRUISE ™ model. The fuel mass flow, $\dot{m}_f$ is integrated into cumulative fuel mass, m_f via the previously explained integrator FMU. The fuel consumption, V_f is calculated as follows:

$$V_f = \frac{m_f}{\rho_{fuel}} \frac{100000}{d}, \tag{6.1}$$

where the ρ_{fuel} is the fuel density, and d the traveled distance. The fuel density was taken from the CRUISE ™ model. The fuel density equals, $\rho_{fuel} = 835$ g/l. Because of the smaller engine operating volume, the vehicle mass was decreased. The vehicle mass for this analysis equals 1179 kg. The corrected fuel consumption, $V_{f,corr}$ will be calculated with the previous statement 4.1.

6.2 NEDC driving cycle

As it was the case with the MHEV CRUISE ™ model, the response of the Overall strategy w/ explicit SoC controller will be shown. Now the simulation results for NEDC cycle follow. Strategies were simulated for three initial battery SoC as follows:

- $SoC_{initial} = 30\%$
- $SoC_{initial} = 50\%$
- $SoC_{initial} = 90\%$

6.2.1 NEDC - $SoC_{initial} = 30\%$

Vehicle response with the Overall hybrid strategy including the explicit SoC controller will be shown on few following figures. On figure 6.1 the vehicle velocity response is shown. The figure shows that the drivability with the Overall hybrid strategy was not compromised. Figure 6.2 shows that the developed strategies were successfully implemented on the Co-

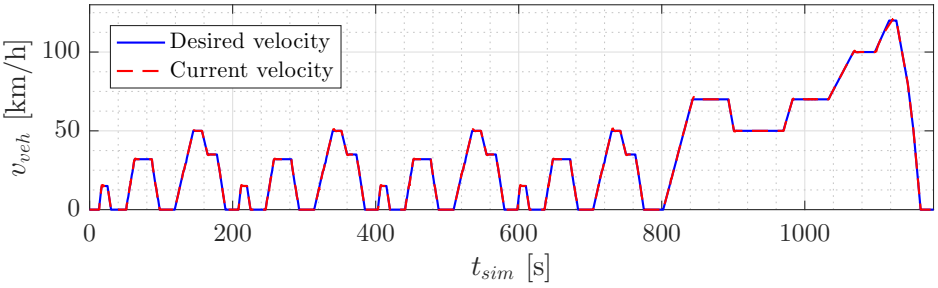

Figure 6.1: Overall strategy response - Velocity - $SoC_{initial} = 30\%$ - NEDC - CoSim

Simulation model. As it was the case in the MHEV CRUISE ™ model, the Co-Simulation model behaves similar. Because of many start-stops, there is a lot of E-Creeping during the cycle. Also, for the big part of the cycle, the LPM functionality is active. At high velocities the Torque Assist and the Sailing functionality activates. Figure 6.3 shows the battery SoC throughout the cycle. The battery SoC was inclining through almost the whole cycle because the LPM tends to charge the battery because of the SoC control error. But at the end of the cycle when the battery SoC reaches the allowed SoC dead zone and the high vehicle velocity becomes constant, the Sailing functionality gets activated and discharges the battery, but the Regenerative braking functionality charges the battery at the end of the cycle so that the final SoC equals 48.43%. The fuel consumption comparison for the Co-simulation model is shown

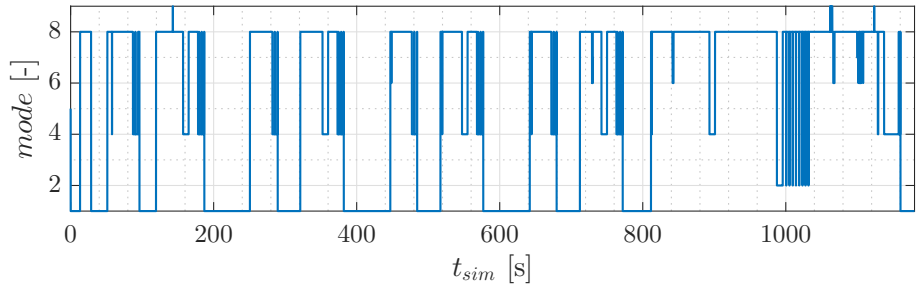

Figure 6.2: Overall strategy response - Modes - $SoC_{initial} = 30\%$ - NEDC - CoSim

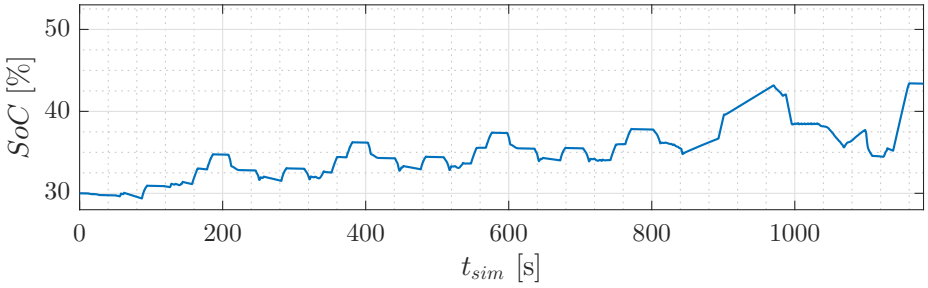

Figure 6.3: Overall strategy response - SoC - $SoC_{initial} = 30\%$ - NEDC - CoSim

Strategy	V_f[l/100km]	$V_{f,corr}$ [l/100km]	SoC_{final} [%]	ΔV[%]
Baseline	3.57	-	-	-
E-Sailing+E-Coast.+E-Creep	3.48	3.27	53.62	-8.40
E-Sailing+E-Coast.+E-Creep+TA	3.42	3.31	42.13	-7.28
'Compact' w/o expl. SoC contr.	3.39	3.43	26.36	-10.84
'Compact' w/ expl. SoC contr.	3.51	3.36	47.34	-6.16
Overall w/o expl. SoC contr.	3.11	3.11	30.32	-12.89
Overall w/ expl. SoC contr.	3.27	3.15	43.38	-11.76

Table 6.1: Fuel consumption comparison - $SoC_{initial} = 30\%$ - NEDC - CoSim

in table 6.1. In the fuel consumption table it is shown that in the Co-Simulation model for the initial battery SoC of 30% the best fuel economy shows the Overall strategy w/o explicit SoC controller. The fuel economy improvement equals 12.89%. The basic functionalities strategy with TA shows engine fuel consumption reduction in comparison with the basic functionality by 7.28%, while the corrected fuel consumption is higher due to the lower final SoC. That indicates that the battery was discharged using the TA functionality. Also, this time the 'Compact' strategy w/ explicit SoC controller shows improvement in the fuel economy in comparison with the baseline control by 6.16%, however the best performance in fuel economy improvement shows the Overall strategy w/o explicit SoC controller because at low velocities, the E-Creep functionality was active and the ICE engine was shut-off, but

at 'Compact' strategies the ICE engine was activated and charged the battery.

6.2.2 NEDC - $SoC_{initial} = 50\%$

On figure 6.4 the vehicle velocity response is shown. Similar as before the drivability with Overall hybrid strategy was not compromised.

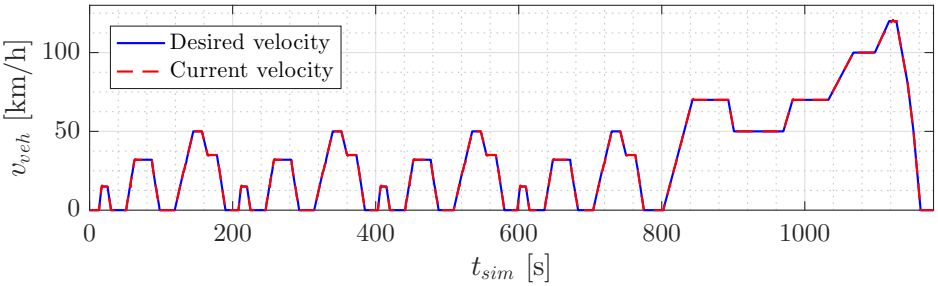

Figure 6.4: Overall strategy response - Velocity - $SoC_{initial} = 50\%$ - NEDC- CoSim

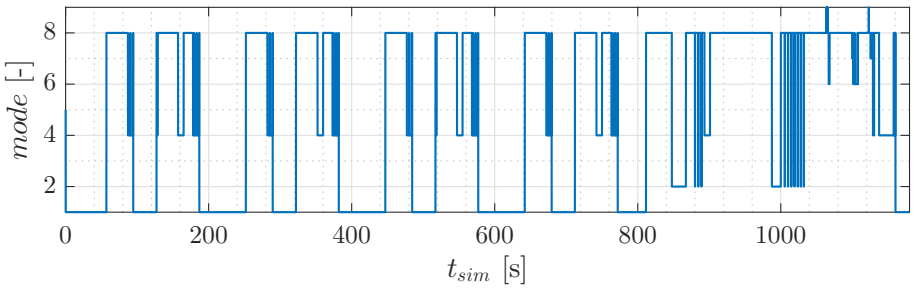

Figure 6.5: Overall strategy response - Modes - $SoC_{initial} = 50\%$ - NEDC - CoSim

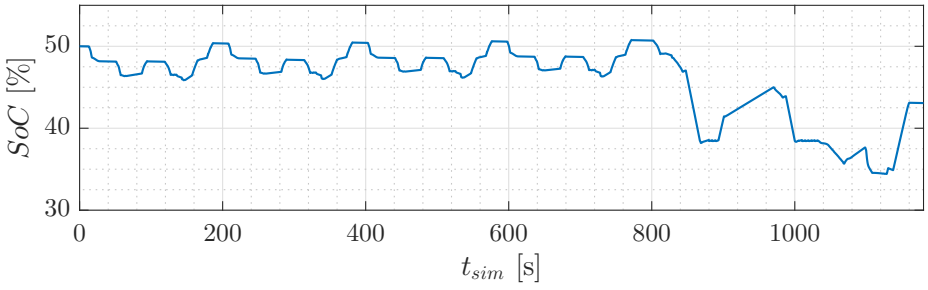

Figure 6.6: Overall strategy response - SoC - $SoC_{initial} = 50\%$ - NEDC - CoSim

Figure 6.5 shows the functionalities that have been active throughout the NEDC cycle. It is noticed that every functionality was activated except the Coasting functionality, like it was the case on all of the cycles. For the most part of the cycle, the LPM and the Regenerative braking functionality were active, but similar as before the Sailing functionality activates at

high and constant vehicle velocities. Similar as before, the E-Boost and TA functionality get activated at the end of the cycle, were there are high torque requests by the driver due to the high vehicle velocities. Figure 6.6 shows the SoC trajectory for the initial battery SoC of 50%. Due to the same desired battery SoC as the initial one the battery SoC stays consistent for the most part of the cycle. The battery has been slowly discharged by the LPM functionality, and charged by the Regenerative braking functionality. At the end of the cycle, the Sailing, TA and E-Boost functionality discharged the battery because of above mentioned reasons. The final battery SoC for this case equaled 43.07%. Table 6.2 presents

Strategy	V_f[l/100km]	$V_{f,corr}$ [l/100km]	SoC_{final} [%]	ΔV[%]
Baseline	3.57	-	-	-
E-Sailing+E-Coast.+E-Creep	3.25	3.22	57.73	-9.80
E-Sailing+E-Coast.+E-Creep+TA	3.13	3.19	41.71	-10.64
'Compact' w/o expl. SoC contr.	2.91	3.12	24.46	-12.61
'Compact' w/ expl. SoC contr.	3.26	3.27	47.08	-8.40
Overall w/o expl. SoC contr.	2.88	3.05	30.34	-14.56
Overall w/ expl. SoC contr.	3.07	3.13	43.07	-12.32

Table 6.2: Fuel consumption comparison - $SoC_{initial} = 50\%$ - NEDC - CoSim

the fuel consumption results for several functionality combinations that make one hybrid control strategy. In comparison with the previous case, this time the basic strategy with TA achieves improvement in the fuel economy in comparison with the baseline and the basic hybrid control strategy. This time the fuel economy improvement reached 10.64%. The 'Compact' strategy w/o explicit SoC controller shows a big fuel consumption reduction in comparison with the baseline strategy but for the cost of halfing the initial battery SoC. The final SoC for this strategy equals 24.46%. The fuel economy improvement equals 12.61%. The Overall strategy w/o explicit SoC controller shows the best fuel economy improvement in comparison to the baseline strategy. The fuel economy improvement equals 14.56%. The Overall strategy w/ explicit SoC controller saved the battery a little more, so that the fuel economy improvement is significant but a less than it was the case with the Overall strategy w/o explicit SoC controller. The fuel economy improvement equals 12.32%.

6.2.3 NEDC - $SoC_{initial} = 90\%$

This subsection shows the Overall strategy w/ explicit SoC controller response on the NEDC cycle for the initial battery SoC of 90%. The figure 6.7 shows that like before, the drivability of the strategy was not compromised.

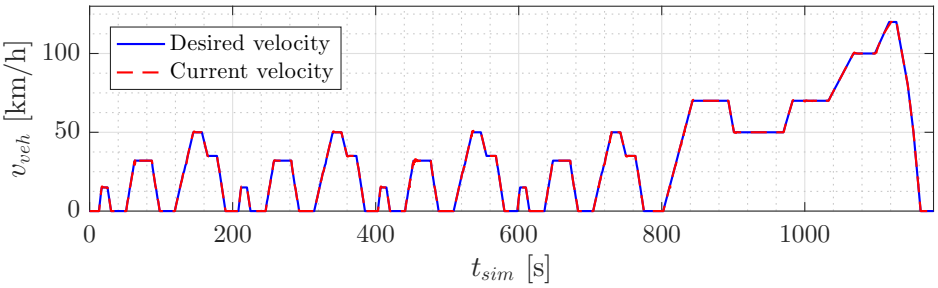

Figure 6.7: Overall strategy response - Velocity - $SoC_{initial} = 90\%$ - NEDC - CoSim

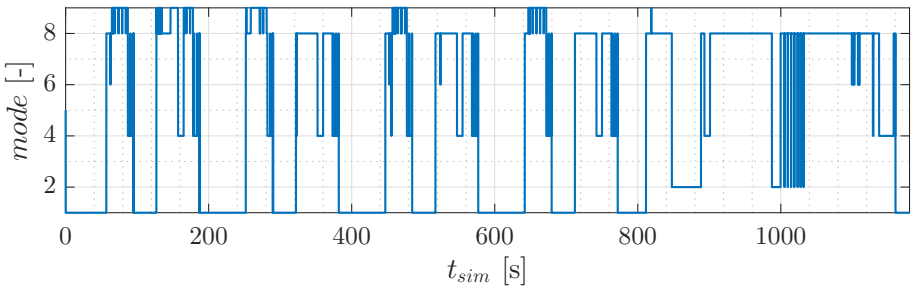

Figure 6.8: Overall strategy response - Modes - $SoC_{initial} = 90\%$ - NEDC - CoSim

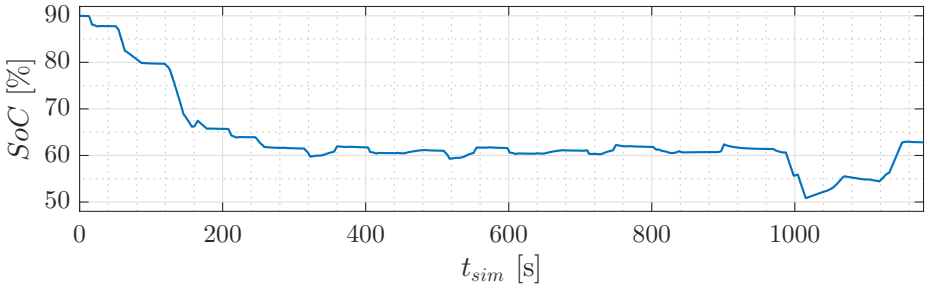

Figure 6.9: Overall strategy response - SoC - $SoC_{initial} = 90\%$ - NEDC - CoSim

Figure 6.8 shows the active functionalities throughout the NEDC cycle. In comparison to the first two initial SoC cases, this time in the beginning of the cycle the LPS functionality gets activated very frequently. This is because in this period the battery SoC is very high, and the explicit SoC controller tends to discharge the battery as fast as it cans. Through that time, it always searches for the best gear ratio in order to discharge the battery in the most efficient way by minimizing the ECMS criteria. At the middle and at the end of the cycle the activated functionalities are similar to the one with previous cases. Figure 6.9 shows the SoC trajectory throughout the cycle. Like it was explained before, the battery SoC is being discharged at the beginning of the cycle by the SoC controller until it reaches the SoC control error dead zone of $\pm 15\%$. Then as it was the case before, the SoC trajectory stayed consistent for the most part of the cycle so that at the end the battery can be discharged and

back charged by the Sailing, TA and Regenerative braking functionalities respectively. Table

Strategy	V_f[l/100km]	$V_{f,corr}$ [l/100km]	SoC_{final} [%]	ΔV[%]
Baseline	3.57	-	-	-
E-Sailing+E-Coast.+E-Creep	2.86	3.18	52.99	-10.92
E-Sailing+E-Coast.+E-Creep+TA	2.79	3.19	43.34	-10.64
'Compact' w/o expl. SoC contr.	2.63	3.13	32.62	-12.32
'Compact' w/ expl. SoC contr.	2.74	3.11	46.96	-12.89
Overall w/o expl. SoC contr.	2.54	3.06	30.14	-14.29
Overall w/ expl. SoC contr.	2.89	3.28	43.55	-8.12

Table 6.3: Fuel consumption comparison - $SoC_{initial} = 90\%$ - NEDC - CoSim

6.3 shows the fuel consumption comparison between the strategies for the initial battery SoC of 90%. The basic strategy with TA shows the fuel economy improvement in comparison with only Basic strategy, but the corrected fuel consumption is larger this time because of the lower final SoC. That means that the battery has been discharged by the TA and saved fuel, but the equivalent energy cost was larger this time. As it was the case with the MHEV CRUISE ™ model the 'Compact' strategy w/ and w/o explicit SoC controller show the significant fuel economy improvement by 12.89 % and 12.32 % respectively. As it was for every case on the NEDC cycle the Overall strategy w/o explicit SoC controller shows the best fuel economy improvement by 14.29%. Similiar as in chapter 5., on figures 6.10 - 6.11 it is shown what an impact different hybrid control strategies have on fuel consumption and SoC trajectories. For example, the Overall startegy and 'Compact' strategy w/ explicit SoC controller tend to force the battery discharge at high battery SoC, while with other strategies that is not the case. Consequently at this point, the cumulative fuel consumption gets reduced.

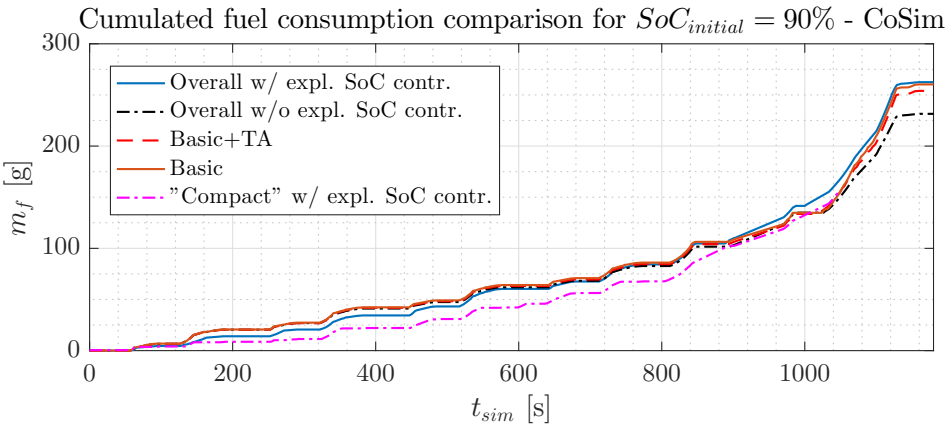

Figure 6.11: Fuel consumption comparison - NEDC - CoSim

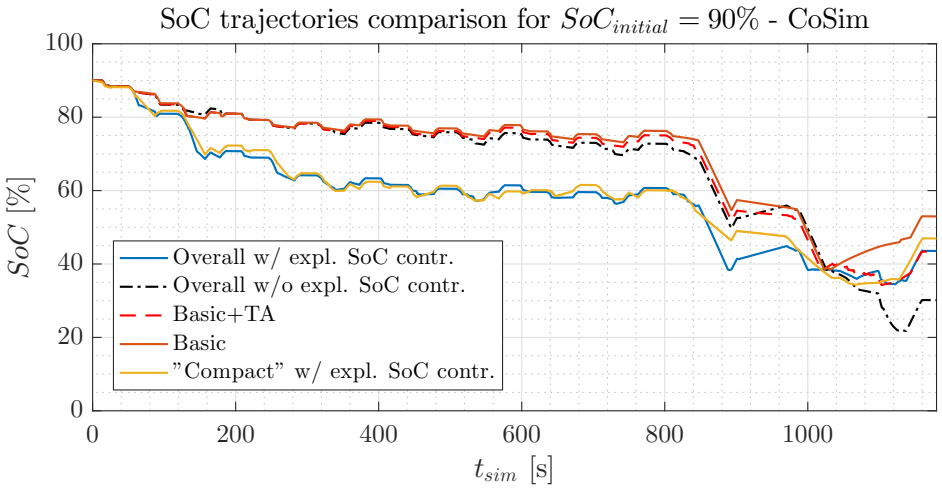

Figure 6.10: SoC trajectories comparison - NEDC - CoSim

6.3 WLTP driving cycle

In this section the Co-Simulation model response will be given for the Overall strategy w/ explicit SoC controller, as it was the case before. Similar as in the MHEV CRUISE ™ model, only the simulation results for the initial battery SoC, $SoC_{initial} = 90\%$ will be presented, while the rest of the fuel consumption tables will be given in the appendix. Figure 6.12 shows the vehicle velocity response. Note that the drivability was a little compromised at around 1600 s because the ICE engine is undersized for this vehicle so it can't provide enough torque to overcome high vehicle loads at those velocities. Figure 6.13 proves that. At that time, the vehicle is forcing E-Boost functionality in order to provide maximal power to successfully follow the desired velocity request. The idea of this analysis was not to dimension the ICE engine, but to analyze the fuel consumption improvements for different hybrid control strategy, so that small velocity control error can be neglected. The figure 6.13 also shows the dynamical alteration between the functionalities. That happens because the WLTP cycle is very dynamical and has sudden accelerations that cause that kind of behavior. Figure 6.14 shows the SoC trajectory throughout the cycle. Similar as it was the case in the NEDC cycle, this time at high SoC levels, the explicit SoC controller tends to discharge the battery in order to correct the SoC control error. Throughout the cycle, the TA functionality gets activated that additionally discharged the battery.

The table 6.4 shows the fuel consumption comparison between the strategies. The basic strategy with TA does not show the overall fuel economy improvement in comparison with the basic strategy even though the basic fuel consumption is smaller than the one with basic strategy, because this strategy ended up on lower final SoC which was in this case 45.21%

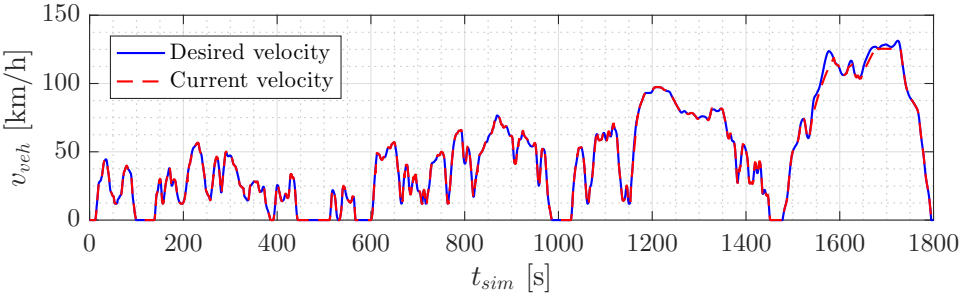

Figure 6.12: Overall strategy response - Velocity - $SoC_{initial} = 90\%$ - WLTP - CoSim

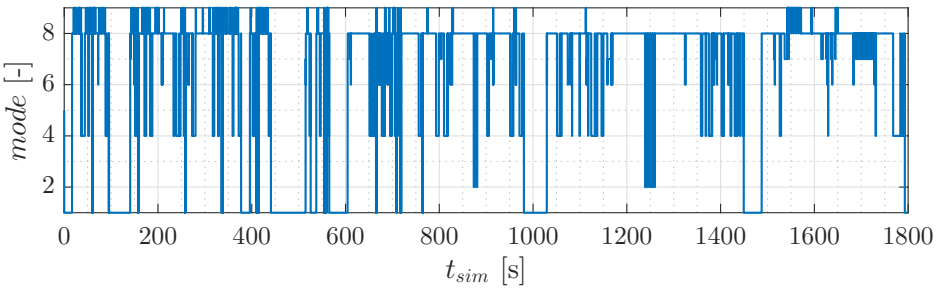

Figure 6.13: Overall strategy response - Modes - $SoC_{initial} = 90\%$ - WLTP - CoSim

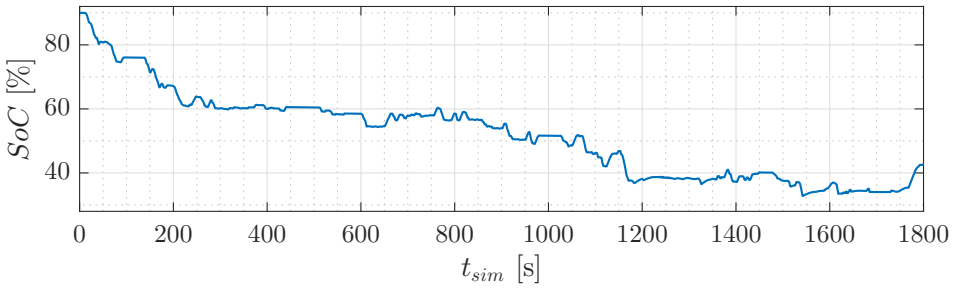

Figure 6.14: Overall strategy response - SoC - $SoC_{initial} = 90\%$ - WLTP - CoSim

Strategy	V_f[l/100km]	$V_{f,corr}$ [l/100km]	SoC_{final} [%]	ΔV[%]
Baseline	4.03	-	-	-
E-Sailing+E-Coast.+E-Creep	3.55	3.87	52.53	-3.97
E-Sailing+E-Coast.+E-Creep+TA	3.53	3.92	45.21	-2.73
'Compact' w/o expl. SoC contr.	3.27	3.85	23.01	-4.47
'Compact' w/ expl. SoC contr.	3.26	3.64	46.09	-9.68
Overall w/o expl. SoC contr.	3.44	4.10	14.82	+1.74
Overall w/ expl. SoC contr.	3.61	4.02	42.52	-0.29

Table 6.4: Fuel consumption comparison - $SoC_{initial} = 90\%$ - WLTP - CoSim

or 7.32% lower than the basic strategy. Note that the 'Compact' strategy w/ explicit SoC controller shows best fuel economy improvement of 9.68%. This time the best strategy in the NEDC cycle, the Overall w/o explicit SoC controller ended up to be worse than the

baseline strategy. That is because it discharged the battery a lot and the fuel consumption correction factor is not real in this case. The problem is that the fuel consumption factor was taken from the MHEV CRUISE ™ model and it doesn't realistically represent the real fuel consuption correction, because with this strategy the basic fuel consumption w/o the correction is 3.44 l/100 km that regarding everything indicates on a large fuel consumption reduction. That fact is also valid for all the other hybrid control strategies.

6.4 US06 driving cycle

In this section the response of the Co-Simulation model will be presented. Like it was the case with the WLTP cycle, only the response and fuel consumption comparison will be given for the initial battery SoC, $SoC_{initial} = 90\%$, while the rest of the results will be given in the appendix. The figure 6.15 shows the velocity response for the Overall strategy w/ explicit SoC controller. In is noticed that this time the drivability was not compromised like before. That's because, in the US06 there aren't that high loads as it was the case with the WLTP cycle. That's why the powertrain can provide enough torque in order to propel and overcome requested vehicle loads. Figure 6.16 shows the functionalities that have been active throughout the cycle. In the figure it is noticeable that at the beginning and at the end of the cycle there were frequent switches between the strategies due to the high dynamic load during these periods. In the middle of the cycle, where the vehicle velocity is relatively high and constant, the active functionality was the LPM that deploys current optimum torques to the both of the power sources. Figure 6.17 shows the SoC trajectory throughout the cycle. The SoC trajectory is similar with the one on the NEDC cycle for same boundary SoC conditions. The SoC controller tended to discharge the battery until it reached the dead zone as it was the case before. At the end of the cycle, an SoC trajectory oscillation is noticed due to the frequent discharging and charging from the TA and the Regenerative braking functionality respectively. Table 6.5 shows the fuel consumption comparison between the hybrid control strategies for the same initial battery SoC of 90%. As it was the case with the WLTP cycle, here the correcting fuel factor that was taken from the MHEV CRUISE ™ has a even bigger influence on the corrected fuel consumption. For example on the case of the Overall strategy w/o explicit SoC controller, the real fuel consumption equals 4.17 l/100km which represents the fuel economy increase of 10.90%, while the corrected fuel consumption equals 4.71% which represents the fuel economy decrease of 0.64%. That means that this factor currently unrealistically punishes the battery equivalent fuel consumption and it needs to be corrected,

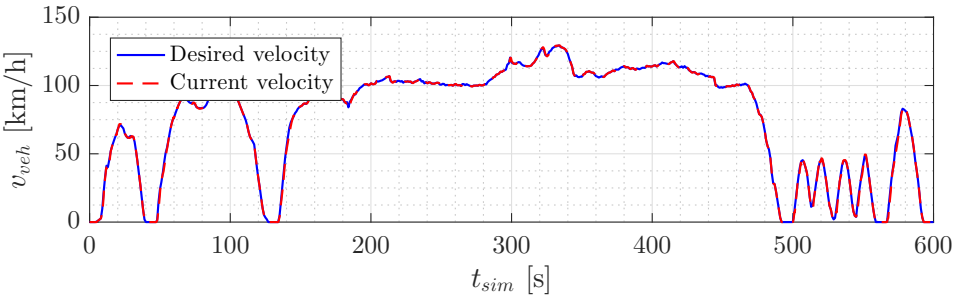

Figure 6.15: Overall strategy response - Velocity - $SoC_{initial} = 90\%$ - US06 - CoSim

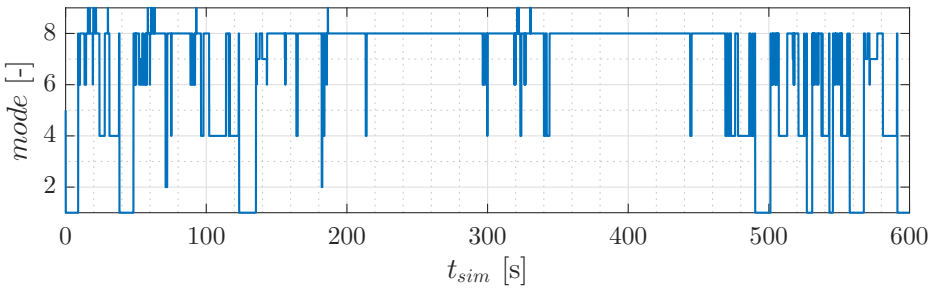

Figure 6.16: Overall strategy response - Modes - $SoC_{initial} = 90\%$ - US06 - CoSim

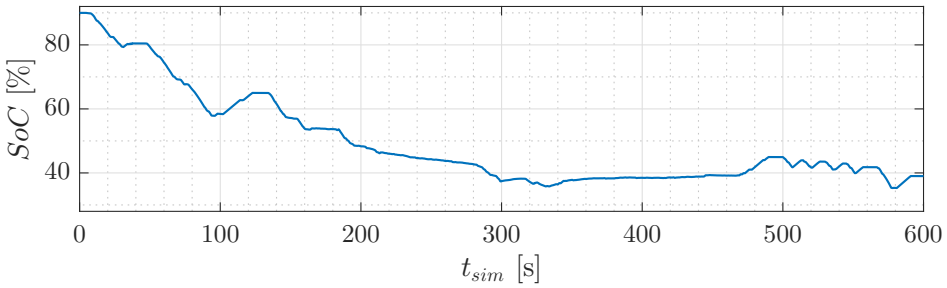

Figure 6.17: Overall strategy response - SoC - $SoC_{initial} = 90\%$ - US06 - CoSim

Strategy	V_f[l/100km]	$V_{f,corr}$ [l/100km]	SoC_{final} [%]	ΔV[%]
Baseline	4.68	-	-	-
E-Sailing+E-Coast.+E-Creep	4.51	4.60	80.44	-1.71
E-Sailing+E-Coast.+E-Creep+TA	4.53	4.77	62.85	+1.92
'Compact' w/o expl. SoC contr.	4.13	4.67	28.22	-0.24
'Compact' w/ expl. SoC contr.	4.15	4.57	42.17	-2.35
Overall w/o expl. SoC contr.	4.17	4.71	27.44	+0.64
Overall w/ expl. SoC contr.	4.24	4.68	39.01	-0.00

Table 6.5: Fuel consumption comparison - $SoC_{initial} = 90\%$ - US06 - CoSim

but for this thesis this was not done, because as it was explained before, the main focus was on the implementation and responses of different hybrid functionalities possible with the P2 parallel architecture. The 'Compact' strategy w/ explicit SoC controller shows the biggest

fuel economy decrease with this current used correcting factor. The fuel economy gained with this strategy in comparison with the baseline strategy equals 2.35%.

Chapter 7

Conclusion

The main goal of this thesis was to develop and implement the following hybrid MHEV functionalities: Torque Assist, E-Boost, Load Point Moving, and Load Point Shifting, integrate them with the previously developed functionalities into one overall hybrid control strategy in order to achieve improved fuel economy. In order to develop and implement the above-mentioned functionalities, the backward mathematical model was developed in the MATLAB environment, while the forward model was given by AVL in the AVL CRUISE ™ environment.The above-mentioned functionalities were described in detail and successfully implemented using the built-in C compiler in the CRUISE ™ environment. After the development and implementation of the functionalities, the integration with the previously developed functionalities was carried out. The integration was done in a way that each of the functionalities can be activated or deactivated by the user. In addition to the integrated overall hybrid control strategy model, a 'Compact' hybrid control strategy model was developed in order to compare the behavior and fuel economy gains using a condensed hybrid control strategy with a 'Rule-based' start-stop functionality that differs from the E-Creep Rolling start-stop functionality in the ways of ICE engine shut-off logic. Hybrid control strategies were tested on different certification driving cycles for different battery SoC initial conditions. It is shown that with the implementation of hybrid control functionalities fuel economy enhancements are significant in comparison to the conventional vehicle. For example, the Overall strategy w/o explicit SoC controller shows fuel economy improvement of 10.67% in comparison with the conventional vehicle on the NEDC driving cycle for initial battery SoC of 50%. On the other hand, the Overall strategies w/ and w/o explicit SoC controller show a slight fuel economy decrease in comparison with only basic hybrid functionalities on the NEDC cycle for initial SoC of 30% and 90 % respectively, but

on the WLTP and the US06 driving cycles that is not the case. That's probably because at the ending of the cycle the Sailing functionality activation gets delayed due to the active TA functionality at high velocities. That indicates that the Sailing functionality with its ICE engine shut-off and pure electrical driving has a bigger influence in fuel economy than the strategy with TA implemented on the NEDC cycle. The best hybrid control strategy, however, was the 'Compact' control strategy w/ explicit SoC controller. That strategy provided the fuel economy enhancement by 22.16% on NEDC cycle for the initial SoC of 90%, 13.86% on the WLTP cycle and 10.59% on the US06 cycle for the same initial SoC boundary condition. That indicates that the developed 'Rule-base' start-stop functionality with the LPM base behaves better than the model with the Overall hybrid control strategy. The assumed reason is that the developed 'Rule-base' start-stop functionality as a part of the 'Compact' strategy has a considerable influence on fuel economy enhancement, while the E-Creep in cooperation with the Regenerative braking functionality penalizes the frequent start-stop activation.

In order to test the control strategy response on a dynamic powertrain model, a Co-Simulation model was developed in the AVL Model.CONNECT ™ environment. The Co-Simulation model consisted of the AVL CRUISE ™ M dynamic ICE engine model, while the rest of the drivetrain stayed in the AVL CRUISE ™ model. All of the above-mentioned functionalities were successfully implemented for the Co-Simulation model in the same way as for the MHEV CRUISE ™ model. It is shown that on the NEDC driving cycle for the initial battery SoC of 30%, the Overall strategy w/ and w/o explicit SoC controller has the highest fuel economy increase in comparison with the conventional vehicle that equals 11.76% and 12.89% respectively. For the same boundary conditions, the 'Compact' strategies w/ and w/o explicit SoC controller show the fuel economy increase of 6.16% and 10.84% respectively. As it was the case before, the largest fuel economy increase is shown at the high initial battery SoC of 90%. The fuel economy increase equaled 14.29% for the Overall strategy w/o explicit SoC controller and 12.89% for the 'Compact' strategy w/ explicit SoC controller. Regarding the WLTP driving cycle, the 'Compact' strategy w/ explicit SoC controller shows fuel economy gain of 9.68%, where, on the other hand, the Overall strategy w/o SoC controller decreased the corrected fuel economy by 1.74% at the initial SoC of 90%. The basic fuel consumption was not compromised (14.64% better fuel economy in comparison with the conventional vehicle), but the energy cost from the battery i.e. the battery consumption in the sum with the basic consumption is larger this time. The first reason why this happened is that the fuel consumption correction factor for the Co-Simulation

model stayed the same, so it does not represent the real battery fuel consumption fairly and it needs to be corrected. The second reason why this happened is, as it was the case before, that 'Rule-based' start-stop has a larger influence on fuel economy gain than the E-Creep start-stop that was used in the Overall strategies. The effect of the fuel consumption correction factor is even larger on the US06 driving cycle, where the battery fuel consumption is more expensive than it was the case on the NEDC and WLTP driving cycles. The 'Compact' strategy w/ explicit SoC controller shows the fuel economy increase by 2.35% in comparison with the conventional vehicle, while the Overall strategy w/o explicit SoC controller, even though it has 10.89% larger basic fuel economy the corrected fuel consumption, shows that fuel economy decreases by 0.64% which is also an impact of fuel consumption correction factor.

In conclusion, the hybrid functionalities were developed, implemented and tested successfully for both of the simulation models. Currently, the 'Compact' strategy w/ explicit SoC controller shows the largest fuel economy increase in comparison with the other developed strategies for almost every simulation case, and it ensures the SoC sustainability. The proposed improvements and further work are as follows:

- implementation of more detailed BSFC maps of the ICE engine and EM efficiency maps,
- potential bug fixes of the C-code,
- proper sizing of the ICE engine in co-simulation model,
- fuel consumption correction factor calculation for the Co-Simulation model,
- P2 architecture components replacement - a larger EM ($\sim$ 20 kW) and a larger battery ($\sim$ 1.5 kWh) [7],
- implementation and testing of the functionalities on other parallel architectures (P0, P3 and P4) [9].

References

[1] Cipek M. *Usporedba različitih struktura hibridnih vozila.* Master's thesis, Faculty of Mechanical Engineering and Naval Architeture, Zagreb, 2009.

[2] Deur J. Cipek M. Škugor B. *Upravljanje električnim i hibridnim vozilima - materijali s predavanja*, 2017.

[3] Petrić J. *Upravljanje električnim i hibridnim vozilima - materijali s predavanja*, 2017.

[4] Cipek M. *Modeliranje, analiza i optimalno upravljanje pogonima hibridnih električnih vozila.* PhD thesis, Faculty of Mechanical Engineering and Naval Architecture, Zagreb, 2015.

[5] *CO_2 facts.* `https://www.co2.earth/global-co2-emissions`, 05.10.2018.

[6] Ehsani M. Gao Y. *Hybrid Electric Vehicle, Overview and State of the Art. IEEE-ISIE*, 2005.

[7] Nazir S. Wong Y.S. Chan C.C. *Encylopedia of Automotive Engineering*, chapter Basic Consideration. John Wiley & Sons, Ltd., 2014.

[8] *Audi A3 Sportback e-tron.* `https://mamotorcars.org/audi-a-3-etron/audi-a-3-etron-beautiful-a3-sportback-e-tron-audi-new-zealand/`, 29.09.2018.

[9] AVL List GmbH. *48V Mild Hybrid*, November 2016.

[10] Hihlik M. *Upravljanje umjereno-hibridiziranim električnim vozilom P2 konfiguracije.* Bachelor thesis, 2018.

[11] Škugor B. Deur J. Cipek M. Pavković D. *Design of a power-split hybrid electric vehicle control system utilizing a rule-based controller and equvalent consupmtion minimisation strategy. Journal of Automobile Engineering*, vol.228(6):631–648, 2014.

[12] Enang W. Bannister C. *Robust proporcional ECMS control of a parallel hybrid electric vehicle. Journal of Automobile Engineering*, pages 1–21, 2016.

[13] Soldo J. Ranogajec V. Škugor B. Deur J. *AVL CRUISE Model-based optimisation of Shift Scheduling Maps for a Parralel Hybrid Electric Vehicle*, 2017.

[14] Pels T. Kaup C. *Encylopedia of Automotive Engineering*, chapter Micro, Mild and Full Hybrids. John Wiley & Sons, Ltd., 2014.

[15] Sundström O. Guzzella L. Soltic P. *Torque-Assist Hybrid Electric Powertrain Sizing: From Optimal Control Towards a Sizing Law. IEEE transactions on control systems technology*, vol.18(4), 2010.

[16] Finkel E.D. *DIRECT Optimization Algorithm User Guide*, 2003.

[17] Škugor B. Ranogajec V. Deur J. *On Smoothing HEV/ERHEV Supervisiory Control Action Using an Extended ECMS Approach.* Faculty of Mechanical Engineering and Naval Architecture Zagreb, EVS27, Barcelona, Spain, November 2013.

[18] Cvok I. *Upravljanje električnim i hibridnim vozilima-Seminarski rad.* Technical report, Faculty of Mechanical Engineering and Naval Architecture Zagreb, 2017.

[19] *The different driving cycles.* `http://www.car-engineer.com/the-different-driving-cycles/`, 5.11.2018.

[20] *What is WLTP and how does it work?* `http://wltpfacts.eu/what-is-wltp-how-will-it-work/`, 5.11.2018.

[21] *SFTP-US06* . `https://www.dieselnet.com/standards/cycles/ftp_us06.php`, 5.11.2018.

[22] *AVL Model.CONNECT^{TM} User's manual.*

[23] Škugor B. *Modeliranje i optimalno punjenje flote električnih dostavnih vozila.* PhD thesis, Faculty of Mechanical Engineering and Naval Architeture, Zagreb, 2016.

[24] Cipek M. Deur J. Petrić J. *Bond Graph Modeling and Analysis of Series-Parallel Hybrid Electric Vehicle Transmissions. SAE International*, 2010.

Appendix A

Bond graph rules

In this appendix, the bond graph rules are given. Each bond represents the direction of power [24]. The bond graphs were used to visualize and model the P2 parallel architecture [24]. The bond graph rules and equation are given in figure A.1 [24].

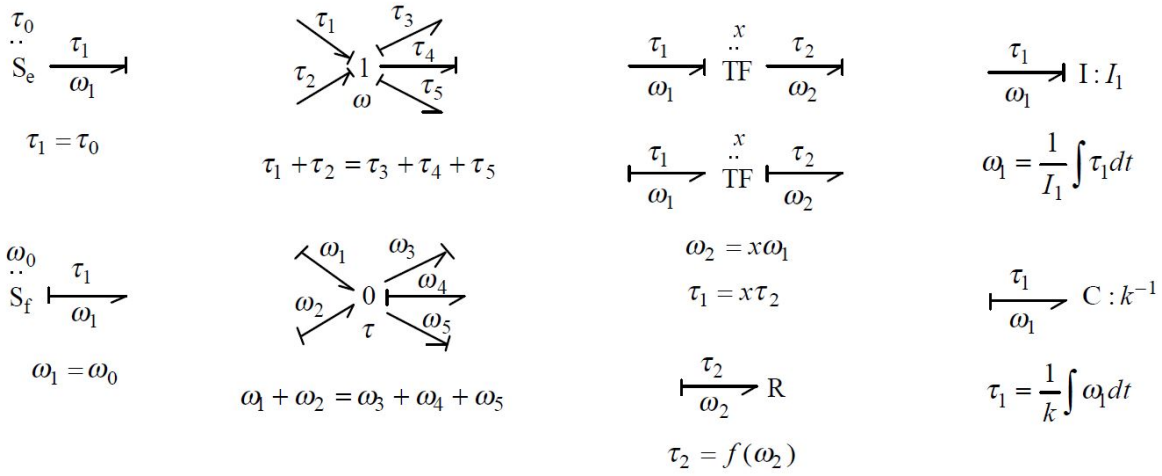

Figure A.1: Bond graph rules and equations

Appendix B

Fuel consumption tables

In this appendix the fuel consumption tables are given for the MHEV CRUISE ™ model and the Co-Sim model.

Strategy	V_f[l/100km]	$V_{f,corr}$ [l/100km]	SoC_{final} [%]	ΔV[%]
Baseline	5.10	-	-	-
E-Sailing+E-Coast.+E-Creep	5.09	4.85	57.05	-4.90
E-Sailing+E-Coast.+E-Creep+TA	5.10	4.88	55.10	-4.31
'Compact' w/o expl. SoC contr.	4.82	4.58	57.29	-9.66
'Compact' w/ expl. SoC contr.	4.56	4.20	71.02	-17.16
Overall w/o expl. SoC contr.	5.12	4.83	63.29	-5.29
Overall w/ expl. SoC contr.	5.09	4.87	55.27	-4.51

Table B.1: Fuel consumption comparison - $SoC_{initial} = 30\%$ - WLTP

Strategy	V_f[l/100km]	$V_{f,corr}$ [l/100km]	SoC_{final} [%]	ΔV[%]
Baseline	5.10	-	-	-
E-Sailing+E-Coast.+E-Creep	4.96	4.91	55.53	-3.73
E-Sailing+E-Coast.+E-Creep+TA	4.98	4.92	56.34	-3.53
'Compact' w/o expl. SoC contr.	4.82	4.58	57.29	-9.66
'Compact' w/ expl. SoC contr.	4.43	4.25	71.02	-16.17
Overall w/o expl. SoC contr.	4.99	4.83	59.29	-3.74
Overall w/ expl. SoC contr.	5.01	4.87	65.92	-4.51

Table B.2: Fuel consumption comparison - $SoC_{initial} = 50\%$ - WLTP

Strategy	V_f[l/100km]	$V_{f,corr}$ [l/100km]	SoC_{final} [%]	ΔV[%]
Baseline	6.27	-	-	-
E-Sailing+E-Coast.+E-Creep	6.22	6.00	54.98	-4.26
E-Sailing+E-Coast.+E-Creep+TA	6.21	5.99	55.14	-4.47
'Compact' w/o expl. SoC contr.	6.01	5.73	61.63	-8.54
'Compact' w/ expl. SoC contr.	5.90	5.58	67.09	-11.05
Overall w/o expl. SoC contr.	6.16	5.96	53.29	-4.94
Overall w/ expl. SoC contr.	6.25	5.99	59.71	-4.47

Table B.3: Fuel consumption comparison - $SoC_{initial} = 30\%$ - US06

Strategy	V_f[l/100km]	$V_{f,corr}$ [l/100km]	SoC_{final} [%]	ΔV[%]
Baseline	6.27	-	-	-
E-Sailing+E-Coast.+E-Creep	6.00	5.96	55.11	-4.94
E-Sailing+E-Coast.+E-Creep+TA	6.02	5.97	55.25	-4.72
'Compact' w/o expl. SoC contr.	5.85	5.73	63.89	-8.63
'Compact' w/ expl. SoC contr.	5.72	5.57	67.09	-11.14
Overall w/o expl. SoC contr.	6.01	5.96	56.09	-4.99
Overall w/ expl. SoC contr.	6.06	5.95	61.83	-5.10

Table B.4: Fuel consumption comparison - $SoC_{initial} = 50\%$ - US06

Strategy	V_f[l/100km]	$V_{f,corr}$ [l/100km]	SoC_{final} [%]	ΔV[%]
Baseline	4.03	-	-	-
E-Sailing+E-Coast.+E-Creep	3.71	3.52	57.74	-12.66
E-Sailing+E-Coast.+E-Creep+TA	3.79	3.66	45.53	-9.18
'Compact' w/o expl. SoC contr.	3.59	3.64	23.34	-9.68
'Compact' w/ expl. SoC contr.	3.67	3.51	47.05	-12.90
Overall w/o expl. SoC contr.	3.69	3.83	14.32	-4.96
Overall w/ expl. SoC contr.	3.85	3.73	42.53	-7.44

Table B.5: Fuel consumption comparison - $SoC_{initial} = 30\%$ - WLTP - CoSim

Strategy	V_f[l/100km]	$V_{f,corr}$ [l/100km]	SoC_{final} [%]	ΔV[%]
Baseline	4.03	-	-	-
E-Sailing+E-Coast.+E-Creep	3.65	3.69	45.05	-8.44
E-Sailing+E-Coast.+E-Creep+TA	3.69	3.73	45.53	-7.44
'Compact' w/o expl. SoC contr.	3.42	3.65	23.27	-9.43
'Compact' w/ expl. SoC contr.	3.52	3.55	46.14	-11.91
Overall w/o expl. SoC contr.	3.61	3.91	15.25	-2.98
Overall w/ expl. SoC contr.	3.75	3.82	42.54	-5.21

Table B.6: Fuel consumption comparison - $SoC_{initial} = 50\%$ - WLTP - CoSim

Strategy	V_f[l/100km]	$V_{f,corr}$ [l/100km]	SoC_{final} [%]	ΔV[%]
Baseline	4.68	-	-	-
E-Sailing+E-Coast.+E-Creep	4.81	4.51	64.74	-3.63
E-Sailing+E-Coast.+E-Creep+TA	4.95	4.76	51.25	+1.71
'Compact' w/o expl. SoC contr.	4.52	4.55	26.67	-2.78
'Compact' w/ expl. SoC contr.	4.61	4.51	41.09	-3.63
Overall w/o expl. SoC contr.	4.70	4.75	24.01	+1.49
Overall w/ expl. SoC contr.	4.67	4.59	39.18	-1.92

Table B.7: Fuel consumption comparison - $SoC_{initial} = 30\%$ - US06 - CoSim

Strategy	V_f[l/100km]	$V_{f,corr}$ [l/100km]	SoC_{final} [%]	ΔV[%]
Baseline	4.68	-	-	-
E-Sailing+E-Coast.+E-Creep	4.61	4.48	65.10	-4.27
E-Sailing+E-Coast.+E-Creep+TA	4.74	4.72	51.85	+0.85
'Compact' w/o expl. SoC contr.	4.39	4.59	26.09	-1.92
'Compact' w/ expl. SoC contr.	4.46	4.53	41.21	-3.21
Overall w/o expl. SoC contr.	4.46	4.67	25.25	-0.21
Overall w/ expl. SoC contr.	4.53	4.63	38.15	-1.07

Table B.8: Fuel consumption comparison - $SoC_{initial} = 50\%$ - US06 - CoSim